

# Simplicial approximation to CW complexes in practice

Raphaël TINARRAGE<sup>1</sup>

**Abstract** We describe an algorithm that takes as an input a CW complex and returns a simplicial complex of the same homotopy type. This algorithm, although well-known in the literature, requires some work to make it computationally tractable. We pay close attention to weak simplicial approximation, which we implement for two subdivisions methods: generalized barycentric and generalized edgewise subdivisions. We also propose a new subdivision process, based on Delaunay complexes. In order to facilitate the computation of a simplicial approximation, we introduce a simplification step, based on edge contractions. We define a new version of simplicial mapping cone, which requires less simplices. Last, we illustrate the algorithm with the real projective spaces, the 3-dimensional lens spaces and the Grassmannian of 2-planes in  $\mathbb{R}^4$ . As applications of these results, we estimate the discrete Lusternik–Schnirelmann category of our lens spaces, and we compute the persistent Stiefel–Whitney classes of a dataset of plane bundles.

**Keywords** Triangulation of manifolds · Simplicial approximation · CW complexes · Delaunay complexes

**MSC codes** 05E45 · 57-04 · 68U05 · 55N31

## Contents

<b>1</b>	<b>Introduction</b>	<b>1</b>
<b>2</b>	<b>Preliminaries</b>	<b>3</b>
2.1	CW complexes . . . . .	4
2.2	Simplicial complexes . . . . .	5
2.3	Simplicial approximation . . . . .	7
<b>3</b>	<b>Weak simplicial approximation</b>	<b>9</b>
3.1	Global subdivisions . . . . .	10
3.2	Subdivisions of the sphere . . . . .	13
3.3	Generalized subdivisions . . . . .	20
3.4	Contraction of codomain . . . . .	24
<b>4</b>	<b>Gluing simplicial cells</b>	<b>28</b>
4.1	Simplicial mapping cone . . . . .	28
4.2	Sketch of algorithm . . . . .	32
4.3	Informatic details . . . . .	36
<b>5</b>	<b>Applications</b>	<b>38</b>
5.1	The projective spaces . . . . .	39
5.2	The 3-dimensional lens spaces . . . . .	40
5.3	The Grassmannian $\mathcal{G}(2,4)$ . . . . .	42
<b>6</b>	<b>Conclusion</b>	<b>45</b>
<b>A</b>	<b>Notations</b>	<b>45</b>
<b>B</b>	<b>Supplementary results</b>	<b>46</b>

<sup>1</sup>FGV EMap, Rio de Janeiro, Brazil. <https://raphaeltinarrage.github.io/>

# 1 Introduction

In combinatorial topology, it is common to represent a topological space  $X$  as a simplicial complex. This representation is the input of many algorithms, as illustrated by all the effort put these last two decades to design softwares for manipulation and computation on simplicial complexes. Some of them are oriented towards algebra, such as `Magma`, `CHomP` and `GAP` [14, 55, 43], other ones towards geometry, in particular of 3-dimensional manifolds, such `regina`, `SnapPy` or `Twister` [16, 23, 8], but also towards data analysis, such as `gudhi`, `TTK` and `ripser` [53, 64, 7], to name a few.

Having access to a triangulation of  $X$  allows to compute algorithmically certain of its topological invariants: its (co)homology groups over  $\mathbb{Z}_p$  or  $\mathbb{Z}$  [44], its fundamental group [59], its Stiefel-Whitney classes [20, 39] or its first Pontryagin class [38].

From a triangulation of  $X$ , one can also study its combinatorial complexity, such as the size of its minimal triangulations [51], or its Lusternik–Schnirelmann category and simplicial versions of it [1, 34].

A last example where having access to triangulations of manifolds is relevant is Topological Data Analysis (TDA), a field at the intersection of computational geometry, algebraic topology and data analysis [17, 19]. Persistent homology, one of the most popular techniques of TDA, allows to infer the singular homology groups of a submanifold, based on a finite sample of it [28, 70, 57]. It has been applied to a wide range of problems, from medicine, physics, computer vision and machine learning, among others [58]. Recently, some works have been proposed towards estimating other topological invariants than homology groups. For instance, in [66], we presented an algorithm to compute the Stiefel-Whitney classes of a vector bundle, from a point cloud observation. This algorithm is based on a triangulation of the Grassmannian  $\mathcal{G}(d, n)$ .

Surprisingly, despite all these potential applications, there are many important manifolds  $X$  for which we do not know explicit triangulations. Namely, in the literature, one finds triangulations of

- $SO(n)$ , the special orthogonal group, only when  $n \leq 4$ ,
- $\mathcal{V}(d, n)$ , the Stiefel manifold of  $d$ -frames in  $\mathbb{R}^n$ , only when  $n \leq 3$ , when  $(d, n) = (3, 4)$ , or when  $d = 1$  (these cases correspond to the spheres),
- $\mathcal{G}(d, n)$ , the Grassmann manifolds of  $d$ -planes in  $\mathbb{R}^n$ , only when  $d = 1$  or  $n - 1$  (these cases correspond to the real projective spaces),
- $\mathbb{C}P^n$ , the complex projective space, only up to  $n = 6$  [62].

In this paper, instead of triangulations, we consider the weaker problem of obtaining simplicial complexes *homotopy equivalent* to the space  $X$ . We implement an algorithm that allows to build such simplicial complexes, based on the notion of *CW structure* on  $X$ . This algorithm, although well-known in the literature, has never been implemented in practice [45, Chapter 2.C].

Taking into account the limitation of computers' performance, we define several variations of the algorithm. We apply and compare the algorithms on the projective spaces  $\mathbb{R}P^n$  ( $n \leq 4$ ), the lens spaces  $L(p, q)$  ( $p, q \leq 7$ ) and the Grassmannian  $\mathcal{G}(2, 4)$ .

As it turns out, verifying the correctness of the algorithm amounts to testing whether two continuous maps between simplicial complexes are homotopic. This question has been subject of various works, but no algorithm has been implemented in practice [35]. Although other techniques exist, we did not investigate further [62, 40]. Consequently, we do not know whether the simplicial complexes we obtained have the correct homotopy type. As a sanity check, we verified that they have the correct fundamental group and the correct homology groups over  $\mathbb{Z}$ , using the package `simpcomp` of `GAP` [30].

Last, we propose applications for each simplicial complexes we computed:

- we compare the size of our triangulations of the projective spaces with other known triangulations,
- we study the discrete Lusternik–Schnirelmann category of the lens spaces,
- we use  $\mathcal{G}(2, 4)$  to compute the persistent Stiefel-Whitney classes of a synthetic 2-dimensional dataset.

**Related works** Explicit triangulations of manifolds can be obtained in three different ways. The first method consists in creating families of triangulations ‘by hand’. As an example, triangulations of  $\mathbb{R}P^n$  have been discovered recently [2], containing less vertices than the classical triangulations of Kühnel [49].

In computational geometry, another way of creating triangulations has been well-studied. It consists in embedding the manifold in some Euclidean space, and generating a finite sample of it. Triangulations are then built on top of these points, using variations of Delaunay triangulations [29, 4, 12].

Last, one can find triangulations via an exhaustive enumeration of combinatorial manifolds, or modifications of already known triangulations. This method has been used to obtain small triangulation of low-dimensional manifolds [51].

An interesting case of triangulation is given by the Grassmann manifolds  $\mathcal{G}(d, n)$ . In the literature, particular attention has been paid to the case  $d = 1$ , that is, to the projective spaces  $\mathbb{R}P^n$ . However, little is known about the case  $1 < d < n$ .

A candidate for a triangulation of  $\mathcal{G}(2, 4)$  is built in [46]. The author obtains a simplicial complex made of 100 vertices, with the correct homology groups over  $\mathbb{Z}/2\mathbb{Z}$  and  $\mathbb{Z}/3\mathbb{Z}$ . However, it is not verified whether this simplicial complex is homotopy equivalent to  $\mathcal{G}(2, 4)$ . Besides, triangulations of Grassmannians using matroids have been presented in [9], but the paper finally appeared to have an error [10]. As an idea of the complexity of this problem, [41] gives some bounds on the minimal number of simplices needed to triangulate  $\mathcal{G}(d, n)$ . In particular,  $\mathcal{G}(2, 4)$  must have at least 14 vertices and 372 simplices.

**Overview of the algorithm** This paper aims at implementing an algorithm to the following problem: given a CW complex  $X$ , return a homotopy equivalent simplicial complex. The reader may refer to Subsections 2.1 and 2.2 for a reminder about CW complexes and simplicial complexes. Roughly speaking, a CW complex is a topological space obtained by iteratively gluing closed balls along their boundary. An example is given in the following figure: the sphere  $\mathbb{S}^2$  can be obtained from a point, by gluing the two ends of an interval, so as to obtain a circle, and then gluing two disks on it, along their boundary. This gives a *filtration* of  $\mathbb{S}^2$  by four sets, denoted  $X_0 \subset X_1 \subset X_2 \subset X_3 = \mathbb{S}^2$ . The set  $X_i$  is called the  $i^{\text{th}}$  *skeleton*.

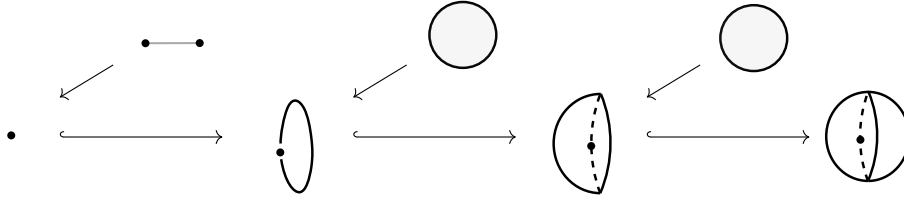


Figure 1: A CW structure on the sphere.

In this context, the balls are called *cells*. If  $\overline{\mathcal{B}}^d$  denotes a closed ball of dimension  $d$ , then its boundary is the  $(d - 1)$ -sphere  $\mathbb{S}^{d-1}$ , and the gluing of  $\overline{\mathcal{B}}^d$  on  $X$  is specified by a map  $\phi: \mathbb{S}^{d-1} \rightarrow X$ , called a *gluing map*. The input of our algorithm will be the collection of such gluing maps. They fit in the following diagram:

$$\begin{array}{ccccccc}
 & & \mathbb{S}^0 \supset \overline{\mathcal{B}}^1 & & \mathbb{S}^1 \supset \overline{\mathcal{B}}^2 & & \mathbb{S}^1 \supset \overline{\mathcal{B}}^2 \\
 & \swarrow \phi_1 & & \swarrow \phi_2 & & \swarrow \phi_3 & \\
 X_0 & \hookrightarrow & X_1 & \hookrightarrow & X_2 & \hookrightarrow & X_3
 \end{array}$$

A convenient feature of CW complexes is that each skeleton  $X_i$  is homeomorphic to the *mapping cone* of the gluing map  $\phi_i$ , denoted  $\text{Cone}(\phi_i)$  (see §2.1.3). Consequently, triangulating  $X$  boils down to triangulating mapping cones.

We will build inductively simplicial complexes  $K_0, \dots, K_3$ , and for each of them a homotopy equivalence  $h_i: X_i \rightarrow |K_i|$ , where  $|K_i|$  denotes the geometric realization of  $K_i$ . To initialize the process,  $K_0$  consists of only one point. Now, if  $K_i$  has been built, we can consider the induced gluing map  $h_i \circ \phi_{i+1}: \mathbb{S}^d \rightarrow |K_i|$ . Using the technique of simplicial approximation, we can find a simplicial equivalent to it. The result is a triangulation  $S_i$  of the sphere, and a simplicial map  $\phi'_{i+1}: S_i \rightarrow K_i$ , homotopy equivalent to  $h_i \circ \phi_{i+1}$ . Subsequently, we can build from  $S_i$  a triangulation of the ball, and glue it on  $K_i$  via  $\phi'_{i+1}$ , giving a simplicial complex  $K_{i+1}$  homotopy equivalent to  $X_{i+1}$ . As it turns out,  $K_{i+1}$  can be described as  $\text{Cone}^s(\phi'_{i+1})$ , the *simplicial mapping cone* (see Subsection 4.1). The following figure represents this process.

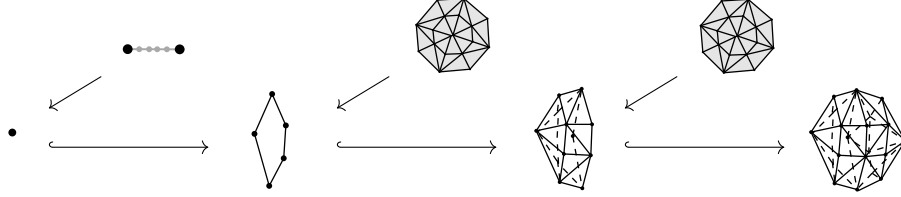


Figure 2: Simplicial version of Figure 1.

In order to obtain a simplicial map  $\phi'_{i+1}$ , we discuss in this paper the notion of *weak simplicial approximation*, and propose Algorithms 1, 2 and 3. We analyse these algorithms for four subdivision methods: barycentric, edgewise, Delaunay barycentric and Delaunay edgewise subdivisions. We also describe a careful implementation of the whole process in Algorithm 4, and apply it on three examples: the projective spaces up to dimension 4, the 3-dimensional lens spaces and the Grassmannian  $\mathcal{G}(2, 4)$ .

As explained in Theorem 4.5, the correctness of Algorithm 4 depends on some verification steps, that must be performed after its execution. We give a few ideas concerning such verifications in §3.1.3, but we do not implement them. The extension of these methods will be the subject of a further work. Thus, for the moment, we do not know whether the simplicial complexes we obtained have the correct homotopy type. We only checked that they have the correct homology.

**Data availability** A Python notebook, presenting an implementation of the algorithm described in this paper, is stored at <https://github.com/raphaeltinarrage/SimplicialApproximationCW>. It gathers applications of the algorithm on the projective spaces, the lens spaces, the Grassmannian  $\mathcal{G}(2, 4)$ , the complex projective space  $\mathbb{C}P^2$  and the special orthogonal group  $SO(3)$ . A text file, representing a simplicial complex potentially homotopy equivalent to the  $\mathcal{G}(2, 4)$ , output by the algorithm, can also be found.

**Outline** The rest of the paper is as follows. In Section 2 we give the mathematical background needed to read this paper. In Section 3 we discuss the problem of simplicial approximation, and how it can be implemented in practice. We define the main algorithm of this paper in Section 4. Notations are listed in Appendix A, and a few supplementary comments are gathered in Appendix B.

## 2 Preliminaries

In this section, we review some usual notions that will be used throughout the paper. We start by discussing CW complexes in Subsection 2.1, simplicial complexes in Subsection 2.2, and the problem of simplicial approximation in Subsection 2.3.

## 2.1 CW complexes

We present here some basic notions of topology, following [45], and then give some background about CW-complexes.

**2.1.1 General topology** A *homeomorphism* between two topological spaces  $X$  and  $Y$  is a continuous bijection  $f: X \rightarrow Y$  with continuous inverse. A *homotopy* between two continuous maps  $f, g: X \rightarrow Y$  is a continuous map  $h: X \times [0, 1] \rightarrow Y$  such that  $x \mapsto h(x, 0)$  is equal to  $f$  and  $x \mapsto h(x, 1)$  is equal to  $g$ . If such a homotopy exists, we say that  $f$  and  $g$  are *homotopic*. A *homotopy equivalence* between  $X$  and  $Y$  is a pair of maps  $f: X \rightarrow Y$  and  $g: Y \rightarrow X$  such that  $g \circ f$  is homotopic to the identity map  $X \rightarrow X$  and  $f \circ g$  is homotopic to the identity map  $Y \rightarrow Y$ . If such a homotopy equivalence exists, we say that  $X$  and  $Y$  are *homotopy equivalent*. In the rest of paper, we may call homotopy equivalence the map  $f$  alone.

A *retraction* of  $X$  onto a subspace  $A$  is a map  $r: X \rightarrow X$  such that  $r(X) = A$  and  $r(a) = a$  for all  $a \in A$ . A *deformation retraction* is a homotopy  $h: X \times [0, 1] \rightarrow X$  from the identity map of  $X$  to a retraction  $r: X \rightarrow X$  that satisfies  $h(a, t) = a$  for all  $a \in A$  and  $t \in [0, 1]$ . The existence of a deformation retraction implies that  $r$  is a homotopy equivalence. We point out that some authors call it a *strong* deformation retraction.

**2.1.2 Gluings** Let  $X$  and  $Y$  be two topological spaces,  $A \subset X$  a subset and  $f: A \rightarrow Y$  a continuous map. The *gluing along  $A$  via  $f$* , denoted  $X \sqcup_f Y$ , is defined as the quotient of the disjoint union  $X \sqcup Y$  by the equivalence relation given by  $\forall x \in A, x \sim f(x)$ .

If  $f: X \rightarrow Y$  is a continuous map, we define the *mapping cylinder* of  $f$ ,  $\text{Cyl}(f)$ , as the gluing  $X \times [0, 1] \sqcup_f Y$ , where  $f$  is seen with domain  $X \times \{1\}$ . One shows that  $\text{Cyl}(f)$  deforms retract on  $Y$ . Besides, the *mapping cone* of  $f$ ,  $\text{Cone}(f)$ , is obtained from  $\text{Cyl}(f)$  by identifying all the points of  $X \times \{0\}$ . Equivalently, the mapping cone can be defined as the gluing  $C(X) \sqcup_f Y$ , where  $C(X)$  is the *cone* obtained from the product  $X \times [0, 1]$  by identifying all the points  $X \times \{0\}$ , and  $f$  is seen with domain  $X \times \{1\} \subset C(X)$ .

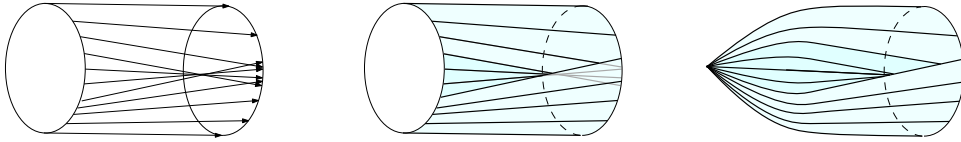


Figure 3: A map  $\mathbb{S}^1 \rightarrow \mathbb{S}^1$ , the corresponding mapping cylinder and mapping cone.

In this paper, we will mainly use mapping cones in the case where  $X$  is a sphere. Let  $\mathbb{S}^d$  be the unit sphere of  $\mathbb{R}^{d+1}$  and  $f: \mathbb{S}^d \rightarrow Y$  a continuous map. The cone  $C(\mathbb{S}^d)$  is homeomorphic to  $\overline{\mathcal{B}}^{d+1}$ , the unit closed ball of  $\mathbb{R}^{d+1}$ . Consequently,  $\text{Cone}(f)$  can be understood as gluing the ball  $\overline{\mathcal{B}}^{d+1}$  on  $Y$  along its boundary. The following lemma states that we do not change the homotopy type of the mapping cone by choosing a homotopy equivalent map.

**Lemma 2.1** ([45, Proposition 0.18]). *If two continuous maps  $f, g: \mathbb{S}^d \rightarrow Y$  are homotopic, then the mapping cones  $\text{Cone}(f)$  and  $\text{Cone}(g)$  are homotopy equivalent.*

We can write down an explicit homotopy equivalence as follows: let  $h: \mathbb{S}^d \times [0, 1] \rightarrow Y$  be a homotopy between  $f$  and  $g$ , and write  $\text{Cone}(f)$  and  $\text{Cone}(g)$  as the gluings  $\overline{\mathcal{B}}^{d+1} \sqcup_f Y$  and  $\overline{\mathcal{B}}^{d+1} \sqcup_g Y$ . Then a homotopy equivalence  $H: \overline{\mathcal{B}}^{d+1} \sqcup_f Y \rightarrow \overline{\mathcal{B}}^{d+1} \sqcup_g Y$  is given by

$$x \mapsto \begin{cases} x & \text{if } x \in Y, \\ 2x & \text{if } x \in \overline{\mathcal{B}}^{d+1} \text{ and } \|x\| \leq \frac{1}{2}, \\ h\left(\frac{x}{\|x\|}, 2\|x\| - 1\right) & \text{if } x \in \overline{\mathcal{B}}^{d+1} \text{ and } \|x\| > \frac{1}{2}. \end{cases} \quad (1)$$

**2.1.3 CW complexes** We shall restrict our definitions to the finite case. Following [54], a *CW complex* is a topological Hausdorff space  $X$  together with a finite partition  $\{e_i \mid i \in \llbracket 0, n \rrbracket\}$  of  $X$  such that:

- For each  $e_i$ , there exists an integer  $d(i)$  and a homeomorphism  $\Phi_i: \mathcal{B}^{d(i)} \rightarrow e_i$ , where  $\mathcal{B}^{d(i)}$  is the unit open ball of  $\mathbb{R}^{d(i)}$ . The integer  $d(i)$  is called the *dimension* of the cell  $e_i$ .
- Moreover, this homeomorphism extends as a continuous map  $\Phi_i: \overline{\mathcal{B}}^{d(i)} \rightarrow X$ , called a *characteristic map* for the cell. We denote by  $\bar{e}_i$  its image.  
The restriction of  $\Phi_i$  to  $\mathbb{S}^{d(i)-1} \subset \overline{\mathcal{B}}^{d(i)}$ , denoted  $\phi_i: \mathbb{S}^{d(i)-1} \rightarrow X$ , is called its *gluing map*.
- Each point  $x \in \bar{e}_i \setminus e_i$  must lie in a cell  $e_j$  of lower dimension.

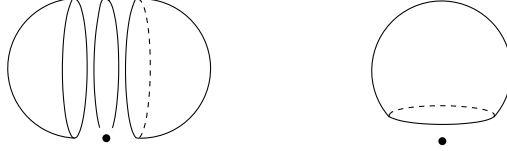


Figure 4: Two CW structures on the sphere. The first one has one cell of dimension 0, one of dimension 1, and two of dimension 2. The second one has one cell of dimension 0, and one of dimension 2.

The CW complexes form a useful class of spaces in algebraic topology: combinatorial in nature, but allowing to describe many important spaces. As reviewed in [52], any smooth manifold is homeomorphic to a CW complex, as well as any topological manifold of dimension  $d \neq 4$ . Moreover, any topological manifold is homotopy equivalent to CW complex.

The goal of this paper is to find a simplicial complex  $K$  homotopy equivalent to a given CW complex  $X$ . To do so, we will use the fact that a CW complex can be built by a sequence of mapping cones. For any  $i \in \llbracket 0, n \rrbracket$ , define the *skeleton*  $X_i = \bigcup_{j \leq i} e_j$ , that is, the union of the first  $i$  cells. We have an increasing sequence of subsets  $X_0 \subset X_1 \subset \dots \subset X_n = X$ . Now, consider the map  $\bar{\Phi}_i: X_i \rightarrow \overline{\mathcal{B}}^{d(i)} \sqcup X_{i-1}$  given by:

$$\bar{\Phi}_i(x) = \begin{cases} \Phi_i^{-1}(x) & \text{if } x \in e_i, \\ x & \text{if } x \in X_{i-1}. \end{cases}$$

Seeing  $\text{Cone}(\phi_i)$ , the mapping cone of  $\phi_i$ , as the quotient  $\overline{\mathcal{B}}^{d(i)} \sqcup_{\phi_i} X_{i-1}$ , we get:

**Lemma 2.2.** *The map  $\bar{\Phi}_i: X^i \rightarrow \text{Cone}(\phi_i)$  is a homomorphism.*

These maps fit in the following diagram:

$$\begin{array}{ccccccc} & \mathbb{S}^{d(1)-1} & & \mathbb{S}^{d(2)-1} & & \mathbb{S}^{d(3)-1} & \\ & \swarrow \phi_1 & & \swarrow \phi_2 & & \swarrow \phi_3 & \\ X_0 & \xrightarrow{\quad} & X_1 & \xrightarrow{\quad} & X_2 & \xrightarrow{\quad} & \dots \xrightarrow{\quad} X_n \\ & & \downarrow \bar{\Phi}_1 & & \downarrow \bar{\Phi}_2 & & \downarrow \bar{\Phi}_n \\ & & \text{Cone}(\phi_1) & & \text{Cone}(\phi_2) & & \text{Cone}(\phi_n) \end{array}$$

Thus, by providing a simplicial equivalent for the mapping cones, we will be able to find a simplicial complex  $K$  homotopy equivalent to  $X$ .

## 2.2 Simplicial complexes

In this subsection, we define the simplicial complexes and their topology, based on [56, Sections 1,2]. We will restrict our definitions to *finite* simplicial complexes.

**2.2.1 Geometric simplicial complexes** Consider a set  $\sigma = \{v_0, \dots, v_p\}$  of  $p+1$  affinely independent points of  $\mathbb{R}^n$ . We define the  $p$ -simplex spanned by  $v_0, \dots, v_p$  as their convex hull:

$$|\sigma| = \left\{ x \in \mathbb{R}^n \mid \exists \lambda_0, \dots, \lambda_p \geq 0, \sum_{0 \leq i \leq p} \lambda_i = 1, x = \sum_{0 \leq i \leq p} \lambda_i v_i \right\}.$$

In this last sum, the numbers  $\lambda_i$  are uniquely defined by  $x$  and are called the *barycentric coordinates* of  $x$  in  $\sigma$ . The *dimension* of  $\sigma$  is defined as  $\dim(\sigma) = p$ . A *face* of  $\sigma$  is a simplex spanned by a subset of its vertices. We also define the *standard  $p$ -simplex*  $\Delta^p$  as the simplex spanned by the canonical basis vectors  $e_1, \dots, e_{p+1}$  of  $\mathbb{R}^{p+1}$ . Now, a *geometric simplicial complex*  $K$  in  $\mathbb{R}^n$  is a collection of simplices in  $\mathbb{R}^n$  such that (1) every face of a simplex of  $K$  is in  $K$  and (2) the intersection of any two simplices is a face of each of them.

Let  $K$  be a geometric simplicial complex, and define  $|K|$  as the subset of  $\mathbb{R}^n$  consisting of the union of the simplices of  $K$ . It is called the *underlying space* or the *geometric realization* of  $K$ . It is given the gluing topology: a subset  $A \subset |K|$  is closed if and only if its intersection  $A \cap \sigma$  with any simplex  $\sigma \in K$  is closed. When  $K$  is finite, it coincides with the subset topology inherited by  $\mathbb{R}^n$ .

According to this construction, each simplex  $\sigma \in K$  is a subset of  $|K|$ . In order to clarify the exposition, we will write  $\sigma$  to denote a simplex seen as an element of the simplicial complex  $K$ , and  $|\sigma|$  to denote its interior, seen as a subset of  $|K| \subset \mathbb{R}^n$ . We consider that the interior of a 0-simplex  $\sigma = \{v\}$  is equal to  $\sigma$  itself.

Note that the set  $\{|\sigma| \mid \sigma \in K\}$  is a partition of  $|K|$ . This allows to define the *location map* of  $K$ . It is the unique map  $\mathcal{L}_K: |K| \rightarrow K$  that satisfies  $x \in |\mathcal{L}_K(x)|$  for all  $x \in |K|$ . From an algorithmic perspective, the location map corresponds to the problem of *location* in a triangulation, that is, finding the simplex that contain a given point. This map is also called *face map* in [66], and *carrier map* in [69]. In the same vein, if  $X$  is a topological space and  $h: X \rightarrow |K|$  any continuous map, we define its *location map* as the unique map  $\mathcal{L}_h: X \rightarrow K$  that satisfies  $x \in |\mathcal{L}_h(x)|$  for all  $x \in X$ .

**2.2.2 Abstract simplicial complexes** Let  $V$  be a set, called the set of *vertices*. An *abstract simplicial complex* on  $V$  is a set  $K$  of finite and non-empty subsets of  $V$ , and such that  $K$  satisfies the following condition: for every  $\sigma \in K$  and every non-empty subset  $v \subseteq \sigma$ ,  $v$  is in  $K$ . The elements of  $K$  are called *simplices* of the simplicial complex  $K$ .

For every simplex  $\sigma \in K$ , we define its dimension as  $\dim(\sigma) = \text{card}(\sigma) - 1$ . The *dimension* of  $K$ , denoted  $\dim(K)$ , is the maximal dimension of its simplices. For every  $i \geq 0$ , the  *$i$ -skeleton*  $K^i$  is defined as the subset of  $K$  consisting of simplices of dimension at most  $i$ . Note that  $K^0$  corresponds to the underlying vertex set  $V$ , and that  $K^1$  is a graph. Given a simplex  $\sigma \in K$ , its (*open*) *star*  $\text{St}(\sigma)$  is the set of all the simplices  $v \in K$  that contain  $\sigma$ . The open star is not a simplicial complex in general. We also define its *closed star*  $\overline{\text{St}}(\sigma)$  as the smallest simplicial subcomplex of  $K$  which contains  $\text{St}(\sigma)$ . The *link* of  $\sigma$  is defined as  $\text{Lk}(\sigma) = \overline{\text{St}}(\sigma) \setminus \text{St}(\sigma)$ . In this paper, we will often use the notation  $\overline{\text{St}}(v)^0$ , where  $v$  is a vertex of  $K$ . According to the notations, it refers to the set of neighbors of  $v$ , with  $v$  included.

Clearly, to any *geometric* simplicial complex  $K'$  in  $\mathbb{R}^n$  is associated an abstract simplicial complex  $K$ , where the vertex set  $V$  of  $K$  is the set of vertices of the simplices of  $K'$ , and the simplices of  $K$  are the subsets of  $V$  that span simplices of  $K'$ . We shall refer to  $K$  as the *underlying abstract simplicial complex* of  $K'$ . Conversely, if  $K$  is an abstract simplicial complex, we call a *geometric realization* of  $K$  a geometric simplicial complex  $K'$  whose underlying abstract simplicial complex is  $K$ . When  $K$  is finite, a geometric realization always exists. In the rest of the paper, we shall say *simplicial complex* to denote either a geometric or an abstract simplicial complex, depending on the context.

**2.2.3 Simplicial maps** A *simplicial map* between geometric simplicial complexes  $K$  and  $L$  is a map between underlying spaces  $g: |K| \rightarrow |L|$  which sends each simplex of  $K$  to a simplex of

$L$  by a linear map that sends vertices to vertices. In other words, for every  $\sigma = [v_0, \dots, v_p] \in K$ , the subset  $[g(v_0), \dots, g(v_p)]$  is a simplex of  $L$ . The map  $g$  restricted to  $|\sigma| \subset |K|$  can be written in barycentric coordinates as

$$\sum_{i=0}^p \lambda_i v_i \mapsto \sum_{i=0}^p \lambda_i g(v_i). \quad (2)$$

A simplicial map  $g: |K| \rightarrow |L|$  is uniquely determined by its restriction to the vertex sets  $g|_{K^0}: K^0 \rightarrow L^0$ .

Reciprocally, let  $f: K^0 \rightarrow L^0$  be a map between vertex sets which satisfies the following condition:

$$\forall \sigma \in K, f(\sigma) \in L. \quad (3)$$

Then  $f$  induces a simplicial map via barycentric coordinates, still denoted  $f: |K| \rightarrow |L|$ . It is called the *geometric realization* of  $f$ . In the rest of this paper, a simplicial map shall either refer to a map  $g: |K| \rightarrow |L|$  which satisfies Equation (2), to a map  $f: K^0 \rightarrow L^0$  which satisfies Equation (3), or to the induced map  $f: K \rightarrow L$ . Note that Equation (3) allows to define the notion of simplicial maps between *abstract* simplicial complexes.

Two simplicial maps  $f, g: K \rightarrow L$  are said *contiguous* if for every simplex  $\sigma \in K$ ,  $f(\sigma) \cup g(\sigma)$  is a simplex of  $L$ . In this case, one shows that their geometric realizations are homotopic.

**2.2.4 Triangulations of manifolds** If  $X$  is any a topological space, a *triangulation* of  $X$  consists of a geometric simplicial complex  $K$  together with a homeomorphism  $h: X \rightarrow |K|$ . All smooth manifolds are triangulable, but this is not the case for topological manifolds. This phenomenon occurs in dimension 4 at least, and an example is given by the  $E_8$  manifold constructed by Freedman [3]. More generally, non-triangulable manifolds exist in every dimension  $d \geq 5$ , as proven recently in [52].

However, in this paper, we are concerned with the following weaker problem: building a simplicial complex *homotopy equivalent* to a given manifold  $X$ . This is possible in general, since any topological manifold is homotopy equivalent to a CW complex, and any CW complex is homotopy equivalent to a simplicial complex [52, Example 2.2].

## 2.3 Simplicial approximation

Let  $f: |K| \rightarrow |L|$  be any continuous map between geometric simplicial complexes. The problem of *simplicial approximation* consists in finding a simplicial map  $g: K \rightarrow L$  with geometric realization  $g: |K| \rightarrow |L|$  homotopy equivalent to  $f$ . A way to solve this problem is to consider the following property.

**2.3.1 Star condition** We say that the map  $f$  satisfies the *star condition* if for every vertex  $v$  of  $K$ , there exists a vertex  $w$  of  $L$  such that

$$f(|\overline{\text{St}}(v)|) \subseteq |\text{St}(w)|. \quad (4)$$

If this is the case, let  $g: K^0 \rightarrow L^0$  be any map between vertex sets such that for every vertex  $v$  of  $K$ , we have

$$f(|\overline{\text{St}}(v)|) \subseteq |\text{St}(g(v))|. \quad (5)$$

Such a map is called a *simplicial approximation* to  $f$ . One shows that it is a simplicial map, and that its geometric realization is homotopic to  $f$  [45, Theorem 2C.1]. We point out that, for some authors, such as [56], the star condition is defined by the property  $f(|\text{St}(v)|) \subseteq |\text{St}(w)|$ . The definition we used above, although harder to satisfy than this one, will be enough for our purposes.

In general, a map  $f$  may not satisfy the star condition. However, there is always a way to ensure that it does, by replacing  $K$  with a finer simplicial complex. We will present two such constructions: the barycentric subdivisions and the edgewise subdivisions.



**2.3.2 Barycentric subdivisions** Let  $\sigma$  be a  $d$ -simplex of  $\mathbb{R}^n$ , with vertices  $v_0, \dots, v_d$ . The *barycentric subdivision* of  $\sigma$ , denoted  $\text{sub}(\sigma)$ , consists in decomposing  $\sigma$  into a simplicial complex with  $2^{d+1} - 1$  vertices and  $(d+1)!$  simplices of dimension  $d$ . More precisely, the new vertices correspond to the barycenters of the vertices of  $\sigma$ , that is, the points  $\sum_{i=0}^d \lambda_i v_i$  for which some  $\lambda_i$  are zero and the other ones are equal. From a combinatorial point of view, we can see this new set of vertices as a the power set of the set of vertices of  $\sigma$ : a vertex  $w = \sum_{i=0}^d \lambda_i v_i$  is associated to the subset  $\hat{w} = \{i \in \llbracket 0, d \rrbracket \mid \lambda_i \neq 0\}$ . Then one defines the simplices of  $\text{sub}(\sigma)$  as the sets  $[w_0, \dots, w_i], i \in \llbracket 0, d \rrbracket$ , such that  $\hat{w}_0 \subsetneq \dots \subsetneq \hat{w}_i$ .

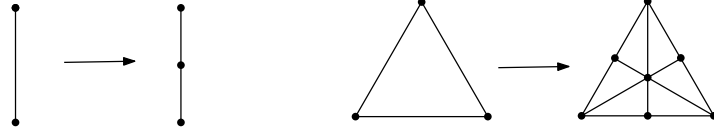


Figure 5: Barycentric subdivision in dimension 1 and 2.

More generally, if  $K$  is a geometric simplicial complex, its barycentric subdivision  $\text{sub}(K)$  is the simplicial complex obtained by subdividing each of its simplices. Applying barycentric subdivision  $n$  times shall be denoted  $\text{sub}^n(K)$ . Note that the underlying abstract simplicial complex of  $\text{sub}^n(K)$  does not depend on a choice of a geometric realization on  $K$ , though the geometric simplicial complex does. Besides, there exists a canonical homeomorphism  $|\text{sub}^n(K)| \rightarrow |K|$ . If  $f: |K| \rightarrow |L|$  is any map, the composition map  $|\text{sub}^n(K)| \rightarrow |L|$  will still be denoted  $f$ .

A key property of the barycentric subdivision is that it shrinks the size of the simplices. If  $K$  is a geometric simplicial complex, let us denote by  $\delta(K)$  the maximal diameter of its simplices (or, equivalently, the maximal length of its edges). Let  $\sigma$  be a geometric  $d$ -simplex. For any  $n \geq 1$ , we have

$$\delta(\text{sub}^n(\sigma)) \leq \left(\frac{d}{d+1}\right)^n \delta(\sigma). \quad (6)$$

As a consequence, if  $K$  is of dimension at most  $d$ , we also have  $\delta(\text{sub}^n(K)) \leq \left(\frac{d}{d+1}\right)^n \delta(K)$ . In other words, iterated barycentric subdivisions allow to make the simplices of  $K$  arbitrarily small. From this property, one deduces the *simplicial approximation theorem*. We now give its proof, following [45, Theorem 2C.1], for we will refer to it later in the paper.

**Theorem 2.3.** *Let  $K, L$  be two geometric simplicial complexes and  $f: |K| \rightarrow |L|$  a continuous map. Then there exists an integer  $n$  such that the induced map  $f: |\text{sub}^n(K)| \rightarrow |L|$  satisfies the star condition.*

*Proof.* Let us endow  $|K| \subset \mathbb{R}^n$  with the geodesic distance induced by the Euclidean metric of  $\mathbb{R}^n$ . In particular, it restricts to the Euclidean metric on each simplex  $|\sigma|$  of  $|K|$ . Now, consider the open cover of  $|K|$  defined as

$$\mathcal{V} = \{f^{-1}(|\text{St}(x)|) \mid x \in L^0\}. \quad (7)$$

Since  $|K|$  is compact, let  $\lambda > 0$  be a Lebesgue number for  $\mathcal{V}$ , that is, a number such that every subset of  $|K|$  of diameter less than  $\lambda$  is included in an element of  $\mathcal{V}$ . As implied by Equation (6), there is a  $n \geq 0$  such that  $\text{sub}^n(K)$  is made of simplices with diameter lower than  $\frac{\lambda}{2}$ . As a consequence, the star of any vertex of  $\text{sub}^n(K)$  has diameter lower than  $\lambda$ , hence is included in an element of  $\mathcal{V}$ . In other words,  $f: |\text{sub}^n(K)| \rightarrow |L|$  satisfies the star condition.  $\square$

**2.3.3 Edgewise subdivisions** From a practical viewpoint, barycentric subdivision is computationally expensive: after one subdivision, the number of vertices of the  $d$ -simplex goes from  $d+1$  to  $2^{d+1} - 1$ . Another subdivision process, known as *edgewise subdivision*, allows to decompose a  $d$ -simplex into a simplicial complex with only  $\frac{d(d+1)}{2}$  vertices: the initial vertices, and the midpoints of its edges. Just as before, the edgewise subdivision of a simplicial complex

$K$  shall be denoted  $\text{sub}(K)$ , and the iterated subdivisions  $\text{sub}^n(K)$ . Instead of giving here the definition, we refer the reader to [27], and represent in the following figure the cases that we will consider in this paper.

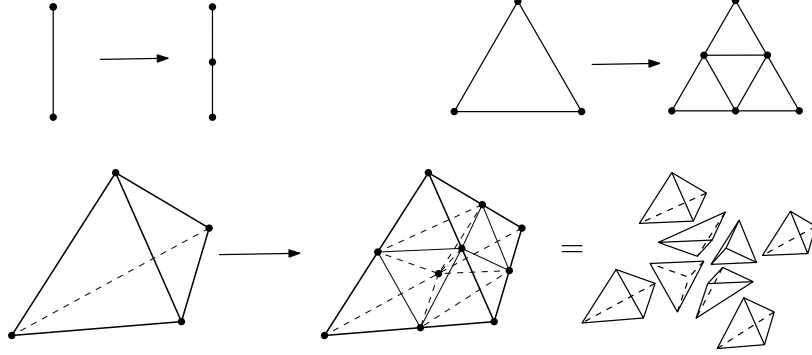


Figure 6: Edgewise subdivision in dimension 1, 2 and 3.

The edgewise subdivision of a 1-simplex is equal to the barycentric subdivision. The simplex is subdivided in two segments, of diameters divided by half. Next, the edgewise subdivision of a 2-simplex consists of four triangles, similar to the original one, with diameters also divided by half. Hence, in both cases, we deduce the bound

$$\delta(\text{sub}^n(\sigma)) \leq \frac{1}{2^n} \delta(\sigma). \quad (8)$$

It is less simpler in dimension 3: from the vertices of a 3-simplex  $\sigma$  and the midpoints of its edges, there exists three different ways of triangulating it again. The subdivided simplex  $\text{sub}(\sigma)$  must contain four tetrahedra, one at each vertex of  $\sigma$ , similar to  $\sigma$ . It remains to subdivide the octahedron inside, which can be done by adding an edge connecting the midpoints of two opposite edges  $e_1$  and  $e_2$ . Let us denote the length of the edges of  $\sigma$  as  $l_1, \dots, l_6$ , where the two first ones correspond to the edges  $e_1$  and  $e_2$ . Elementary geometry shows that the distance between their midpoints is

$$\frac{1}{2} \sqrt{l_3^2 + l_4^2 + l_5^2 + l_6^2 - l_1^2 - l_2^2}.$$

In particular, if  $l_1, l_2$  go to zero, and if the other edges have equal length, then we can make  $\delta(\text{sub}(\sigma))$  arbitrarily close to  $\delta(\sigma)$ . Therefore, there is no inequality  $\delta(\text{sub}(\sigma)) \leq \alpha \delta(\sigma)$  with  $\alpha < 1$  for edgewise subdivisions in dimension 3. Fortunately, we can obtain the following bound:

$$\delta(\text{sub}^n(\sigma)) \leq \frac{\sqrt{3}}{2^n} \delta(\sigma). \quad (9)$$

More generally, edgewise subdivision in dimension  $d$  satisfies  $\delta(\text{sub}^n(\sigma)) \leq \frac{\sqrt{d}}{2^n} \delta(\sigma)$ . This is a consequence of the fact that iterating  $n$  edgewise subdivisions is equivalent to applying a  $2^n$ -fold edgewise subdivision, and that a  $2^n$ -fold subdivision can be obtained by cutting the simplex  $2^n$  times [27, Main Theorem]. As a consequence, for any geometric simplicial complex  $K$ , we have  $\delta(\text{sub}^n(K)) \leq \frac{\sqrt{d}}{2^n} \delta(K)$ , which goes to zero, hence the simplicial approximation theorem also holds for edgewise subdivisions.

### 3 Weak simplicial approximation

We now gather some ideas to allow the use of simplicial approximation in practice. Throughout this section, we will consider two geometric simplicial complexes  $|K|$  and  $|L|$ , and a continuous map  $f: |K| \rightarrow |L|$ . In our examples, the simplicial complexes will be chosen homeomorphic to

the  $d$ -sphere for  $d = 1$  or  $2$ , and  $f$  will be the identity map. In order to distinguish more clearly between the various notions of subdivisions that we will introduce, we may call *global subdivisions*, instead of simply subdivision, the usual barycentric or edgewise subdivisions defined in Subsection 2.3.

As it is defined in Equation (4), the star condition cannot be used in practice. In Subsection 3.1, we propose a way around this problem with the weak simplicial approximations. We pay particular attention to the case where  $K$  is a sphere in Subsection 3.2, and define the notion of Delaunay subdivisions. In Subsection 3.3, we study generalized subdivisions, a more economical approach than global subdivisions. We also introduce the notion of Delaunay simplification. Last, we present in Subsection 3.4 the operation of edge contraction, and explain how contracting the complex  $L$  may simplify the problem of simplicial approximation.

### 3.1 Global subdivisions

Let us consider a continuous map  $f: |K| \rightarrow |L|$  between two geometric simplicial complexes. As discussed in Subsection 2.3, the problem of simplicial approximation consists in finding a simplicial map  $g: K \rightarrow L$  whose topological realization  $g: |K| \rightarrow |L|$  is homotopic to  $f$ . The problem is easily solved if  $f$  satisfies the star condition, that is, if for every vertex  $v$  of  $K$ , there exists a vertex  $w$  of  $L$  such that

$$f(|\overline{\text{St}}(v)|) \subseteq |\text{St}(w)|.$$

From a practical point of view, one can compute the closed star  $\overline{\text{St}}(v)$  from the simplicial complex  $K$ . However, computing  $f(|\overline{\text{St}}(v)|)$  requires to evaluate  $f$  on the infinite set  $|\overline{\text{St}}(v)|$ . In order to reduce the problem to a finite number of evaluations of  $f$ , we shall consider a related property.

**3.1.1 Weak simplicial approximation** It has been introduced in [66]. Consider a vertex  $v \in K^0$ . We say that map  $f$  satisfies the *weak star condition at  $v$*  if there exists a vertex  $w \in L^0$  such that

$$|f(\overline{\text{St}}(v)^0)| \subseteq |\text{St}(w)|, \quad (10)$$

where we remind the reader that  $\overline{\text{St}}(v)^0$  denotes the 0-skeleton of  $\overline{\text{St}}(v)$ , i.e., the set of neighbors of  $v$ , with  $v$  included. Moreover, we say that map  $f$  satisfies the *weak star condition* if it does for every vertex of  $K$ . Suppose now that it is the case. Let  $g: K^0 \rightarrow L^0$  be a map between vertex sets such that for every  $v \in K^0$ ,

$$|f(\overline{\text{St}}(v)^0)| \subseteq |\text{St}(g(v))|. \quad (11)$$

Such a map is called a *weak simplicial approximation to  $f$* . One shows that  $g$  is a simplicial map [66, Lemma 5.2]. Moreover, any two weak simplicial approximations are contiguous, hence homotopy equivalent.

If  $f$  satisfies the star condition, then it also satisfies the weak star condition, and any weak star approximation  $g$  is homotopic to  $f$  [66, Proposition 5.5]. However, in general,  $g$  and  $f$  may not be homotopic. In order to verify that they are, a further verification step must be used. We present such ideas in §3.1.3. It is worth noting that, in practice, this verification step must involve an additional knowledge about  $f$  (such as a Lipschitz constant, or its induced map between homology groups). Without further hypothesis, we might not be able to actually verify that  $g$  is homotopic to  $f$ .

When  $f$  does not satisfy the weak star condition, the simplicial complex  $K$  must be subdivided. Following Subsection 2.3, let us choose a subdivision method between barycentric and edgewise, and consider the sequence of subdivided complexes  $(\text{sub}^i(K))_{i \geq 0}$ . As a consequence of the simplicial approximation theorem (Theorem 2.3), the induced map  $f: |\text{sub}^i(K)| \rightarrow |L|$  satisfies the star condition at some point, hence the weak star condition too. In other words, the following algorithm terminates.

---

**Algorithm 1** Weak simplicial approximation via global subdivisions
 

---

**Input:** a continuous map  $f: |K| \rightarrow |L|$   
**Output:** a weak simplicial approximation  $g$  to  $f$   
 1: **while**  $f: |K| \rightarrow |L|$  does not satisfy the star condition **do**  
   2:   let  $K$  be  $\text{sub}(K)$   
 3: **end while**  
 4: let  $g$  be a weak simplicial approximation to  $f$   
 5: **return**  $g$

---

**Proposition 3.1.** *Given any continuous map  $f: |K| \rightarrow |L|$ , Algorithm 1 terminates.*

An illustration of this algorithm is given in the following figure, where  $f$  is the identity map between two triangles, represented as  $\partial\Delta^2$ , the boundary of the 2-simplex. After two subdivisions, the map satisfies the weak star condition.

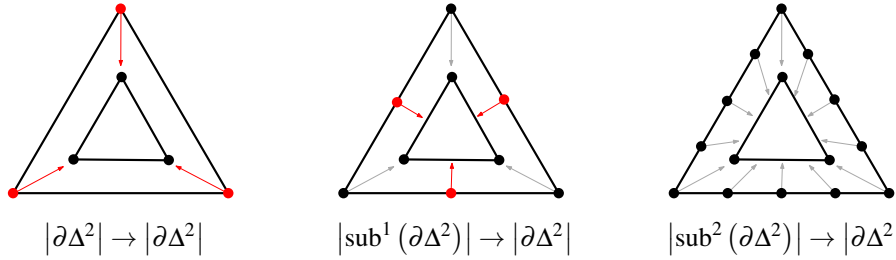


Figure 7: Run of Algorithm 1 on the identity map  $|\partial\Delta^2| \rightarrow |\partial\Delta^2|$ . Vertices where the map does not satisfy the weak star condition are represented in red.

*Remark 3.2.* We point out that the notion of weak simplicial approximation is merely a tool to find a homotopic simplicial map  $g: K \rightarrow L$ . To find so, various other ideas may be used. For instance, one could design a general algorithm that, given the map  $f: |K| \rightarrow |L|$ , returns a simplicial map  $g: K \rightarrow L$  such that

$$|f(v)| \in |\text{St}(g(v))|$$

for each vertex  $v \in K^0$ . In the case where  $K$  is a graph, this is known as the *list homomorphism problem*, and it is NP in general [33]. Another natural idea consists in weakening Equation (10) as follows, giving the notion of *closed weak star condition*:

$$\left| f\left(\overline{\text{St}}(v)^0\right) \right| \subseteq \left| \overline{\text{St}}(w) \right|. \quad (12)$$

Then, by mimicking Equation (11), one can define a notion of *closed weak star approximation*. In some cases,  $f$  may not satisfy the weak star condition, but satisfy the closed weak star condition. However, closed weak simplicial approximations suffer from a crucial issue: they are not simplicial maps in general.

**3.1.2 Alternative formulation** One has a convenient formulation of the weak star condition, using the *location map* of  $L$ . We remind the reader that, as defined in §2.2.1, it is the unique map  $\mathcal{L}_L: |L| \rightarrow L$  that satisfies  $x \in |\mathcal{L}_L(x)|$  for every  $x \in |L|$ . It is clear that the map  $f: |K| \rightarrow |L|$  satisfies the weak star condition if and only if for every vertex  $v$  of  $K$ , the intersection of the locations of the neighbors of  $v$  is non-empty:

$$\bigcap_{v' \in \text{St}(v)^0} \mathcal{L}_L(f(v')) \neq \emptyset.$$

Consequently, in order to verify the weak star condition, and to run Algorithm 1, one only has to have access to an implementation of  $f$  and  $\mathcal{L}_L$ .

Given a map that satisfies the weak star condition, we can define a weak simplicial approximation  $g$  by mapping each vertex  $v \in K^0$  to an element of  $\bigcap \mathcal{L}_L(f(v'))$ . In practice, we will choose such an element at random, leading to the consequence that two runs of the algorithm may give different outputs.

**3.1.3 Checking homotopy equivalence** As pointed out before, a weak simplicial approximation may not be homotopy equivalent to the initial map. This would have been the case in Figure 7 if we had chosen a homeomorphism  $|\partial\Delta^2| \rightarrow |\partial\Delta^2|$  that sent the three vertices of  $\partial\Delta^2$  on a single edge. Algorithm 1 would have returned a map  $g$  homotopic to a constant map. Therefore, a verification step must be used after running the algorithm. We present here two such ideas.

The first method consists in verifying that the weak simplicial approximation  $g: K \rightarrow L$  actually is a simplicial approximation to  $f: |K| \rightarrow |L|$ . This requires the knowledge of a Lipschitz constant  $\lambda$  for  $f$ , where we endowed the geometric complexes with the geodesic distance induced by the Euclidean metric. Let us choose  $\varepsilon > 0$  and suppose that, for any vertex  $v \in K^0$ , we have access to a subset  $\mathcal{N}_\varepsilon(v) \subset |\text{St}(v)|$  which is  $\varepsilon$ -dense, that is, such that any point  $x \in |\text{St}(v)|$  admits a point  $y \in \mathcal{N}_\varepsilon(v)$  at distance most  $\varepsilon$ . Now, we can check the following condition: for any vertex  $v \in K^0$  and any point  $x \in \mathcal{N}_\varepsilon(v)$ ,  $x$  is included in  $|\text{St}(g(v))|$  and at distance at least  $\frac{\varepsilon}{\lambda}$  from its boundary. It is clear that this condition implies that  $f(|\text{St}(v)|) \subseteq |\text{St}(g(v))|$ , hence that  $g$  is a simplicial approximation.

For the second method, we adopt an algebraic point of view. Let  $[|K|, |L|]$  denote the set of homotopy classes of maps from  $|K|$  to  $|L|$ . Note that when  $K$  is homeomorphic to the sphere  $\mathbb{S}^d$ , this set can be identified with the  $d^{\text{th}}$  homotopy group  $\pi_d(|L|)$ . Now, determining whether  $g$  and  $f$  are homotopy equivalent boils down to testing the equality of elements in  $[|K|, |L|]$ . Computing this set has been the subject of various works, such as [35] and references therein. All the proposed algorithms rely on various hypothesis about  $K$  and  $L$ , notably on the fact that the fundamental group  $\pi_1(|L|)$  is trivial (otherwise the problem is known to be undecidable). Unfortunately, as far as we know, these algorithms are not implemented and available to the user.

Using more accessible techniques, we can try to identify the homotopy classes at the level of homology groups. To start, let us suppose that both  $K$  and  $L$  are homeomorphic to the sphere  $\mathbb{S}^d$ . In this case, their  $d^{\text{th}}$  homology groups are  $\mathbb{Z}$ , and the Hopf theorem states that the set of homotopy classes  $[|K|, |L|]$  is in bijection with  $\mathbb{Z}$ . More precisely, to any map  $f: |K| \rightarrow |L|$  is associated its *degree*, the unique integer  $\deg(f)$  such that the induced morphism  $f_*: H_d(K) \rightarrow H_d(L)$  is equal to  $x \mapsto \deg(f) \cdot x$ . Two maps  $f, g$  are homotopy equivalent if and only if  $\deg(f) = \deg(g)$ . This gives another way of verifying that the maps are homotopy equivalent, provided that we know the degree of  $f$ , and that we are able to compute the degree of  $g$ . The problem of computing the degree as deserved some attention, as we can see in [37]. In these works, the usual hypotheses are a Lipschitz constant for the map, or an explicit algebraic expression. However, in our case,  $g$  is a simplicial map, and a simpler method can be proposed. Let us consider  $\text{Cone}^s(g)$ , the simplicial mapping cone of  $g$ , that we will define later in Subsection 4.1. It is a simplicial complex, homotopy equivalent to  $\text{Cone}(g)$ , the topological mapping cone. It comes with a long exact sequence:

$$\dots \longrightarrow H_k(K) \xrightarrow{g_*} H_k(L) \longrightarrow H_k(\text{Cone}^s(g)) \longrightarrow H_{k-1}(K) \longrightarrow \dots$$

Since  $H_{d+1}(K) = H_{d+1}(\mathbb{S}^d) = 0$ , we deduce that  $H_d(\text{Cone}^s(g))$  is isomorphic to the quotient  $H_k(L)/\text{Im}(g_*)$ , that is,  $\mathbb{Z}/\deg(g)\mathbb{Z}$ . Hence the degree of  $g$  can be read on the homology groups of  $\text{Cone}^s(g)$ : if  $H_d(\text{Cone}^s(g)) = \mathbb{Z}/a\mathbb{Z}$ , then  $\deg(g)$  is either  $a$  or  $-a$ . We can then determine the sign of  $\deg(g)$  by checking if  $g$  is orientation-preserving or orientation-reversing.

In general, when  $K$  and  $L$  are not spheres, it is not true anymore that the homotopy class of  $f$  only depends only on the morphism  $f_*$  between homology groups. An example is given

by the projective plane  $\mathbb{R}P^2$ , studied in Subsection 5.1. Let  $f: \mathbb{S}^2 \rightarrow \mathbb{R}P^2$  be the quotient map, and  $g: \mathbb{S}^2 \rightarrow \mathbb{R}P^2$  a constant map. They correspond to different classes in  $\pi_2(\mathbb{R}P^2) = \mathbb{Z}$ , hence are not homotopy equivalent. However, since  $H_2(\mathbb{R}P^2) = 0$ , both induced morphisms  $f_*$  and  $g_*$  are zero, and the mapping cones  $\text{Cone}(f)$  and  $\text{Cone}(g)$  have the same homology groups. In this case, more refined techniques might be used, as we plan to study in a future work. An idea would be to use spectral sequences, as presented in [47, Section 16].

In Section 5, we will give concrete examples of simplicial approximation. However, we will not put in practice the methods described above. Instead, we will simply compute the homology groups of  $\text{Cone}^s(g)$ , and verify that they correspond to the ones of  $\text{Cone}(f)$ , that we know in advance.

## 3.2 Subdivisions of the sphere

In this paper, we will mainly consider the problem of weak simplicial approximation to a map  $f: |K| \rightarrow |L|$  where  $K$  is triangulation of the sphere  $\mathbb{S}^d$ . We describe in this subsection how such triangulations are built.

**3.2.1 Triangulation of the sphere** Let  $d$  be a positive integer. The simplest simplicial complex homeomorphic to the  $d$ -sphere is  $\partial\Delta^{d+1}$ , the boundary of the  $(d+1)$ -simplex. We shall give it a geometric realization in  $\mathbb{R}^{d+1}$ . As described in Subsection 2.2,  $\Delta^{d+1}$  is endowed with a canonical geometric realization  $|\Delta^{d+1}| \subset \mathbb{R}^{d+2}$ , where its vertices are identified with the canonical basis of  $e_0, \dots, e_{d+1}$  of  $\mathbb{R}^{d+2}$ . Based on this embedding, we can embed  $\Delta^{d+1}$  in  $\mathbb{R}^{d+1}$  as follows: we project the vertices in the  $d+1$ -dimensional affine space they span, with origin their barycenter. The resulting points, once normalized, form a family  $x_0, \dots, x_{d+1}$  of regularly spaced points on  $\mathbb{S}^d \subset \mathbb{R}^{d+1}$ . A computation shows that these points are explicitly given by

$$\begin{cases} -(d+1)^{-\frac{3}{2}}(\sqrt{d+1}+1)(1, \dots, 1) + \sqrt{1+(d+1)^{-1}}e'_i & \text{for } i \in \llbracket 0, d \rrbracket, \\ -(d+1)^{-\frac{1}{2}}(1, \dots, 1) \end{cases} \quad (13)$$

where  $e'_0, \dots, e'_d$  denote the canonical basis of  $\mathbb{R}^{d+1}$ . The Euclidean distance between two of these vertices is  $\sqrt{2\frac{d+2}{d+1}}$ . Using these coordinates, we also get an embedding of  $\partial\Delta^{d+1}$  into  $\mathbb{R}^{d+1}$ .

Denote  $K = \partial\Delta^{d+1}$ . We now wish to define a homeomorphism  $\mathbb{S}^d \rightarrow |K|$ . There are two natural candidates: the *metric projection*  $p: \mathbb{S}^d \rightarrow |K|$ , for which  $p(x)$  is the point of  $|K|$  that minimizes the Euclidean distance  $\|x - p(x)\|$ , and the *radial projection*  $r: \mathbb{S}^d \rightarrow |K|$ , where  $r(x)$  is defined as the unique intersection point between  $|K|$  and the half-line spanned by  $x$  (see Figure 8). Since  $K$  is built on the points defined by Equation (13), both these maps are well-defined and are homeomorphisms.



Figure 8: The metric and the radial projections  $p, r: \mathbb{S}^1 \rightarrow K$

In the rest of the paper, we will use the radial projection only, since it turns out more convenient to work with, both in the proofs and the implementations. We will describe an implementation of  $\mathcal{L}_r$ , the location map of the radial projection, in §4.3.1.

**3.2.2 Iterated subdivisions** As explained in Subsection 2.3, if  $\text{sub}(K)$  is any subdivision of a geometric simplicial complex  $K$ , then it is naturally given a realization  $|\text{sub}(K)|$ , by seeing  $|\text{sub}(K)| = |K|$ . However, in practice, we will use a variation of this geometric realization: all the vertices of  $\text{sub}(K)$ , seen in  $\mathbb{R}^{d+1}$ , are normalized, so as to belong to  $\mathbb{S}^d$  (as in Figure 9). In this paragraph, let us denote  $|\text{sub}(K)|'$  this new geometric realization.

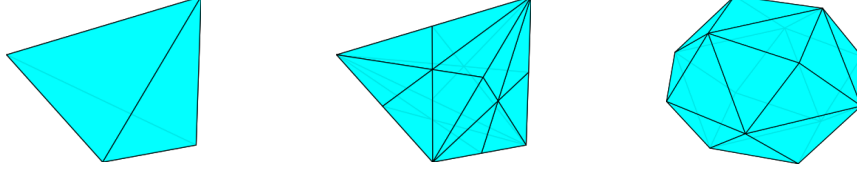


Figure 9: The geometric realizations  $|\partial\Delta^3|$ ,  $|\text{sub}(\partial\Delta^3)|$  and  $|\text{sub}(\partial\Delta^3)|'$ . We used a barycentric subdivision.

Consider a continuous map  $\mathbb{S}^d \rightarrow |L|$ , and define the composition  $f: |K| \rightarrow \mathbb{S}^d \rightarrow |L|$ , where the first map is the inverse radial projection. We wish to find a weak simplicial approximation to  $f$ . We choose a subdivision method, between barycentric or edgewise, and consider the sequence of subdivided complexes  $(K_i)_{i \geq 0}$  defined as  $K_0 = K$  and  $K_{i+1} = \text{sub}(K_i)$ . At each step, we endow  $K_{i+1}$  with the geometric realization  $|\text{sub}(K_i)|'$ . We point out that this normalization must be performed at each step, indeed, the normalization procedure and the subdivision do not commute. This construction leads to a variation of Algorithm 1:

---

**Algorithm 2** Weak simplicial approximation via global subdivisions and normalization

---

**Input:** a continuous map  $\mathbb{S}^d \rightarrow |L|$ , a triangulation  $|K| \rightarrow \mathbb{S}^d$

**Output:** a weak simplicial approximation  $g$  to  $f: |K| \rightarrow |L|$

- 1: **while**  $f: |K| \rightarrow |L|$  does not satisfy the star condition **do**
  - 2:   let  $K$  be  $\text{sub}(K)$
  - 3:   normalize the vertices of  $K$
  - 4: **end while**
  - 5: let  $g$  be a weak simplicial approximation to  $f$
  - 6: **return**  $g$
- 

In practice, and as we will illustrate in Example 3.5, we observed better performances of the algorithm by normalizing the vertices of  $\text{sub}(K)$ . Let us consider the problem of termination of Algorithm 2. Contrary to Algorithm 1, it does not directly follow from the simplicial approximation theorem. In order to track the evolution of the diameter of the simplices of  $(K_i)_{i \geq 0}$  in the algorithm, it is convenient to work with the *geodesic distance*  $d_{\mathbb{S}^d}(\cdot, \cdot)$  on the sphere. We remind the reader that, for two points  $u, v \in \mathbb{S}^d$ , their Euclidean and geodesic distance are related by  $d_{\mathbb{S}^d}(u, v) = 2 \arcsin\left(\frac{\|x-y\|}{2}\right)$ . Now, let us consider the maximal geodesic edge length of  $K_i$ :

$$\delta_{\mathbb{S}^d}(K_i) = \sup \{d_{\mathbb{S}^d}(u, v) \mid [u, v] \in K_i\}.$$

As in the proof of the simplicial approximation theorem, there exists an  $\varepsilon > 0$  such that the map  $f: |K_i| \rightarrow |L|$  satisfies the star condition when  $\delta_{\mathbb{S}^d}(K_i) < \varepsilon$ . Hence, proving the termination of Algorithm 2 boils down to showing that  $\delta_{\mathbb{S}^d}(K_i)$  goes to zero with  $i$ .

However, in this case, the usual bounds on the diameter of the subdivided simplices, in Equations (6) and (9), do not hold anymore. The problem comes from the curvature of the sphere, which tends to enlarge small distances, and reduce large distances, as shown in the following figure.



Figure 10: Left: the edgewise subdivision of a 2-simplex in the plane reduces the edge lengths by half. Right: it is not true anymore for a triangle on the sphere.

Nonetheless, we will show that these bounds are still valid, up to a small error. The first step consists bounding the distance between a simplex and its radial projection on the sphere.

**Lemma 3.3.** *Consider a  $d$ -simplex  $\sigma$  with vertices included in  $\mathbb{S}^d$ , and suppose that its (Euclidean) diameter  $\delta$  is upper bounded by  $\sqrt{2\frac{d+1}{d}}$ . Then, for any  $x \in |\sigma|$ , we have  $\|x - \frac{x}{\|x\|}\| \leq \ell(\delta)$  where*

$$\ell(\delta) = 1 - \sqrt{1 - \frac{1}{2} \frac{d}{d+1} \delta^2}.$$

Remark that, for  $\delta$  close to 0, we have the equivalent  $\ell(\delta) \sim \frac{1}{4} \frac{d}{d+1} \delta^2$ , and for all  $\delta \leq \sqrt{2\frac{d+1}{d}}$ , we have  $\ell(\delta) \leq \frac{1}{2} \frac{d}{d+1} \delta^2$ .

*Proof.* Let us consider the minimal enclosing ball of  $\sigma$  in  $\mathbb{R}^{d+1}$ , that is, the closed ball of minimal radius that contains all its vertices. Let  $x_*$  be its center and  $r$  its radius. By Jung's theorem, we have  $r \leq \delta \sqrt{\frac{1}{2} \frac{d}{d+1}}$ . Moreover,  $x_*$  belongs to the convex hull  $|\sigma|$ : it is either the circumcenter of its vertices  $\sigma^0$ , or of a subset of it.

Next, consider the intersection of  $\mathbb{S}^d$  with the ball of center  $x_*$  and radius  $r$ , denoted  $\mathcal{D}$ , and the intersection with the corresponding sphere, denoted  $\mathcal{C}$ . The set  $\mathcal{D}$  is a ‘dome’ of base  $\mathcal{C}$ . By definition of the minimal enclosing ball, the vertices of  $\sigma$  are included in  $\mathcal{D}$ . Moreover,  $\mathcal{C}$  is a  $(d-1)$ -sphere of radius  $r$ . Now, for any  $x$  in the convex hull  $|\sigma|$ , we can find two points  $y, y' \in \mathbb{S}^d$  such that  $\|z - z'\| \leq 2r$ . They are obtained by cutting  $\mathcal{D}$  along the affine hyperplane orthogonal to  $[0, x_*]$  and passing through  $x$ . The situation is represented in the following figure.

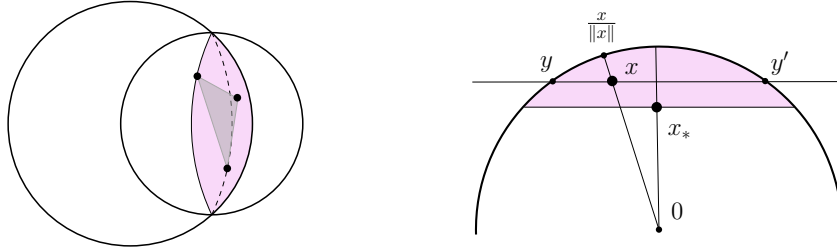


Figure 11: Left: the dome  $\mathcal{D}$ , in pink, contains the vertices of  $\sigma$ . Right: the point  $x$  lies on the segment  $[y, y']$ .

Now we can bound the norm  $\|x - \frac{x}{\|x\|}\|$ . We see that this quantity is maximal when  $x$  is the midpoint of  $[y, y']$ . Using the Pythagorean theorem, we get that  $\|x\| \leq \sqrt{1 - r^2}$ . We deduce that  $\|x - \frac{x}{\|x\|}\| \leq 1 - \sqrt{1 - r^2}$ , and the bound on  $r$  yields the result.  $\square$

This lemma can be used as follows: let  $\text{sub}(\sigma)$  be any subdivision of  $\sigma$ ,  $|\text{sub}(\sigma)|$  its geometric realization, where the vertices are not normalized and  $|\text{sub}(\sigma)|'$  where they are. If  $[x, y]$  is an edge of  $|\text{sub}(\sigma)|$ , then the corresponding edge  $[\frac{x}{\|x\|}, \frac{y}{\|y\|}]$  of  $|\text{sub}(\sigma)|'$  has length upper



bounded by:

$$\begin{aligned} \left\| \frac{x}{\|x\|} - \frac{y}{\|y\|} \right\| &\leq \|x - y\| + \left\| x - \frac{x}{\|x\|} \right\| + \left\| y - \frac{y}{\|y\|} \right\| \\ &\leq \|x - y\| + 2\ell(\delta). \end{aligned} \quad (14)$$

In other words, any bound on the length of the edges of  $|\text{sub}(\sigma)|$  also holds on  $|\text{sub}(\sigma)|'$ , up to the quadratic error  $2\ell(\delta)$ . We can deduce the following:

**Proposition 3.4.** *Consider a geometric simplicial complex  $K$  with  $|K^0| \subset \mathbb{S}^d$  and such that  $K$  is homeomorphic to  $\mathbb{S}^d$  via the radial projection map. Denote by  $\delta$  the maximal (Euclidean) edge length of  $K$ . Also, consider a continuous map  $\mathbb{S}^d \rightarrow |L|$ , and define the composition  $f: |K| \rightarrow |L|$ . With barycentric subdivisions, Algorithm 2 terminates, provided that  $\delta^{-1}\ell(\delta) < \frac{1}{2(d+1)}$ . With edgewise subdivisions, the algorithm terminates, provided that  $\delta^{-1}\ell(\delta) < \frac{1}{4} \left( \frac{\log(d)}{2\log(2)} + 1 \right)^{-1}$ .*

Using the upper bound  $\ell(\delta) \leq \frac{1}{2} \frac{d}{d+1} \delta^2$ , we see that the first condition is implied by  $\delta \leq \frac{1}{d}$ , and the second one by  $\delta \leq \frac{1}{2} \frac{d+1}{d} \left( \frac{\log(d)}{2\log(2)} + 1 \right)^{-1}$ , or more simply  $\delta \leq \frac{1}{\log(d)}$ .

*Proof.* In both cases, and as in the proof of the simplicial approximation theorem, it is enough to show that, in the sequence of simplicial complexes  $(\text{sub}^i(K))_{i \geq 0}$ , the maximal geodesic length  $\delta_{\mathbb{S}^d}(\text{sub}^i(K))$  goes to zero. Equivalently, we have to show that the Euclidean length  $\delta(\text{sub}^i(K))$  goes to zero.

Starting with barycentric subdivision, we have seen in Equation (6) that it reduces the length of the edges by a factor  $\frac{d}{d+1}$ . After normalization, and as shown by Equation (14),  $\text{sub}(K)$  is made of edges of length lower than  $\frac{d}{d+1} \delta + 2\ell(\delta)$ . Now, the assumption on  $\delta$  gives that  $2\ell(\delta) < \frac{1}{d+1} \delta$ , and we deduce that  $\delta(\text{sub}(K)) < \alpha \delta$  with  $\alpha < 1$ . Repeating this process, it is clear that  $\delta(\text{sub}^i(K))$  goes to zero.

With edgewise subdivisions, we have to proceed a bit differently. As shown in Equation (9), we start to have a bound  $\delta(\text{sub}^i(K)) \leq \frac{1}{2} \delta$  when  $i$  is such that  $\frac{\sqrt{d}}{2^i} \leq \frac{1}{2}$ , i.e., when  $i \geq \frac{\log(d)}{2\log(2)} + 1$ . However, the geometric simplicial complex  $\text{sub}^i(K)$  given by the algorithm is not the one used in Equation (9): in the algorithm, each subdivided complex has its vertices renormalized. According to Lemma 3.3, at each step, the vertices are perturbed by a distance at most  $\ell(\delta)$ . Consequently, the vertices of  $\text{sub}^i(K)$  are perturbed by a distance at most  $i\ell(\delta)$ , hence its edge lengths by at most  $2i\ell(\delta)$ . We deduce that  $\delta(\text{sub}^i(K)) < \frac{1}{2} \delta + 2i\ell(\delta)$ . According to the assumption on  $\delta$ , we have  $2i\ell(\delta) < \frac{1}{2} \delta$ , hence  $\delta(\text{sub}^i(K)) < \alpha \delta$  with  $\alpha < 1$ . By repeating this process  $n$  times, we have that  $\delta(\text{sub}^{ni}(K)) \leq \alpha^n \delta(K)$ . As a consequence,  $(\delta(\text{sub}^j(K)))_{j \geq 0}$  goes to zero.  $\square$

The previous proposition justifies the use of Algorithm 2, as long as the initial complex is made of sufficiently small simplices. Moreover, and as shown in the following example, it may perform better than Algorithm 1. In addition to these facts, our choice of using the normalization step is motivated by the two following reasons: it yields more readable figures, and it will be more convenient to define a triangulation of the ball  $\overline{\mathcal{B}}^{d+1}$  in §4.3.3.

**Example 3.5.** In order to compare Algorithms 1 and 2, let us consider the identity map  $|\partial \Delta^3| \rightarrow |L|$  where  $L$  is an arbitrary triangulation of the sphere on ten vertices, represented in Figure 12. By applying Algorithm 1, we have to subdivide five times, both for barycentric and edgewise subdivisions. The resulting complexes have 15'554 and 2050 vertices. In comparison, by applying Algorithm 2, we have to subdivide four times only. The resulting complexes have 2594 and 514 vertices. As we can see on the figure, the normalization step allows to obtain simplicial complexes whose simplices, seen on the sphere, seem more uniform.

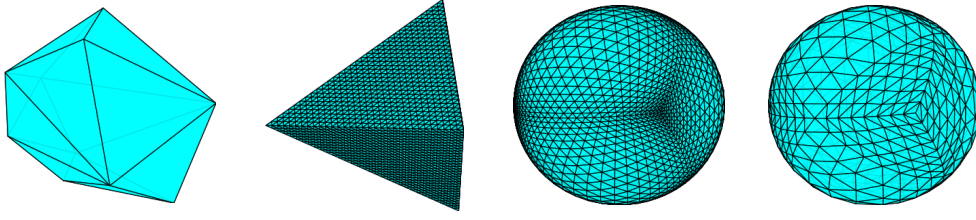


Figure 12: The complex  $L$ , the output of Algorithm 1, the same complex with vertices normalized, and the output of Algorithm 2. We used edgewise subdivisions.

**3.2.3 Delaunay triangulations** Until here, we obtained triangulations of the sphere  $\mathbb{S}^d$  by embedding  $\partial\Delta^{d+1}$  into  $\mathbb{R}^{d+1}$ , and then performing subdivisions. We shall now present another solution. First, we recall the notion of Delaunay complex in the Euclidean space. We refer the reader to [11] for further explanations. Let  $X \subset \mathbb{R}^n$  be a finite subset. We say that a subset of  $n+1$  points of  $X$  has the *empty circle property* if it has a circumscribing (open) ball empty of points of  $X$ . The collection of such subsets form the maximal simplices of a simplicial complex called the *Delaunay complex*, denoted  $\text{Del}(X)$ . In general,  $\text{Del}(X)$  is not embeddable in  $\mathbb{R}^n$ . However, under the following genericity assumption, it is true that the vertex set  $X \subset \mathbb{R}^n$  induces a natural embedding of  $\text{Del}(X)$ : no subset of  $n+2$  points of  $X$  lie on the same sphere.

Secondly, we can adapt these definitions to obtain the notion of *Delaunay complex on the sphere*: the set  $X$  is now a subset of  $\mathbb{S}^d \subset \mathbb{R}^{d+1}$ , and the empty circle property is to be understood with respect to the geodesic distance on  $\mathbb{S}^d$  [60, 18]. We shall also denote the corresponding Delaunay complex  $\text{Del}(X)$ . Under the assumption that no subset of  $d+2$  points lie on the same geodesic sphere,  $\text{Del}(X)$  is naturally embedded in  $\mathbb{R}^{d+1}$ . In the remaining of the paper, we shall implicitly make this assumption.

Equivalently, the complex  $\text{Del}(X)$  can be defined as the boundary of the convex hull of  $X$  [15, 63]. We will use this definition to compute the complex in practice, using the package Qhull [6].

Using these notions, we are now able to define triangulations of the sphere by considering a subset  $X \subset \mathbb{S}^d$  and computing the corresponding complex  $\text{Del}(X)$ . The radial projection map  $r: \mathbb{S}^d \rightarrow |\text{Del}(X)|$ , defined in §3.2.1, is well-defined when the origin is included in the convex hull of  $X$ . Consequently, in this case,  $\text{Del}(X)$  is a triangulation of the sphere. This condition is satisfied for the points defined in Equation (13). In what follows, we will always make sure to build Delaunay complexes on sets  $X$  that contain these points.

**3.2.4 Delaunay subdivisions** We now propose a sort of subdivision process adapted to Delaunay complexes. Let  $\text{Del}(X)$  be the Delaunay complex on a subset of the sphere  $\mathbb{S}^d$ . Let  $X'$  be the set of vertices of the barycentric subdivision of  $\text{Del}(X)$ , with the vertices normalized, so as to make them belong to  $\mathbb{S}^d$ . We call *Delaunay barycentric subdivision* the Delaunay complex  $\text{Del}(X')$  built on  $X'$ . Similarly, if  $X'$  denotes the set of vertices of the edgewise subdivision of  $\text{Del}(X)$ , the corresponding Delaunay complex  $\text{Del}(X')$  is called the *Delaunay edgewise subdivision*. As for usual subdivisions, the subdivided complexes will be denoted  $\text{sub}(K)$ , and iterated subdivisions  $\text{sub}^i(K)$ .

It is worth noting that, strictly speaking,  $\text{Del}(X')$  is not a subdivision of  $\text{Del}(X)$ , in the sense that each simplex  $|\sigma|$  of  $\text{Del}(X')$  would be included in a simplex  $|\nu|$  of  $\text{Del}(X)$ . Indeed, adding points to a Delaunay complex may change its combinatorial structure, as shown in the following figure.

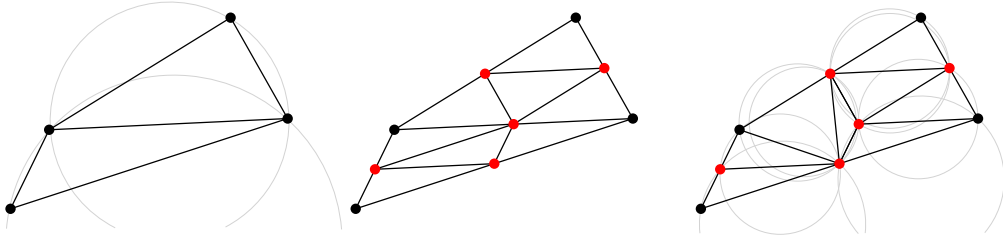


Figure 13: Left: the Delaunay complex  $\text{Del}(X)$  on a set of four points. Middle: its edgewise subdivision. Right: its Delaunay edgewise subdivision. The new vertices are represented in red.

Algorithm 2 directly adapts to Delaunay subdivisions: starting with a continuous map  $\mathbb{S}^d \rightarrow |L|$  and  $K = \text{Del}(X)$  is a Delaunay complex, we can consider the sequence of Delaunay subdivisions  $(\text{sub}^i(K))_{i \geq 0}$ , until the map satisfies  $f: |K| \rightarrow |L|$  the weak star condition. However, and as illustrated in Figure 13, it is not clear that repeated subdivisions decrease the diameter of the simplices of  $\text{Del}(X)$ , and that Algorithm 2 terminates. In fact, we are only able to prove it for the Delaunay barycentric subdivisions up to dimension three, and for the Delaunay edgewise subdivisions up to dimension two. To prove so, we first we state a result that allows to control the diameter of the simplices of  $\text{Del}(X)$  based on the *density* of  $X$ . In what follow, we say that  $X$  is  $\varepsilon$ -dense in  $\mathbb{S}^d$  if for any point  $x \in \mathbb{S}^d$ , there exists a point  $v \in X$  such that  $d_{\mathbb{S}^d}(x, v) \leq \varepsilon$ .

**Lemma 3.6.** *If  $X$  is  $\varepsilon$ -dense in  $\mathbb{S}^d$ , then  $\text{Del}(X)$  is made of edges of geodesic length at most  $2\varepsilon$ .*

*Proof.* Let  $\sigma$  be a  $d$ -simplex of  $\text{Del}(X)$ , and denote by  $r$  the radius of its circumscribing ball. Using the empty circle property and the density of  $X$ , we deduce that  $r \leq \varepsilon$ . Consequently,  $\sigma$  has diameter bounded above by  $2\varepsilon$ .  $\square$

**Proposition 3.7.** *Consider a subset  $X \subset \mathbb{S}^d$  such that  $K = \text{Del}(X)$  is homeomorphic to  $\mathbb{S}^d$  via the radial projection map, and denote by  $\delta$  the maximal (Euclidean) edge length of  $K$ . Also, consider a continuous map  $\mathbb{S}^d \rightarrow |L|$ , and define the composition  $f: |K| \rightarrow |L|$ . With Delaunay barycentric subdivisions, Algorithm 2 terminates, provided that  $d \leq 3$  and  $\delta^{-1} \ell(\delta) \leq \frac{1}{4}(1 - \sqrt{2}(\frac{d}{d+1})^{\frac{3}{2}})$ . With Delaunay edgewise subdivisions, the algorithm terminates, provided that  $d \leq 2$  and  $\delta \leq \frac{1}{2}$ .*

Using the bound  $\ell(\delta) \leq \frac{1}{2} \frac{d}{d+1} \delta^2$ , we see that the first condition is valid when  $\delta \leq \frac{1}{2} \frac{d+1}{d} (1 - \sqrt{2}(\frac{d}{d+1})^{\frac{3}{2}})$ . For  $d = 1, 2$  and  $3$ , this upper bound is approximately  $0.5, 0.2$  and  $0.05$ . For  $d = 4$ , it becomes negative, and our proof does not work anymore.

*Proof.* We start with the barycentric subdivisions. As in the proof of Proposition 3.4, we will show that the iterated Delaunay subdivisions reduce the diameter of the simplices. Consider the barycentric subdivision (non-Delaunay) of  $K$ , denoted  $K_*$ , its vertex set  $X_*$ , and  $X'$  this set of vertices normalized. Consequently, the Delaunay barycentric subdivision  $\text{sub}(\text{Del}(X))$  can be written  $\text{Del}(X')$ . Let us denote  $\delta_{\mathbb{S}^d}$  the maximal edge length of  $K$  with respect to the geodesic distance. The first step consists in showing that  $X'$  is sufficiently dense in  $\mathbb{S}^d$ .

Let  $x \in \mathbb{S}^d$ . Since the radial projection  $r: \mathbb{S}^d \rightarrow K_*$  is a homeomorphism, there exists a simplex  $\sigma$  of  $K_*$  such that  $x$  belongs to  $r^{-1}(|\sigma|)$ . Let us denote  $r(x)$  the radial projection of  $x$ , which belongs to  $|\sigma|$ . According to Equation (6),  $\sigma$  is made of edges of length at most  $\frac{d}{d+1} \delta$ . Consider the minimal enclosing ball of its vertices. By Jung's theorem, its radius is at most  $\sqrt{\frac{1}{2} \frac{d}{d+1} \frac{d}{d+1}} \delta$ . Hence, using Lemma 3.8 stated below, we deduce that there exists a vertex  $z \in \sigma^0$  such that

$$\|r(x) - z\| \leq \sqrt{\frac{1}{2} \frac{d}{d+1} \frac{d}{d+1}} \delta = \frac{1}{\sqrt{2}} \left( \frac{d}{d+1} \right)^{3/2} \delta.$$

Projecting  $z$  and  $r(x)$  onto the sphere, and using Equation (14), we obtain

$$\|x - r^{-1}(z)\| \leq \frac{1}{\sqrt{2}} \left( \frac{d}{d+1} \right)^{3/2} \delta + 2\ell(\delta).$$

According to the assumption on  $\delta^{-1}\ell(\delta)$ , we deduce  $\|x - r^{-1}(z)\| \leq \frac{1}{2}\alpha\delta$  with  $\alpha < 1$ .

Now, let  $h: x \mapsto 2\arcsin\left(\frac{x}{2}\right)$  be the map that converts Euclidean into geodesic distance. We have  $d_{\mathbb{S}^d}(x, r^{-1}(z)) = h(\|x - r^{-1}(z)\|)$ . Moreover, since  $h$  is convex and increasing on  $[0, 2]$ , we have

$$d_{\mathbb{S}^d}(x, r^{-1}(z)) \leq h\left(\frac{1}{2}\alpha\delta\right) \leq \frac{1}{2}\alpha h(\delta) \leq \frac{1}{2}\alpha\delta_{\mathbb{S}^d}.$$

That is, we found a vertex of  $X'$  at geodesic distance at most  $\frac{1}{2}\alpha\delta_{\mathbb{S}^d}$  from  $x$ . This being true for any  $x \in \mathbb{S}^d$ , we deduce that  $X'$  is  $(\frac{1}{2}\alpha\delta_{\mathbb{S}^d})$ -dense in  $\mathbb{S}^d$ . Hence, by Lemma 3.6,  $\text{Del}(X')$  is made of edges with geodesic lengths at most  $\alpha\delta_{\mathbb{S}^d}$ . In other words, the simplices have been reduced by a factor  $\alpha < 1$ . By repeating this process, we obtain iterated Delaunay subdivisions whose simplices can be made arbitrarily small. The result follows.

This proof also holds for Delaunay edgewise subdivisions, if we replace Equation (6) by (8). When  $d \leq 2$ , the simplices of the edgewise subdivision  $K_*$  are reduced by half, hence we obtain the same result as barycentric subdivisions for  $d = 1$ .  $\square$

We now state the lemma used in the proof.

**Lemma 3.8.** *Let  $\sigma$  be a simplex embedded in  $\mathbb{R}^n$ , and  $r$  the radius of its minimal enclosing ball. For any point  $x \in |\sigma|$ , there exists a vertex  $z$  of  $\sigma$  such that  $\|x - z\| \leq r$ .*

*Proof.* Let  $\overline{\mathcal{B}}(x, r)$  denote the closed ball of center  $x$  and radius  $r$  of  $\mathbb{R}^n$ . By contradiction, we suppose that  $\overline{\mathcal{B}}(x, r)$  is empty of vertices of  $\sigma$ , that is,  $\overline{\mathcal{B}}(x, r) \cap |\sigma^0| = \emptyset$ . Let  $y$  be the center of the minimal enclosing ball of  $\sigma$ . By definition, we have  $|\sigma^0| \subset \overline{\mathcal{B}}(y, r)$ . Now, consider the perpendicular bisector to the segment  $[x, y]$ . It is a hyperplane, that cuts  $\mathbb{R}^n$  into two closed half-spaces,  $H_x$  which contains  $x$  and  $H_y$  which contains  $y$ . Similarly,  $\overline{\mathcal{B}}(y, r)$  is cut into  $\overline{\mathcal{B}}(y, r) \cap H_x$  and  $\overline{\mathcal{B}}(y, r) \cap H_y$ . Since points in  $H_x$  are closer to  $x$  than  $y$ , we have  $\overline{\mathcal{B}}(y, r) \cap H_x \subset \overline{\mathcal{B}}(x, r)$ . Besides, using that  $\overline{\mathcal{B}}(x, r)$  is empty of vertices of  $\sigma$ , we deduce  $\overline{\mathcal{B}}(y, r) \cap H_x \cap |\sigma^0| = \emptyset$ . In other words, all the vertices of  $\sigma$  belong to  $H_y$ . Consequently,  $|\sigma| \subset H_y$ , hence  $x$  cannot belong to the convex hull of  $\sigma$ .  $\square$

**Example 3.9.** As an experimental study, let us compare, on a practical case of approximation, the four subdivisions we encountered so far. The map  $f: |K| \rightarrow |L|$  will be the identity map between two triangulations of the sphere:  $K$  is the boundary of the 3-simplex  $\partial\Delta^3$ , and  $L$  its barycentric subdivision  $\text{sub}^n(\partial\Delta^3)$  for  $n = 0, 1, 2$  and 3. We apply subdivisions until obtaining a weak simplicial approximation, with (1) barycentric subdivisions, (2) edgewise subdivisions, (3) Delaunay barycentric subdivisions and (4) Delaunay edgewise subdivisions. We gather in the following table the number of subdivisions needed, as well as the number of vertices of the subdivided complex. We also represent in Figure 14 the resulting simplicial complexes for  $L = \text{sub}^1(\partial\Delta^3)$ .

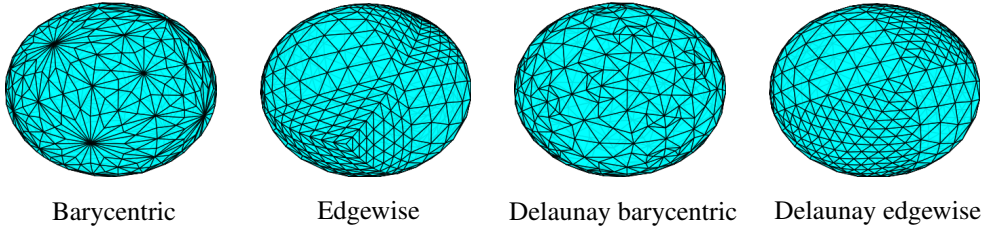


Figure 14: Resulting complexes after applying the subdivision process to the identity map  $|\partial\Delta^3| \rightarrow |\text{sub}^1(\partial\Delta^3)|$ .

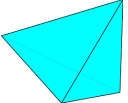
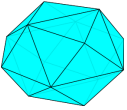
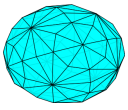
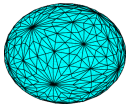
				
	$\partial\Delta^3$	$\text{sub}^1(\partial\Delta^3)$	$\text{sub}^2(\partial\Delta^3)$	$\text{sub}^3(\partial\Delta^3)$
Barycentric	2 (74)	3 (434)	4 (2'594)	5 (15'554)
Edgewise	2 (34)	4 (514)	5 (2'050)	7 (32'770)
Delaunay barycentric	2 (74)	3 (434)	5 (15'554)	6 (93'314)
Delaunay edgewise	2 (34)	4 (514)	5 (2'050)	7 (32'770)

Table 1: Number of subdivisions needed to obtain a weak simplicial approximation to the identity map  $|\partial\Delta^3| \rightarrow |\text{sub}^n(\partial\Delta^3)|$ . We indicate in parenthesis the final number of vertices.

### 3.3 Generalized subdivisions

Consider a map  $f: |K| \rightarrow |L|$  to which we wish to find a weak simplicial approximation. As we have seen with Algorithms 1 and 2, the problem is solved by subdividing  $K$  sufficiently many times, where the subdivisions can be barycentric, edgewise, Delaunay barycentric or Delaunay edgewise. However, from a computational point of view, iterated subdivisions are time-consuming, and potentially redundant: in the process, we may subdivide simplices that already satisfy the weak star condition. We will present in this subsection a way to improve these subdivisions.

**3.3.1 Generalized subdivisions** Let  $K$  be a geometric simplicial complex and  $K' \subset K$  a simplicial subcomplex. Following [56, Chapter 16], we define the *generalized barycentric subdivision of  $K$  holding  $K'$  fixed* iteratively as follows. Let  $J^0$  be the vertex set  $K^0$ . From  $J^i$ , define  $J^{i+1}$  as the simplicial complex of dimension  $i+1$  containing:

- all the simplices of  $J^i$ ,
- all the  $(i+1)$ -simplices of  $K'$ ,
- the cones  $\hat{\sigma} * \partial\sigma$  for any  $(i+1)$ -simplex  $\sigma$  of  $K \setminus K'$ .

In the notation  $\hat{\sigma} * \partial\sigma$ ,  $\hat{\sigma}$  is understood as a new vertex, the barycenter of  $\sigma$ , and  $\partial\sigma$  is defined as the subcomplex  $\{\eta \in J^i \mid |\eta| \subset \overline{|\sigma|}\}$ . The cone  $\hat{\sigma} * \partial\sigma$  is then defined as the set of simplices  $\{\hat{\sigma}\} \cup \eta$  for  $\eta \in \partial\sigma$ . At the end of this process, we obtain the simplicial complex  $J^{\dim(K)}$ , the generalized barycentric subdivision of  $K$ , that we denote  $\text{sub}(K; K')$ . An illustration is given in Figure 16.

This definition can be adapted to obtain the notion of *generalized edgewise subdivisions*: we start with the fixed complex  $K'$ , then we add all the vertices of  $K \setminus K'$  as well as the midpoint of its edges, and we complete the triangulation of  $K \setminus K'$ . However, in this case, the construction is not canonical: there are two way of triangulating the 2-simplex when adding the midpoints of two edges.



Figure 15: With edgewise subdivisions, one can subdivide the 2-simplex, holding an edge fixed, in two ways.

Choosing such a subdivision of the simplex  $\sigma$  among the various possibilities will be called a *reparation* of  $\sigma$ . It is equivalent to endow  $\sigma$  with a total order of its vertices, and to refer to a list of arbitrary choices, such as the one in Appendix B. Therefore, from now on, we will suppose that  $K$  is endowed with a total order of its vertices. We define a sequence of simplicial

complexes, starting with  $J^0 = K^0$ , to which we add a new vertex  $\hat{\sigma}$  for each edge  $\sigma$  in  $K \setminus K'$ . Then, we define  $J^{i+1}$  from  $J^i$  as the simplicial complex containing:

- all the simplices of  $J^i$ ,
- all the  $(i+1)$ -simplices of  $K'$ ,
- for each  $(i+1)$ -simplex  $\sigma$  of  $K \setminus K'$ , we repair  $\sigma$  by adding a collection of simplices whose union is  $|\sigma|$ .

The last complex,  $J^{\dim(K)}$ , is called the generalized edgewise subdivision of  $K$  holding  $K'$  fixed, and is denoted  $\text{sub}(K; K')$ . An illustration is given in the following figure.

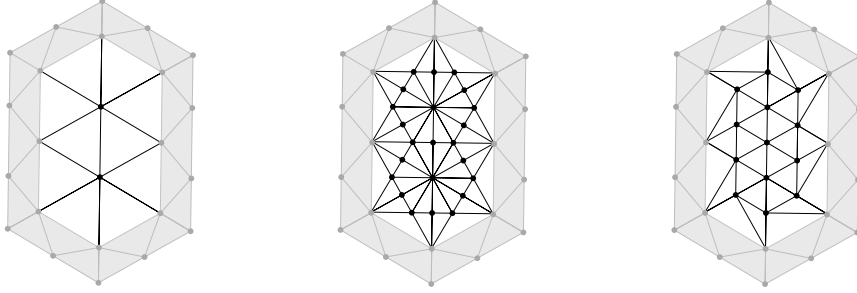


Figure 16: Left: a simplicial complex  $K$  and a subcomplex  $K'$  in grey. Middle: the generalized barycentric subdivision  $\text{sub}(K; K')$ . Right: the generalized edgewise subdivision  $\text{sub}(K; K')$ .

**3.3.2 Application to weak simplicial approximation** In order to see how these generalized subdivisions fit into the problem of simplicial approximation, let us consider a continuous map  $f: |K| \rightarrow |L|$ . Define the set

$$K' = \{\sigma \in K \mid f \text{ satisfies the weak star condition on each vertex of } \sigma\}, \quad (15)$$

where we remind the reader that the weak star condition has been defined in Equation (10). The set  $K'$  is a simplicial subcomplex of  $K$ . Equivalently,  $K'$  can be defined as the complement

$$K' = K \setminus \bigcup_{v \in V} \text{St}(v), \quad (16)$$

where  $V$  is the set of vertices of  $K$  where  $f$  does not satisfy the star condition. The generalized subdivision of  $K$  holding  $K'$  fixed,  $\text{sub}(K; K')$ , has the effect of keeping the simplices of  $K'$  intact, and of reducing the diameter of the stars of vertices in  $V$ . As an illustration, Figure 16 above represents the complex  $\text{sub}(K; K')$  where  $V$  consists of the two vertices at the center.

More precisely, the simplices of  $\text{sub}(K; K') \setminus K'$  fall into two groups: the simplices  $\sigma$  such that  $\sigma \cap V \neq \emptyset$ , that we call *globally subdivided*, and the others, *semi-subdivided*. The diameter of the globally subdivided simplices follows the bounds of Equations (6) and (9), but this does not hold in general for the semi-subdivided ones.

These considerations lead naturally to the following procedure: we build the sequence of simplicial complexes  $(K_i)_{i \geq 0}$  defined by  $K_0 = K$  and  $K_{i+1} = \text{sub}(K_i; K'_i)$  for all  $i \geq 0$ . Written as an algorithm, it reads:

---

**Algorithm 3** Simplicial approximation via generalized subdivisions

---

**Input:** a continuous map  $f: |K| \rightarrow |L|$   
**Output:** a weak simplicial approximation  $g$  to  $f$   
1: **while**  $f: |K| \rightarrow |L|$  does not satisfy the star condition **do**  
2:   let  $K'$  be defined as in Equation (15)  
3:   let  $K$  be  $\text{sub}(K; K')$   
4:   (normalize the vertices of  $K$ )  
5: **end while**  
6: let  $g$  be a weak simplicial approximation to  $f$   
7: **return**  $g$

---

This algorithm can be seen as a variation of Algorithm 1. Moreover, if  $f$  comes from a map  $\mathbb{S}^d \rightarrow |L|$ , we can also choose to normalize the new vertices of  $K$  at each step, giving a variation of Algorithm 2. In practice, and as illustrated in Example 3.12, we observed that Algorithm 3 performs significantly better than Algorithms 1 and 2, in the sense that it leads to simplicial complexes with fewer vertices.

However, this algorithm does not terminate in general. We give in Example 3.11 a configuration where the map  $f: |K_i| \rightarrow |L|$  never satisfies the weak star condition. This example uses edgewise subdivisions, but a similar case can be built for barycentric subdivisions. If the user observe that the algorithm does not seem to terminate, they would have to stop it, and run Algorithm 1 or 2 instead, for which we have proven that they terminate (Propositions 3.1, 3.4 and 3.7). We do not know if Algorithm 3 can be modified so as to ensure its termination. To this end, a natural idea would be to modify Equation (16) and define the fixed simplicial complex as

$$K' = K \setminus \bigcup_{v \in V} \text{St}^2(v), \quad (17)$$

where the double star  $\text{St}^2(v)$  of a vertex is defined as the union of the stars of its neighbors, itself included. Even so, one can design a variation of Example 3.11 to show that the algorithm would not terminate in general.

Surprisingly, in the applications we propose in Section 5, we always observed that Algorithm 3 terminates. In other words, these examples correspond to configurations on which the algorithm terminates. The following lemma is a result towards understanding such configurations.

**Proposition 3.10.** *Endow  $|K|$  and  $|L|$  with the geodesic distance induced by the Euclidean metric. Suppose that the map  $f: |K| \rightarrow |L|$  is convex, in the sense that the preimage of a geodesically convex set is a geodesically convex set. Then Algorithm 3 terminates, where the subdivisions can be barycentric or edgewise.*

*Proof.* Let us denote  $(K_i)_{i \geq 0}$  the sequence of simplicial complexes built by the algorithm and, for all  $i \geq 0$ ,  $V_i$  the set of vertices of  $K_i$  on which  $f$  does not satisfy the weak star condition. Consider also the cover  $\mathcal{V} = \{f^{-1}(|\text{St}(x)|) \mid x \in L^0\}$  of  $|K|$ . In order to clarify the proof, let us denote  $\text{St}_{K_i}(v)$  and  $\overline{\text{St}}_{K_i}(v)$  the open and closed stars in  $K_i$  of a vertex  $v$ , and  $f_i: |K_i| \rightarrow |L|$  the map  $f$  seen with domain  $|K_i|$ . With these notations,  $V_i$  can be described as the set of vertices  $v \in K_i^0$  such that the set  $|\overline{\text{St}}_{K_i}(v)|^0$  is not included in a member of  $\mathcal{V}$ . Since the map  $f$  is convex, and since the complexes are obtained by subdivision, one deduces the following *hereditary property*: if  $f_i$  satisfies the weak star condition at a vertex  $v$  of  $K_i$ , then so does  $f_j$  for every  $j > i$  and at every vertex  $w$  of  $K_j$  such that  $w \in |\text{St}_{K_i}(v)|$ .

We shall now proceed by contradiction. Suppose that the algorithm does not terminate. We will build a sequence of vertices  $(x_i)_{i \geq 0}$  with  $x_i \in V_i$ , and such that any simplex  $\sigma \in \text{St}_{K_{i+1}}(x_{i+1})$  is globally subdivided. As a consequence, the diameter of  $\text{St}_{K_i}(x_i)$  goes to zero, hence  $f_i$  satisfies the weak star condition at  $x_i$  at some point, which is absurd.

In order to build this sequence, we will use the sets  $W_i = \bigcup_{j \geq i} V_j$ , which are infinite by assumption. First, consider the cover of  $K$  by its open stars. By compactness of  $K$ , at least one



of these open sets must contain infinitely many elements of  $W_0$ . Let  $x_0$  be the center of such a star. Now, let us suppose that  $x_i$  has been defined. In  $K_{i+1}$ , we can cover  $|\text{St}_{K_i}(x_i)|$  by the open stars of the vertices of  $K_{i+1}$  included in  $|\text{St}_{K_i}(x_i)|$ . As before, at least one of these stars must contain infinitely many elements of  $W_{i+1}$ . We define  $x_{i+1}$  as the center of such a star. Let us now show that the simplices in  $\text{St}_{K_{i+1}}(x_{i+1})$  are globally subdivided. If  $x_{i+1} = x_i$ , this is obvious. Otherwise, there exists a neighbor  $y$  of  $x_i$  in  $K_i$  such that  $x_{i+1} \in |\text{St}_{K_i}(y)|$ . The hereditary property stated above yields that  $f_i$  does not satisfy the weak star condition at  $y$ . Besides, any simplex  $\sigma \in \text{St}_{K_{i+1}}(x_{i+1})$  contains either  $x_i$  or  $y$ , hence is globally subdivided. Thus we have constructed the desired sequence of vertices.  $\square$

**Example 3.11.** Let us denote  $(K_i)_{i \geq 0}$  the sequence of simplicial complexes built by Algorithm 3, using edgewise subdivisions. Consider also the cover  $\mathcal{V} = \{f^{-1}(|\text{St}(x)|) \mid x \in L^0\}$  of  $|K|$ . The following figure shows a configuration where the map never satisfies the weak star condition. In other words, the algorithm does not terminate. The cover  $\mathcal{V}$  is made of three sets, two of which are not connected. One sees that, at each step, there are two vertices  $v$  of  $K_i$  such that the set of neighbors  $|\overline{\text{St}}(v)^0|$  is not included in a member of  $\mathcal{V}$ . Note also that the two vertices at the bottom left and right are always included in a semi-subdivided simplex, but never in a globally subdivided one.

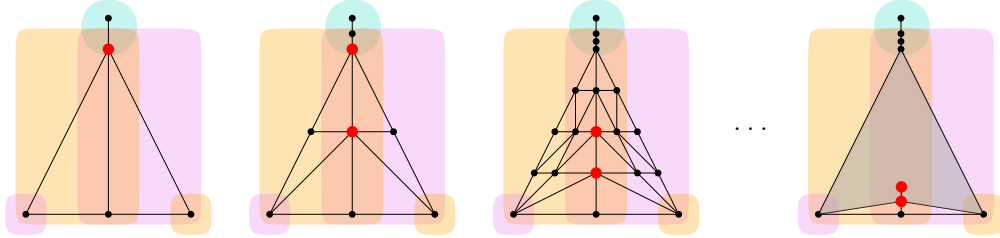


Figure 17: Run of Algorithm 3 with edgewise subdivisions. The filled shapes represent the cover  $\mathcal{V}$ . At each step, vertices where  $f$  does not satisfy the star condition are represented in red. We do not represent the full complex in the last picture.

**3.3.3 Generalized Delaunay subdivisions** The previous notions directly adapt to Delaunay complexes (defined in §3.2.3). Let  $X$  be a subset of the sphere  $\mathbb{S}^d$  and  $K = \text{Del}(X)$  the corresponding Delaunay complex. Let  $K' \subset K$  be a simplicial sub-complex, and let  $X'$  be the set of vertices of the generalized barycentric (resp. edgewise) subdivision  $\text{sub}(K; K')$ , where we normalize the vertices so as they belong to  $\mathbb{S}^d$ . The Delaunay complex built on  $X'$ ,  $\text{Del}(X')$ , is called the *generalized Delaunay barycentric* (resp. *edgewise*) *subdivision of  $K$  holding  $K'$  fixed*, denoted  $\text{sub}(K; K')$ . We point out that, as it is the case for global Delaunay subdivisions,  $\text{sub}(K; K')$  may not be a subdivision of  $K$  (see Figure 13).

Algorithm 3 also directly adapts: if  $K$  is a Delaunay complex, the simplicial complex  $K'$  can be defined as in Equation (15), and we can consider the generalized Delaunay subdivision  $\text{sub}(K; K')$ . As before, the algorithm does not terminate in general.

**Example 3.12.** In order to illustrate the benefits of generalized subdivisions over global subdivisions, let us consider a problem of weak simplicial approximation to a map  $|K| \rightarrow |L_\varepsilon|$ , where  $K$  is the usual triangulation of  $\mathbb{S}^2$  via  $\partial\Delta^3$ , and  $L_\varepsilon$  is a triangulation of  $\mathbb{S}^2$  containing a small simplex. More precisely, for  $\varepsilon \in (0, 1]$ , we define the simplicial complex  $L_\varepsilon$  as the Delaunay complex on the sphere given by the set  $X = \{x_0, x_1, x_2, x_\varepsilon\}$ , where the first three vertices are those defined in Equation (13), and  $x_\varepsilon$  is a point at distance  $\varepsilon$  from  $x_0$ . We apply Algorithm 3 to the identity map  $|K| \rightarrow |L_\varepsilon|$  for a few values of  $\varepsilon$ , and the four generalized subdivisions methods we defined. We collect in Table 2 the number of vertices of the resulting simplicial complexes  $K_i$ . We also represent in Figure 18 these complexes for  $\varepsilon = 0.1$ . One observe that, in this case, edgewise and Delaunay edgewise subdivisions perform better, in the sense that they yield simplicial complexes with less vertices.



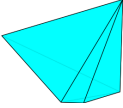
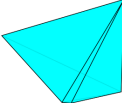
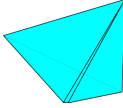
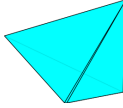
				
	$L_{0.25}$	$L_{0.1}$	$L_{0.05}$	$L_{0.01}$
Barycentric	136	452	836	3138
Edgewise	64	77	88	110
Delaunay barycentric	101	159	192	208
Delaunay edgewise	52	72	93	99

Table 2: Number of vertices of  $K$  after applying Algorithm 3 to the identity map  $|K| \rightarrow |L_\varepsilon|$ .

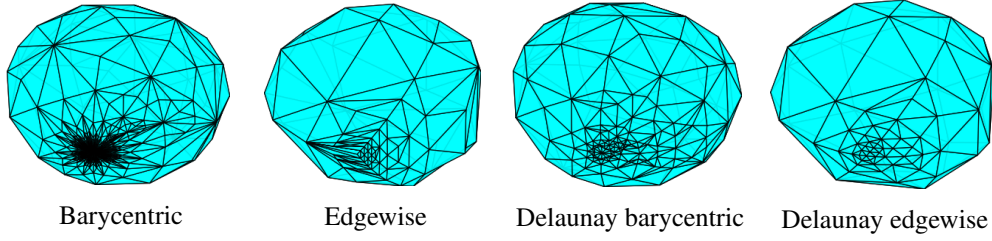


Figure 18: Resulting complexes after applying the subdivision process to the identity map  $|K| \rightarrow |L_{0.1}|$ .

**3.3.4 Delaunay simplifications** When working with Delaunay complexes, we can define a simplification procedure that, given a simplicial  $g: \text{Del}(X) \rightarrow L$ , search for a subset  $X' \subset X$  and a simplicial map  $g': \text{Del}(X') \rightarrow L$  homotopy equivalent to  $g$ . To do so, we say that a vertex  $v \in X$  satisfies the *simplex condition* if

$$g(\overline{\text{St}}(v)^0) \in L.$$

We can define a map between vertex sets  $g': \text{Del}(X \setminus \{v\})^0 \rightarrow L^0$  by restricting  $g$  to  $X \setminus \{v\}$ .

**Lemma 3.13.** *If  $v$  satisfies the simplex condition, then  $g'$  is a simplicial map and is homotopy equivalent to  $g$ .*

*Proof.* This is a consequence of the fact that removing a vertex  $v$  from  $\text{Del}(X)$  only changes its structure in the open star  $\text{St}(v)$ . For any new simplex  $\sigma \in \text{Del}(X \setminus \{v\}) \setminus \text{Del}(X)$ , its image  $g(\sigma)$  is a simplex of  $L$  by the simplex condition. Therefore  $g'$  is simplicial. For the same reason, the maps  $g$  and  $g'$  are contiguous, hence homotopy equivalent.  $\square$

As a consequence, we can simplify the map  $g: \text{Del}(X) \rightarrow L$  incrementally by removing a vertex of  $X$  that satisfies the simplex condition, computing again the Delaunay complex, and repeating the process. We must take care of not removing the initial  $d+2$  vertices of  $\partial\Delta^{d+1}$ , defined in §3.2.1, in order to ensure that the radial projection map  $r: \mathbb{S}^d \rightarrow \text{Del}(X)$  remains well-defined.

**Example 3.14.** We reproduce Example 3.12, but now applying the simplification process for Delaunay complexes. The number of vertices of the final complexes are collected in the following table. The number of vertices before applying the simplification are also given in parenthesis. We can observe a significant improvement.

### 3.4 Contraction of codomain

In the previous subsections we explained how to find a weak simplicial approximation to a map  $f: |K| \rightarrow |L|$ . Here, we shall discuss how the notion of edge contractions may simplify this

	$L_{0.25}$	$L_{0.1}$	$L_{0.05}$	$L_{0.01}$
Delaunay barycentric	11 (101)	9 (159)	10 (192)	9 (208)
Delaunay edgewise	8 (52)	10 (72)	9 (93)	11 (99)

Table 3: Number of vertices of  $K$  after applying Algorithm 3 to the identity map  $|K| \rightarrow |L_\varepsilon|$ , followed by the Delaunay simplification. We indicate in parenthesis the results without Delaunay simplification.

problem. Namely, by contracting the complex  $L$ , we obtain a simpler complex  $L'$ , for which the induced map  $|K| \rightarrow |L'|$  may be easier to approximate. We will not state actual results on this matter, but only propose a heuristic discussion and some experiments.

**3.4.1 Edge contractions** It is an usual tool in computational topology, used to reduce a simplicial complex  $L$  [25, 5, 26]. Let  $[a, b]$  be an edge of  $L$ , and  $c \notin L^0$  a new vertex. We define the *quotient map* as

$$q: L^0 \longrightarrow (L^0 \setminus \{a, b\}) \cup \{c\}$$

$$x \longmapsto \begin{cases} c & \text{if } x = a \text{ or } b, \\ x & \text{else.} \end{cases} \quad (18)$$

Seeing  $q$  as a map with domain the whole simplicial complex  $L$ , we can define the *contracted complex* as its image  $L' = \{q(\sigma) \mid \sigma \in L\}$ . An example is given in Figure 19. From a combinatorial point of view, the contraction is a local process: the structure of  $L$  is altered only in  $\text{St}(a) \cup \text{St}(b)$ , the open stars of  $a$  and  $b$ . In other words, the simplicial complex  $L \setminus (\text{St}(a) \cup \text{St}(b))$  is included in  $L'$ .

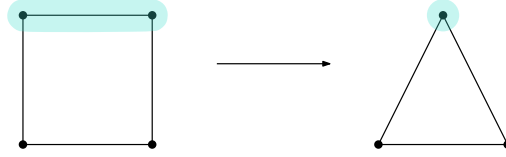


Figure 19: Contracting the upper side of a square yields a triangle.

The quotient map induces a surjective simplicial map  $q: L \rightarrow L'$ . The following lemma gives a criterion to check whether this map is a homotopy equivalence, known as the *link condition*. We remind the reader that the notion of link has been defined in Subsection 2.2.

**Lemma 3.15.** *The map  $q$  is a homotopy equivalence when the edge  $[a, b]$  satisfies  $\text{Lk}(ab) = \text{Lk}(a) \cap \text{Lk}(b)$ .*

*Proof.* The fact that  $L$  and  $L'$  are homotopy equivalent as already been proven in [5, Theorem 2]. We will verify here that the quotient map gives a homotopy equivalence. Their proof goes as follows: let  $\mathcal{U}'$  be the cover of  $|L'|$  by the closed simplices  $|\bar{\sigma}|$  for  $\sigma \in L'$ . Let  $\mathcal{N}'$  be the nerve of  $\mathcal{U}'$ . Since intersection of simplices are simplices, and therefore are contractible, the nerve theorem yields that  $\mathcal{N}'$  has the homotopy type of  $L'$ . Next, consider the cover  $\mathcal{U}$  of  $L$  defined as the collection of the preimages  $q^{-1}(|\bar{\sigma}|)$  for  $\sigma \in L'$ , and  $\mathcal{N}$  its nerve. The authors show that the nerve theorem still applies, hence that  $\mathcal{N}$  has the homotopy type of  $L$ . Now, it is direct to see that  $\mathcal{N}$  and  $\mathcal{N}'$  are equal, and we deduce that  $L$  and  $L'$  are homotopy equivalent.

In order to show that  $q$  is a homotopy equivalence, we shall use another notion. Following [45, Section 4.G], let us denote  $X_{\mathcal{U}}$  and  $X_{\mathcal{U}'}$  the *complexes of spaces* given by the covers  $\mathcal{U}$  and  $\mathcal{U}'$ . These are simplicial complexes that encode the combinatorial structure of the covers. To each of them is associated a topological space, denoted  $\Delta X_{\mathcal{U}}$  and  $\Delta X_{\mathcal{U}'}$ , obtained by a series of mapping cones, as well as maps  $p: \Delta X_{\mathcal{U}} \rightarrow |L|$  and  $p': \Delta X_{\mathcal{U}'} \rightarrow |L'|$ . It is proven in [45,

Subsection 4G.2] that these maps are homotopy equivalences provided that  $\mathcal{U}$  and  $\mathcal{U}'$  are *open* covers. Here the covers are closed, but the result still holds since we consider covers that are made of unions of simplices.

Now, for any simplex  $\sigma \in L'$ , both  $|\overline{\sigma}|$  and  $q^{-1}(|\overline{\sigma}|)$  are contractible [5, Lemma 2]. Hence the map  $q: q^{-1}(|\overline{\sigma}|) \rightarrow |\overline{\sigma}|$  is a homotopy equivalence. Consequently,  $q$  induces a homotopy equivalence  $\Delta q: \Delta X_{\mathcal{U}} \rightarrow \Delta X_{\mathcal{U}'}$  [45, Proposition 4G.1]. Moreover, it fits in the following commutative diagram:

$$\begin{array}{ccc} \Delta X_{\mathcal{U}} & \xrightarrow{\Delta q} & \Delta X_{\mathcal{U}'} \\ \downarrow p & & \downarrow p' \\ |L| & \xrightarrow{q} & |L'| \end{array}$$

By the 2-out-of-3 property of homotopy equivalences, we conclude that  $q$  is a homotopy equivalence.  $\square$

*Remark 3.16.* We point out that this construction of edge contraction does not give  $L'$  a canonical geometric realization  $|L'|$  inherited from  $|L|$ . A natural idea, that consists in deducing  $|L'|$  from  $|L|$  by assigning to  $c$  the coordinate of  $a$  or  $b$ , does not give an embedding of  $L'$  in general.

**3.4.2 Repeated edge contractions** In order to reduce the simplicial complex  $L$ , we can build a sequence of complexes  $L_0, L_1, \dots$ , starting with  $L_0 = L$ , and defining  $L_{i+1}$  from  $L_i$  by choosing an edge that satisfies the link condition and contracting it. If no edge satisfies the link condition, the process stops, and we denote the last complex  $L'$ . The composition of all the quotient maps  $L_i \rightarrow L_{i+1}$  gives, as in Lemma 3.15, a homotopy equivalence  $L \rightarrow L'$ .

It is worth noting that this process depends on a choice of edges: different contracted edges may lead to a different output  $L'$ . In practice, we observed that the number of vertices of the output may vary significantly. However, we did not investigate whether there would be a criterion, or heuristic ideas, which would lead to minimal outputs. In practice, we use an algorithm that selects at each step an edge at random among all the edges that satisfy the link condition.

**3.4.3 Application to simplicial approximation** We now study how edge contractions can be used in our problem. Let  $f: |K| \rightarrow |L|$  be a continuous map, to which we wish to find a simplicial approximation. Let  $L'$  be obtained from  $L$  by a series of edge contractions, and consider the composition

$$\begin{array}{ccccc} |K| & \xrightarrow{f} & |L| & \xrightarrow{q} & |L'| \\ & \searrow & & \nearrow & \\ & & f' & & \end{array}$$

Following the proof of the simplicial approximation theorem (Theorem 2.3), consider the following covers of  $L$ :

$$\mathcal{U} = \{|\text{St}(x)| \mid x \in K^0\} \quad \text{and} \quad \mathcal{V} = \{f^{-1}(|\text{St}(x)|) \mid x \in L^0\}.$$

The map  $f$  satisfies the star condition (and consequently the weak star condition) if  $\mathcal{U}$  *refines*  $\mathcal{V}$ , that is, if each element of  $\mathcal{U}$  is included in an element of  $\mathcal{V}$ . Now, define

$$\mathcal{V}' = \{f'^{-1}(|\text{St}(x)|) \mid x \in L'^0\}.$$

Similarly,  $f'$  satisfies the star condition if  $\mathcal{U}$  *refines*  $\mathcal{V}'$ . In order to compare the covers  $\mathcal{V}$  and  $\mathcal{V}'$ , remark that for any vertex  $x'$  of  $L'$ , pulling it back into  $L$  gives

$$q^{-1}(\text{St}(x')) = \bigcup_{x \in q^{-1}(\{x'\})} \text{St}(x).$$

In other words,  $q$  has the effect of merging the stars of  $L$ . Therefore, the cover  $\mathcal{V}'$  can be obtained from  $\mathcal{V}$  by merging the elements that correspond to vertices identified by  $q$ . We deduce that  $\mathcal{V}$  refines  $\mathcal{V}'$ , and that  $f'$  satisfies the star condition if  $f$  does. This shows why contracting  $L$  simplify the problem of simplicial approximation. An illustration is given in the next figure, where  $f: K \rightarrow L$  is the identity map between two squares, and  $L'$  is a triangle.

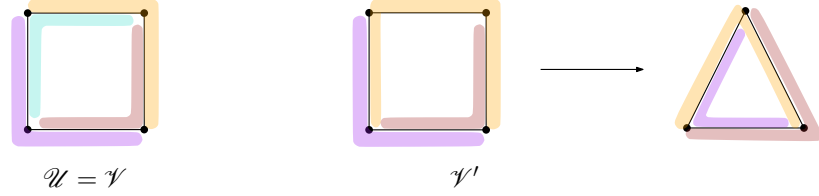


Figure 20: Left: cover of the square by its stars. Right: cover of the square by pulling back the stars of the triangle via  $q$ .

In order to quantify this improvement, let us endow  $|K|$  with a metric, and let  $\lambda > 0$  be the supremum of the Lebesgue numbers of  $\mathcal{V}$ . This number is such that any subset of  $|K|$  with diameter less than  $\lambda$  is included in an element of  $\mathcal{V}$ . Consequently,  $f$  satisfies the star condition if every star of  $K$  has diameter less than  $\lambda$ . Let also  $\lambda'$  be the supremum of the Lebesgue numbers of  $\mathcal{V}'$ . Clearly, we have  $\lambda \leq \lambda'$ , but the inequality is not strict in general. An example of this phenomenon is given in Figure 20: on the square of side 1, we have  $\lambda = \lambda' = 1$ .

At this point, it is natural to consider a local notion of Lebesgue number. Namely, define the *local Lebesgue number* of  $\mathcal{V}$  as the map  $\Lambda: |K| \rightarrow [0, +\infty)$  that assigns to any point  $x \in |K|$  the supremum of the values  $\lambda$  such that every set of  $|K|$  with diameter less than  $\lambda$  and containing  $x$  is included in a member of the cover. Let  $\Lambda'$  denote the local Lebesgue number of  $\mathcal{V}'$ . Coming back to the examples of Figure 20, we see that  $\Lambda$  is constant equal to 1, while  $\Lambda'$  is greater than 1 on the interior of the upper edge (with maximum 1.5).

These considerations work in pair with the notion of generalized subdivisions, introduced in Subsection 3.3. Indeed, it is clear that  $f$  satisfies the star condition under the following criterion:

$$\forall x \in K^0, \text{diam}(\text{St}(x)) < \Lambda_{\mathcal{V}}(x).$$

Hence, one can ensure that  $f$  satisfies the star condition by subdividing  $K$  where  $\Lambda$  is too small. This is the behavior we observed in practice by running Algorithm 3, as we now illustrate.

**Example 3.17.** Define  $K = \partial\Delta^3$ , seen as a triangulation of  $\mathbb{S}^2$ , and let  $L = \text{sub}^3(\partial\Delta^3)$  be its third barycentric subdivision. After performing edge contractions on  $L$ , we obtain a simplicial complex  $L'$  consisting of 4 vertices. The following figure represents the cover  $\mathcal{V}'$  of  $L'$  obtained by pulling back the star of  $L'$ . As one can observe, elements of the cover tend to have a large diameter, but do not intersect much. That is to say, the local Lebesgue number is large inside the elements of the cover, but low at their intersections.

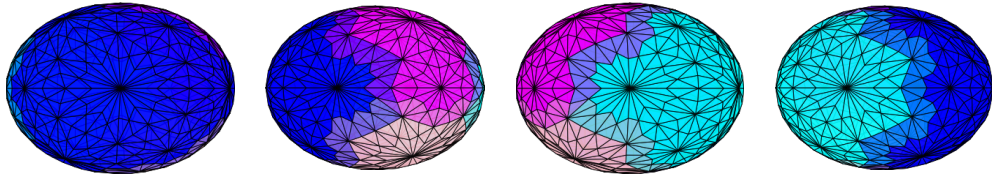


Figure 21: Four views of the covering  $L$ . The cover consists of four sets, represented in blue, cyan, magenta and pink. When two sets intersect, the colors are averaged.

We now apply Algorithm 3, so as to obtain a weak simplicial approximation to  $f': |K| \rightarrow |L'|$ . We compare the results of barycentric, edgewise, Delaunay barycentric and Delaunay edgewise

subdivisions. At the end of the algorithm, the simplicial complexes consist of 4'032, 865, 2'149 and 784 vertices. They are represented in Figure 22. This is to be compared with Table 1, where we applied the subdivision process to the map  $f: |K| \rightarrow |L|$ , obtaining simplicial complexes with 15'554, 32'770, 93'314 and 32'770 vertices respectively.

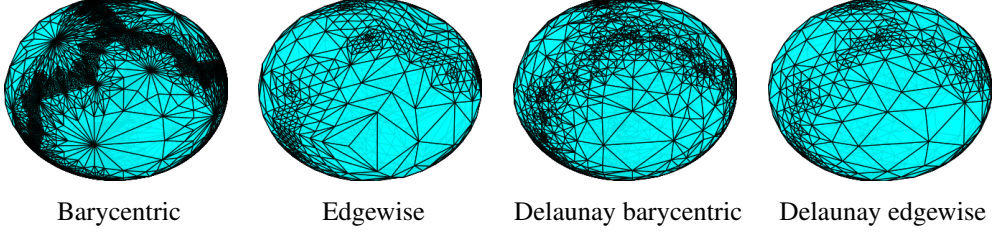


Figure 22: Resulting complexes after applying Algorithm 3 to the map  $|\partial\Delta^3| \rightarrow |L'|$ , where  $L'$  is the result of a series of edge contractions on  $\text{sub}^3(\partial\Delta^3)$ .

**3.4.4 Unfoldings** As we have seen above, the quotient map  $q: L \rightarrow L'$  of an edge contraction yields a cover  $\mathcal{V}'$  of  $|K|$  whose (global) Lebesgue number may be low. In order to improve this cover, one could consider another map than  $q$ , for instance homeomorphisms, if they exist. In [25] is introduced the following notion: an *unfolding* of  $q$  is a map  $i: |L| \rightarrow |L'|$  that is a *simplicial homeomorphism*, that is, such that there exist subdivisions of  $L$  and  $L'$  on which  $i$  is a bijective simplicial map. For simplicial complexes of dimension up to three, the authors give a criterion under which the quotient map of an edge contraction admits an unfolding.

Using unfoldings  $i: |L| \rightarrow |L'|$  instead of the quotient map, we may be able to obtain covers  $\mathcal{V}'$  with larger Lebesgue number. An example is given in the following figure: the new cover of the square has a constant local Lebesgue number equal to 1.5, improving the cover of Figure 20. In the remaining in the paper, however, we will not implement such a technique.

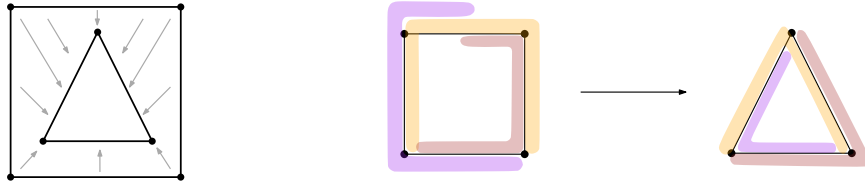


Figure 23: Left: a homeomorphism  $i: |L| \rightarrow |L'|$ . Right: cover of the square by pulling back the stars of the triangle via  $i$ .

## 4 Gluing simplicial cells

As described in Subsection 2.1, building a CW complex  $X$  amounts to gluing its cells, by building mapping cones. The aim of this section is to provide a simplicial equivalent to this process. In Subsection 4.1, we define a notion of simplicial mapping cone. By applying this construction to CW complexes, we obtain the main algorithm of this paper. An overview of the algorithm is given in Subsection 4.2, and a few technical details are discussed in Subsection 4.3.

### 4.1 Simplicial mapping cone

In this subsection, we suppose that  $f: K \rightarrow L$  is a simplicial map between geometric simplicial complexes, and we consider  $\text{Cone}(f)$ , the mapping cone of  $f$  (defined in §2.1.2). We will present the construction of a simplicial equivalent of the mapping cone, that is, a simplicial complex  $\text{Cone}^s(f)$  homotopy equivalent to  $\text{Cone}(f)$ . Let us mention that the construction of a

homeomorphic simplicial complex will not be addressed here. Throughout this subsection, we will take as an illustration a simplicial approximation to the identity map between two circles, represented in Figure 24.

We will proceed by first proposing a simplicial equivalent to the product  $|K| \times [0, 1]$ , then to the mapping cylinder  $\text{Cyl}(f)$ , and last to the mapping cone  $\text{Cone}(f)$ . We point out that such a construction is already well-known in algebraic topology literature [68, 21]. Nonetheless, motivated by practical applications, we present here a simpler version, in the sense that our simplicial mapping cone requires less simplices. We compare these various constructions in Remark 4.3.

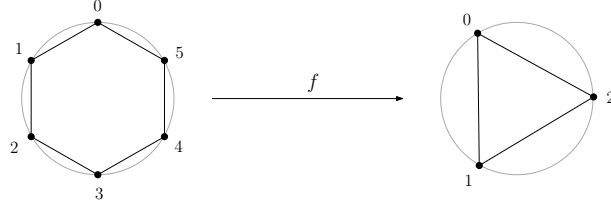


Figure 24: The identity map  $f: K \rightarrow L$ , defined as  $0, 1, 2, 3, 4, 5 \mapsto 0, 0, 1, 1, 2, 2$ .

**4.1.1 Triangulation of the product** The first step consists in triangulating the product  $|K| \times [0, 1]$ , or equivalently the product  $|K| \times |I|$ , where  $I = \{\{0\}, \{1\}, \{0, 1\}\}$  is the standard 1-simplex. There exists a notion of product of two simplicial complexes  $K$  and  $K'$ , denoted here  $K \times K'$ , whose geometric realization is homeomorphic to the product  $|K| \times |K'|$  [31, Definition 8.8]. However, one has to pay attention to the fact that the product used here is not the product in the category of the simplicial complexes, but of those ordered. If  $K$  and  $K'$  are respectively endowed with a total order of their vertices, consider the lexicographic order on the set  $K^0 \times K'^0$ , that is, the (partial) order given by  $(a, b) < (a', b')$  if and only if  $a < a'$  and  $b < b'$ . The product  $K \times K'$  is defined as the simplicial complex whose vertex set is the Cartesian product  $K^0 \times K'^0$ , and whose simplices are the subsets of  $K^0 \times K'^0$  totally ordered by the lexicographic order.

In the particular case of  $K \times I$ , the construction can be described as follows. Let  $x_0 < x_1 < \dots < x_n$  be an order of the vertices of  $K$ . Take two copies of  $K$ , identified with  $K \times \{0\}$  and  $K \times \{1\}$ . For every  $m \in \llbracket 0, n \rrbracket$  and every  $m$ -simplex  $\sigma = [x_0, \dots, x_m]$  of  $K \times \{0\}$ , with vertices ordered, consider the corresponding vertices of  $K \times \{1\}$ , denoted  $x'_0 < \dots < x'_m$ . Now, for every  $k \in \llbracket 0, m \rrbracket$ , define the  $(m+1)$ -simplex

$$\sigma_k = [x_0, \dots, x_k, x'_k, \dots, x'_m]. \quad (19)$$

Their collection form the simplices of  $K \times I$ . In what follows, we may refer to  $K \times \{0\}$  as the *inner layer*, and  $K \times \{1\}$  as the *outer layer*.

If  $K$  is endowed with a geometric realization  $|K| \subset \mathbb{R}^N$ , and if  $|I| \subset \mathbb{R}^2$  is the standard 1-simplex, then the cartesian product  $|K| \times |I| \subset \mathbb{R}^{N+2}$  is clearly a geometric realization of  $K \times I$ . As a consequence, the points of  $|K \times I|$  can be written as  $(x, t)$  for  $x \in |K|$  and  $t \in [0, 1]$ .

It is worth noting that the product  $K \times I$  depends on a particular choice of an order of the vertices, hence the construction is not canonical. Some examples are given in Figure 25. In practice, we choose an arbitrary order.

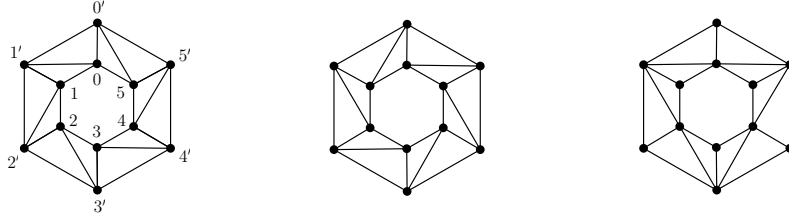


Figure 25: Three versions of the simplicial product  $K \times [0, 1]$ , respectively for the order  $0 < 1 < 2 < 3 < 4 < 5$ , the order  $5 < 4 < 3 < 2 < 1$  and  $0 < 2 < 4 < 5 < 3 < 1$ .

**4.1.2 Triangulation of the mapping cylinder** We now obtain the *simplicial mapping cylinder*, denoted  $\text{Cyl}^s(f)$ , by identifying  $K \times \{1\}$ , the outer layer of  $K \times I$ , with  $L$  via the simplicial map  $f$ . In other words,  $\text{Cyl}^s(f)$  is the simplicial complex with vertex set  $K^0 \sqcup L^0$ , and whose simplices are:

- the simplices  $\sigma \in L$ ,
- the simplex  $[x_0, \dots, x_k, f(x'_k), \dots, f(x'_m)]$  for any simplex  $[x_0, \dots, x_k, x'_k, \dots, x'_m]$  of  $K \times I$  (as in Equation (19)).

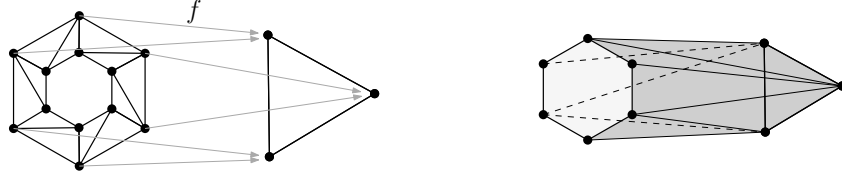


Figure 26: The simplicial mapping cone is obtained as a quotient of  $K \times I \sqcup L$ .

If  $K$  and  $L$  are endowed with geometric realizations  $|K| \subset \mathbb{R}^N$  and  $|L| \subset \mathbb{R}^{N'}$ , we can define a geometric realization  $|\text{Cyl}^s(f)|$  for  $\text{Cyl}^s(f)$  by seeing it as a subset of  $|K| \times |L| \subset \mathbb{R}^{N+N'}$ . Besides, it is clear that the map  $f$  induces a simplicial map  $K \times I \rightarrow \text{Cyl}^s(f)$ , from which we get a continuous map  $h': |K| \times [0, 1] \rightarrow |\text{Cyl}^s(f)|$ .

Now, let us consider  $\text{Cyl}(f)$ , the (topological) mapping cone of  $f$ . Let  $h: |K| \times [0, 1] \sqcup |L| \rightarrow \text{Cyl}(f)$  be the quotient map. We can make  $h'$  descend to the quotient and obtain a continuous map  $q: \text{Cyl}(f) \rightarrow |\text{Cyl}^s(f)|$ .

$$\begin{array}{ccc}
 & |K \times I| \sqcup |L| & \\
 h \swarrow & & \searrow h' \\
 \text{Cyl}(f) & \xrightarrow{q} & |\text{Cyl}^s(f)|
 \end{array}$$

**Lemma 4.1.** *The quotient map  $q: \text{Cyl}(f) \rightarrow |\text{Cyl}^s(f)|$  is a homotopy equivalence.*

*Proof.* We shall first give the mapping cylinder a CW structure. Since  $K$  and  $L$  are simplicial complexes, hence CW complexes, the quotient map  $|K \times I| \sqcup |L| \rightarrow \text{Cyl}(f)$  restricted to each simplex can be seen as a characteristic map. Their collection form a CW structure on  $\text{Cyl}(f)$  (more particularly, a  $\Delta$ -complex structure, as in [45]).

Both  $h$  and  $h'$  are injective on  $|L|$ , but their behavior may differ on  $|K \times I|$ . To see so, let  $\sigma = [x_0, \dots, x_m, y_0, \dots, y_n]$  be a simplex of  $K \times I$ , with  $x_0, \dots, x_m \in K \times \{0\}$  and  $y_0, \dots, y_n \in K \times \{1\}$ . We have that:

- $|h(\sigma)|$  is homeomorphic to the quotient  $|\sigma|/f$ , where only the outer layer is affected,
- $|h'(\sigma)|$  is the simplex spanned by  $[x_0, \dots, x_m, f(y_0), \dots, f(y_n)]$ .

In particular, if  $f$  is not injective,  $h'(\sigma)$  may be of lower dimension than  $h(\sigma)$ , as shown in the following figure.

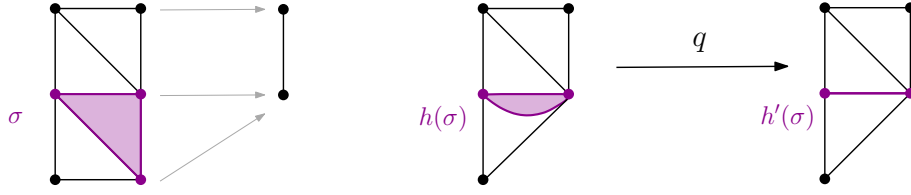


Figure 27: Left: the map  $f: K \times \{1\} \rightarrow L$ . Right:  $q: \text{Cyl}(f) \rightarrow |\text{Cyl}^s(f)|$  is not a homeomorphism here.

Note that, by using the map  $h$ , we can write the points of  $|h(\sigma)|$  in barycentric coordinates as

$$\sum_{i=0}^m t_i x_i + \sum_{i=0}^n t'_i y_i \quad \text{with} \quad \sum_{i=0}^m t_i + \sum_{i=0}^n t'_i = 1.$$

Now, let us see  $|h'(\sigma)|$  as a subset of  $\text{Cyl}(f)$ . We define a retraction  $r_\sigma: |h(\sigma)| \rightarrow |h'(\sigma)|$  by

$$\sum_{i=0}^m t_i x_i + \sum_{i=0}^n t'_i y_i \mapsto \sum_{i=0}^m t_i x_i + \sum_{i=0}^n t'_i f(y_i).$$

This retraction comes from a deformation retraction, for instance the linear interpolation between the identity and  $r_\sigma$ . According to Lemma B.1 stated in Appendix B, the quotient  $\text{Cyl}(f) \rightarrow \text{Cyl}(f)/r_\sigma$  is a homotopy equivalence. By repeating this operation for each simplex of  $K \times I$ , we obtain a sequence of homotopy equivalences whose last term is  $\text{Cyl}^s(f)$ :

$$\text{Cyl}(f) \longrightarrow \text{Cyl}(f)/r_\sigma \longrightarrow (\text{Cyl}(f)/r_\sigma)/r_{\sigma'} \longrightarrow \cdots \longrightarrow \text{Cyl}^s(f).$$

Since this composition is equal to  $q$ , we deduce the result.  $\square$

**4.1.3 Triangulation of the mapping cone** The last part of our construction consists in coning  $K \times \{0\}$ , the inner layer of  $\text{Cyl}^s(f)$ , at a new vertex  $x^*$ . More precisely, the *simplicial mapping cone*,  $\text{Cone}^s(f)$ , is the simplicial complex whose vertex set is  $\text{Cyl}^s(f)^0 \sqcup \{x^*\}$  and whose simplices are

- the simplices  $\sigma \in \text{Cyl}^s(f)$ ,
- the simplex  $\sigma \cup \{x^*\}$  for any simplex  $\sigma \in K \times \{0\}$ .

The simplicial complex  $\text{Cone}^s(f)$  is endowed with a geometric realization  $|\text{Cone}^s(f)| \subset |\text{Cyl}^s(f)| \times \mathbb{R} \subset \mathbb{R}^{N+1}$ , where  $|\text{Cyl}^s(f)| \subset \mathbb{R}^N$  is the geometric realization of  $\text{Cyl}^s(f)$  previously defined, and where  $x^*$  is identified with  $(0, \dots, 0, 1) \in \mathbb{R}^{N+1}$ .



Figure 28: The simplicial mapping cone is obtained by coning the mapping cylinder.

In practice, it may be more convenient to see this construction the other way around: we can define  $\text{Cone}^s(f)$  by first coning the inner layer of  $K \times I$ , and then gluing its outer layer to  $L$ . Namely, let  $\text{C}^s(K)$  denote the simplicial complex obtained from  $K \times I$  by adding a new vertex  $x^*$  and all the simplices  $\sigma \cup \{x^*\}$  for  $\sigma \in K \times \{0\}$ . It is clear that  $\text{Cone}^s(f)$  can be obtained from  $\text{C}^s(K) \sqcup L$  by identifying the vertices of  $K \times \{1\}$  to  $L$  via  $f$ .

In order to define a continuous map  $\text{Cone}(f) \rightarrow |\text{Cone}^s(f)|$ , we can start with a homeomorphism  $\text{C}(|K|) \rightarrow |\text{C}^s(K)|$ , where  $\text{C}(|K|)$  is the topological cone on  $|K|$ , as defined in §2.1.2. Such a homeomorphism is not canonical, and we will suppose from now on that one has been



choosen. We will expose our choices later in §4.3.3. From this homeomorphism, we deduce a quotient map  $C(|K|) \sqcup |L| \rightarrow |C^s(K)| \sqcup |L|$ , which descends to the quotient to give a continuous map  $q' : \text{Cone}(f) \rightarrow |\text{Cone}^s(f)|$ .

$$\begin{array}{ccc} C(|K|) \sqcup |L| & \longrightarrow & |C^s(K)| \sqcup |L| \\ \downarrow & & \downarrow \\ \text{Cone}(f) & \xrightarrow{q'} & |\text{Cone}^s(f)| \end{array} \quad (20)$$

The same proof as Lemma 4.1 yields the following:

**Lemma 4.2.** *The quotient map  $q' : \text{Cone}(f) \rightarrow |\text{Cone}^s(f)|$  is a homotopy equivalence.*

*Remark 4.3.* Compared to other constructions of simplicial mapping cones already studied in the literature, ours has the advantage of requiring fewer simplices. Unfortunately, it has the inconvenience of not being canonical: in order to build the product  $K \times I$ , an order of the vertices of  $K$  has to be choosen. However, this drawback will not be a problem for developing the algorithm in the next subsection.

A first construction can be found in [68, Section 6], where  $K \times I$  is triangulated with three layers:  $K$ , the barycentric subdivision of  $K$ , and  $K$  again. The outer layer is identified to  $L$  via the simplicial map  $f$ . It is shown that this simplicial mapping cylinder is homeomorphic to the topological mapping cylinder [67, Section 10]. This homeomorphism, however, is not given by the quotient map defined in Lemma 4.1. A similar construction can be found in [21, Section 4], where the inner layer  $K$  is removed. It is shown to be homeomorphic to the first construction. This simplicial mapping cylinder is also used in [45, Theorem 2C.5]. We compare in the following figure these constructions.

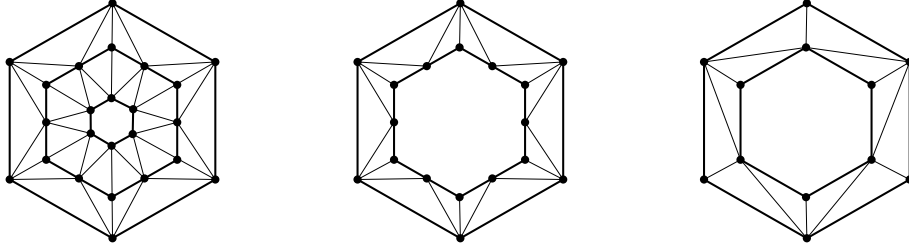


Figure 29: The triangulation of  $K \times I$  in [68], the one in [21], and the one presented in this paper.

## 4.2 Sketch of algorithm

We now describe the main algorithm of this paper. We first gather the mathematical results obtained so far, and then describe a concrete implementation in pseudo-code. The input of the algorithm will be a CW complex  $X$ . More precisely, and using the notations of §2.1.3, we consider that  $X$  is a subset of a Euclidean space  $\mathbb{R}^N$ , and that we are given the partition  $\{e_i \mid i \in \llbracket 0, n \rrbracket\}$  of  $X$  into cells, with their dimensions  $d(i)$ , the gluing maps  $\phi_i : \mathbb{S}^{d(i)-1} \rightarrow X$  and the inverse characteristic maps  $\Phi_i^{-1} : e_i \rightarrow \mathcal{B}^{d(i)}$ .

**4.2.1 Mathematical formulation** By defining the skeleta  $X_i = \bigcup_{j \leq i} e_j$  we obtain an increasing sequence of subsets  $X_0 \subset X_1 \subset \dots \subset X_n = X$ . We wish to build a sequence of simplicial complexes  $K_0, \dots, K_n$  and for each of them a homotopy equivalence  $h_i : X_i \rightarrow |K_i|$ . Sequentially, we obtain  $K_{i+1}$  from  $K_i$  as follows:

- we find a triangulation  $\iota_{i+1} : |S_{i+1}| \rightarrow \mathbb{S}^{d(i+1)-1}$  of the sphere such that the composition  $h_i \circ \phi_{i+1} \circ \iota_{i+1} : |S_{i+1}| \rightarrow |K_i|$  satisfies the weak star condition,
- we choose a weak simplicial approximation  $\phi'_{i+1} : S_{i+1} \rightarrow K_i$  to  $h_i \circ \phi_{i+1} \circ \iota_{i+1}$  such that they are homotopy equivalent,

- we define the simplicial mapping cone  $K_{i+1} = \text{Cone}^s(\phi'_{i+1})$ .

The first two points can be achieved using Algorithms 1, 2 or 3. The maps then fit in the following diagram, commutative up to homotopy:

$$\begin{array}{ccccc}
 |S_{i+1}| & \xrightarrow{t_{i+1}} & \mathbb{S}^{d(i+1)-1} & \xrightarrow{\phi_{i+1}} & X_i & \xrightarrow{h_i} & |K_i| \\
 & & & & \searrow & \nearrow & \\
 & & & & \phi'_{i+1} & & 
 \end{array} \quad (21)$$

We obtain a homotopy equivalence  $h_{i+1}: X_{i+1} \rightarrow |K_{i+1}|$  as a consequence of several previous results. Namely, we define  $h_{i+1}$  as the composition

$$X_{i+1} \xrightarrow{\bar{\Phi}_{i+1}} \text{Cone}(\phi_{i+1}) \xrightarrow{H} \text{Cone}(\phi'_{i+1}) \xrightarrow{q'} |\text{Cone}^s(\phi'_{i+1})|$$

where the homotopy equivalences  $\bar{\Phi}_{i+1}$ ,  $H$  and  $q'$  are given respectively by Lemmas 2.2, 2.1 and 4.2.

Therefore our problem is solved, if it were not for the following issue: the map  $H$ , given by Lemma 2.1, depends on a homotopy  $h$  between  $h_i \circ \phi_{i+1} \circ t_{i+1}$  and  $\phi'_{i+1}$ , which may be unknown in practice. As a consequence, we might not be able to compute the map  $h_{i+1}$ , and glue the following cells. In order to circumvent this issue, we will assume that  $\phi'_{i+1}$  actually is a *simplicial approximation* to  $h_i \circ \phi_{i+1} \circ t_{i+1}$ . Indeed, in this case, the homotopy  $h$  is simply given by linear interpolation. As a consequence of this discussion, we obtain the following:

**Proposition 4.4.** *The map  $h_{i+1}: X_{i+1} \rightarrow |K_{i+1}|$  is a homotopy equivalence. Moreover, if  $\phi'_{i+1}$  is a simplicial approximation, then the location map of  $h_{i+1}$ , denoted  $\mathcal{L}_{h_{i+1}}: X_{i+1} \rightarrow K_{i+1}$ , can be computed as follows: if  $x \in X_i$ , return  $\mathcal{L}_{h_i}(x)$ . If  $x \in X_{i+1} \setminus X_i$ , consider  $y = \bar{\Phi}_{i+1}(x)$  and*

- if  $\|y\| \geq \frac{1}{2}$ , let  $x' = \phi_{i+1}\left(\frac{y}{\|y\|}\right)$  and return  $\mathcal{L}_{h_i}(x')$ ,
- if  $\|y\| < \frac{1}{2}$ , let  $\sigma = \mathcal{L}_{h_i}(2y)$ , and return  $\phi'_{i+1}(\sigma)$ .

An implementation of  $\mathcal{L}_{h_{i+1}}$  will be given below in Algorithm 5.

**4.2.2 Concrete implementation** We now describe an implementation of the algorithm. From an informatic perspective, we encode the cells of the CW complex in a data structure, denoted `Cells[0]`, `Cells[1]`, ..., containing:

- `Cells[i].Dimension`: an integer, the dimension of the cell  $e_i$ .
- `Cells[i].Domain`: a function that takes as an input an element  $x \in \mathbb{R}^N$ , and returns `True` if  $x$  is in the cell  $e_i$  or `False` otherwise.
- `Cells[i].GluingMap`: a function representing the gluing map. It takes as an input an element  $x \in \mathbb{S}^{d(i)-1}$ , and returns the element  $\phi_i(x)$  of  $X \subset \mathbb{R}^N$ .
- `Cells[i].InverseCharacteristicMap`: a function representing the inverse characteristic map. It takes as an input an element  $x \in e_i$ , and returns the element  $\Phi_i^{-1}(x)$  of  $\mathcal{B}^{d(i)} \subset \mathbb{R}^{d(i)}$ .

To simplify the exposition, we suppose that  $e_0$  is the unique cell of dimension 0. The algorithm works iteratively, by building the simplicial complexes  $K_0, \dots, K_n$  of §4.2.1. In order to encode the homotopy equivalence  $h_i$  of Proposition 4.4, we should use a data structure, denoted `Skeleta[0]`, `Skeleta[1]`, ..., that contain:

- `Skeleta[i].Complex`: a simplicial complex, representing  $K_i$ .
- `Skeleta[i].LocationMap`: a function, representing the location map  $\mathcal{L}_{h_i}$  of  $h_i$  in Proposition 4.4. It takes as an input an element  $x \in X_i \subset \mathbb{R}^N$  and returns the simplex  $\sigma$  of  $K_i$  such that  $h_i(x) \in |\sigma|$ .

In order to build mapping cones, we also consider the data structures `Spheres[0]`, `Spheres[1]`, ..., containing

- `Spheres[i].Complex`: a simplicial complex, representing  $S_i$ .

- `Spheres[i].Coordinates`: a dictionary, representing the map  $\iota_i$  of Equation (21). It takes as an input a vertex  $x \in S_i^0$  and returns the element  $\iota_i(x)$  of  $\mathbb{S}^{d(i)-1}$ .

We also consider `Balls[0], Balls[1], ...,` containing

- `Balls[i].Complex`: a simplicial complex, representing the simplicial cone  $C^s(S_i)$ .
- `Balls[i].Coordinates`: a dictionary, representing the coordinates of  $C^s(S_i)$ . Further details are given in §4.3.3.

The algorithm reads as follows. A visual representation is given in Figure 30.

---

**Algorithm 4** Simplicial approximation to CW-complexes

---

**Input:** a CW structure given by `Cells[0], Cells[1], ...`  
**Output:** a simplicial complex

```

1: Skeleta[0] = CreateZeroCell()
2: for i = 1, ..., n do
3:   Spheres[i] = TriangulateSphere(Cells[i].Dimension)
4: end for
5: IsSimplicial, Vertices = CheckWeakStarCondition(Spheres[i], Skeleta[i-1],
   Cells[i].GluingMap)
6: while not IsSimplicial do
7:   Spheres[i] = GeneralizedSubdivision(Spheres[i], Vertices)
8:   IsSimplicial, Vertices = CheckWeakStarCondition(Spheres[i], Skeleta[i-1],
   Cell[i].GluingMap)
9: end while
10: Balls[i] = TriangulateBall(Spheres[i])
11: Skeleta[i] = GlueCell(Skeleta[i-1], Balls[i], Cells[i], Vertices)
12: return Skeleta[n]
```

---

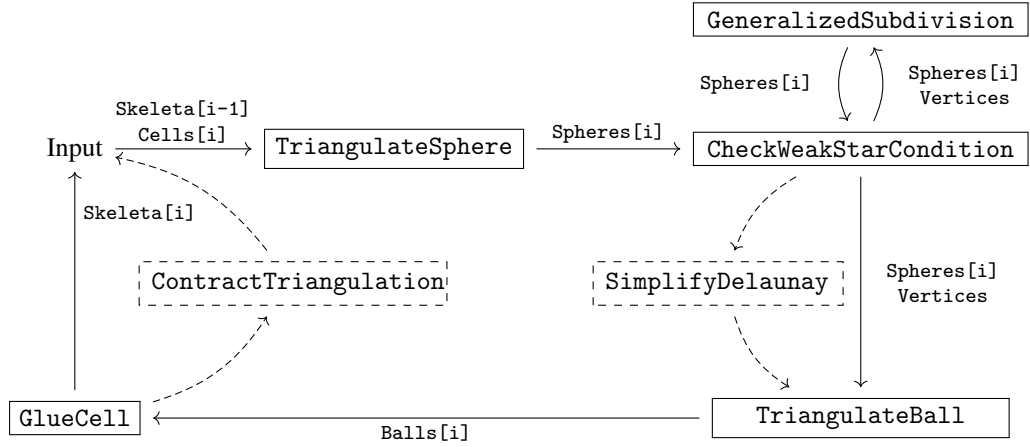


Figure 30: Diagrammatic representation of Algorithm 4. The variables on the arrows are the output of the functions in the boxes. Optional steps are represented in dashed.

The two simplifications procedures—the contraction of the codomain (presented in Subsection 3.4) and the Delaunay simplifications (presented in §3.3.4)—are represented in Figure 30 but not in Algorithm 4.

Let us now describe each of the functions involved in the algorithm.

- `CreateZeroCell`: returns a triangulation of the topological space consisting of only one point.

- **TriangulateSphere**: returns a triangulation of the sphere  $\mathbb{S}^d$ , based on the embedding of  $\partial\Delta^{d+1}$  in  $\mathbb{R}^{d+1}$  described in §3.2.1. Further details are given in §4.3.1.
- **CheckWeakStarCondition**: checks whether the map  $\text{Cells}[i].\text{GluingMap}$ , from  $\text{Spheres}[i].\text{Complex}$  to  $\text{Skeleta}[i-1].\text{Complex}$ , satisfies the weak star condition. If it does not,  $\text{IsSimplicial}$  is `False`, and  $\text{Vertices}$  is the list of vertices where the map does not satisfy the weak star condition. If it does,  $\text{IsSimplicial}$  is `True`, and  $\text{Vertices}$  is a dictionary representing a weak simplicial approximation. In practice, it is chosen randomly among all the weak simplicial approximations.
- **GeneralizedSubdivision**: performs a generalized subdivision to the simplicial complex given in  $\text{Spheres}[i]$ , and following the procedure described in §3.3.2. We draw the attention of the reader to the fact that the loop **CheckStarCondition-GeneralizedSubdivision** is exactly the Algorithm 3 presented before.
- **TriangulateBall**: builds the simplicial cone on  $\text{Spheres}[i]$ , as described in §4.1.3. Further details are given in §4.3.3.
- **GlueCell**: builds the simplicial mapping cone of the simplicial map  $\text{Vertices}$  by identifying the outer part of  $\text{Balls}[i]$  with  $\text{Skeleta}[i-1]$ . In order to define its location map, implemented below, the output  $\text{Skeleta}[i]$  is endowed with the following information:  $\text{Skeleta}[i].\text{Cell} = \text{Cells}[i]$ ,  $\text{Skeleta}[i].\text{Ball} = \text{Balls}[i]$  and  $\text{Skeleta}[i].\text{LowerSkeleton} = \text{Skeleta}[i-1]$ .

Moreover, the optional steps presented in Figure 30 are the following:

- **ContractTriangulation**: contracts the triangulation  $\text{Skeleta}[i]$  by repeated edge contractions, as described in §3.4.2.
- **SimplifyDelaunay**: simplifies the simplicial map  $\text{Vertices}$ , following the Delaunay simplification procedure described in §3.3.4.

Each function that returns a triangulation also endows it with its location map. Details about the implementation of the location map of  $\text{Spheres}[i]$  and  $\text{Balls}[i]$  are given in the next subsection. The location map of  $\text{Skeleta}[i]$  is given as a direct implementation of Proposition 4.4:

---

**Algorithm 5** Location map of the simplicial mapping cone

---

**Input:** a vector  $x$   
**Output:** a simplex

```

1: if self.Cell.Domain( $x$ ) then
2:    $u = \text{self.Cell.InverseCharacteristicMap}(x)$ 
3:   if norm( $u$ ) < 1/2 then
4:      $u = 2*u$ 
5:     simplexBall = self.Ball.LocationMap( $u$ )
6:     simplex = [self.CharacteristicMap[i] for i in simplexBall]
7:     return simplex
8:   else
9:      $u = u/\text{norm}(u)$ 
10:     $x = \text{self.Cell.GluingMap}(u)$ 
11:    return self.LocationMap( $x$ )
12:   end if
13: elsereturn self.LowerSkeleton.LocationMap( $x$ )
14: end if

```

---

**4.2.3 Termination and correctness** As it is presented, Algorithm 4 may not terminate. This behavior may occur when one of the weak simplicial approximations  $\phi'_i$  to  $\phi_i$  is not a simplicial approximation. In this case, Proposition 4.4 might not apply. Therefore the implementation of the location map given in Algorithm 5 might represent a discontinuous map, hence the next gluing map  $\mathbb{S}^d \rightarrow |K_i|$  might not admit a weak simplicial approximation. The algorithm would then be stuck in the loop **CheckWeakStarCondition-GeneralizedSubdivision**. In order

to ensure that the algorithm terminates, one has to verify that each of these maps are simplicial approximations, using for instance the methods sketched in §3.1.3.

Even under this assumption, the algorithm may not terminate, since the `CheckStarCondition-GeneralizedSubdivision` loop does not in general, as we showed in Example 3.11. This loop, which is Algorithm 3, may be substituted by Algorithm 1 or 2, that we know terminate. These results are gathered in the following.

**Theorem 4.5.** *Let  $X$  be a CW complex, and run Algorithm 4 on it.*

*Correctness:* Suppose that each weak simplicial approximation  $\phi_i^l$  computed by the algorithm is homotopy equivalent to  $\phi_i$ . If the algorithm terminates, then it returns a simplicial complex homotopy equivalent to  $X$ .

*Termination:* Suppose that each weak simplicial approximation  $\phi_i^l$  computed by the algorithm is a simplicial approximation to  $\phi_i$ . The termination of Algorithm 4 depends on the algorithm used for the subdivision loop, the subdivision method, and the dimension  $d$  of the complex. It is described in the following table, where a cross indicates that the algorithm does not terminate in general.

	Algorithm 1	Algorithm 2	Algorithm 3
Barycentric	any $d$	any $d$	×
Edgewise	any $d$	any $d$	×
Delaunay barycentric		$d \leq 4$	×
Delaunay edgewise		$d \leq 3$	×

*Proof.* As consequence of Proposition 4.4, the output has the correct homotopy type. Moreover, the termination of the algorithm follows from Propositions 3.1 and 3.4 for barycentric or edgewise subdivisions, and Proposition 3.7 for Delaunay subdivisions.  $\square$

In practice, if the user cannot verify that each  $\phi_i^l$  is homotopic to  $\phi_i$ , they can use the following pre-processing step, that may help the algorithm to terminate. To each `Spheres[i]` output by `TriangulateSphere`, we apply an arbitrary number of global subdivisions before sending it to `CheckWeakStarCondition`. We observed that one or two global subdivisions were enough to ensure that the algorithm terminates on the examples of Subsections 5.1 and 5.3.

### 4.3 Informatic details

We discuss in this subsection a few technical details needed to implement Algorithm 4: the computation of the location map of the sphere and of the ball.

**4.3.1 Triangulation of the sphere** As presented in the previous subsection, the algorithm rely on a function `TriangulateSphere` which, given a positive integer  $d$ , returns a simplicial complex  $K$  and a homeomorphism  $\mathbb{S}^d \rightarrow |K|$ . Our construction has already been given in §3.2.1:  $K$  is the boundary of the standard  $d + 1$ -simplex, embedded in  $\mathbb{R}^{d+1}$  via Equation (13), and the homeomorphism is the radial projection map  $r$ .

From an algorithmic point of view, the map  $r: \mathbb{S}^d \rightarrow |K|$  is given via its location map  $\mathcal{L}_r$  (see §2.2.1). We can compute it following [66, Lemma 9]: given a  $x \in \mathbb{S}^d$ ,

- for each maximal simplex  $\sigma$  of  $K$ , let  $\langle \sigma \rangle \subset \mathbb{R}^{d+1}$  denote the affine hyperplane it spans. Compute whether half-line spanned by  $x$  intersects  $\langle \sigma \rangle$ .
- If it does, check whether this intersection point is inside the convex hull of  $\sigma$ .
- Return the intersection of such all simplices  $\sigma$ .

Each of these processes amount to performing a QR factorization on a  $(d + 1) \times (d + 1)$  matrix. More precisely, given a simplex  $\sigma$  of dimension  $d$  in  $\mathbb{R}^{d+1}$ , one can check if a point  $x$  is inside its convex hull by computing its barycentric coordinates, and by verifying whether they all are greater or equal to zero.

*Remark 4.6.* These previous computations are subject to float-precision errors, which could affect the correctness of the algorithm. In practice, a test of the form ‘ $a \geq 0$ ’ is replaced by ‘ $a \geq -\varepsilon$ ’ with  $\varepsilon$  a small positive number. We did not study the impact of such an approximation.

**4.3.2 Fast location in the sphere** The implementation of the location map of  $r: \mathbb{S}^d \rightarrow |K|$  described above suffers from a crucial problem in practice: all the maximal simplices have to be tested, what may result in a long computation time if  $K$  is large. This is the case when  $K$  has been obtained by repeated subdivisions. In order to speed up this process, we propose to organize the maximal simplices, so as to reduce the number of tests.

First, suppose that  $\text{sub}(K)$  is a barycentric or edgewise subdivision of  $K$ , global or generalized. Using the canonical homeomorphism  $|K| \rightarrow |\text{sub}(K)|$ , we can associate to each maximal simplex  $\sigma$  of  $K$  a collection of maximal simplices of  $\text{sub}(K)$ : those who are contained in it. This collection is denoted  $\mathcal{T}(\sigma)$ . The operator  $\mathcal{T}$  can be seen as a collection of rooted trees of height 2, whose roots are the maximal simplices of  $K$  and whose leaves are the maximal simplices of  $\text{sub}(K)$ . Now, in order to compute the location map of  $\mathbb{S}^d \rightarrow |\text{sub}(K)|$ , it is enough to compute the location map of  $\mathbb{S}^d \rightarrow |K|$ , with output  $\sigma$ , and then to test the simplices of  $\text{sub}(K)$  included in  $\mathcal{T}(\sigma)$ .

In general, if the simplicial complex is the result of a series of subdivisions  $K, \text{sub}^1(K), \dots, \text{sub}^n(K)$ , we can build similarly a collection of rooted trees  $\mathcal{T}$ , whose roots are the maximal simplices of  $K$ , and whose depth  $i$  nodes are maximal simplices of  $\text{sub}^i(K)$ . The successors of a simplex  $\sigma$  in  $\text{sub}^i(K)$  are the simplices of  $\text{sub}^{i+1}(K)$  that contain it. Now, in order to locate a point  $x$  in  $\text{sub}^n(K)$ , it is enough to find a depth-0 simplex that contains it, and to repeat the process with its successors, until reaching a simplex in  $\text{sub}^n(K)$ .

As a first complexity analysis, let us suppose that  $\text{sub}^n(K)$  has been obtained by repeated global barycentric subdivisions on  $K = \partial\Delta^{d+1}$ , the triangulation of  $\mathbb{S}^d$ . The simplicial complex  $K$  has  $d+2$  maximal faces. Since a barycentric subdivision subdivides a  $d$ -simplex into  $(d+1)!$  maximal simplices, we deduce that each  $\text{sub}^i(K)$  has  $(d+2) \times ((d+1)!)^i$  maximal simplices. Hence, the naive implementation of the location map requires  $(d+2) \times ((d+1)!)^n$  operations. In comparison, by using the structure  $\mathcal{T}$ , only  $(d+1)!$  simplices have to be checked at each positive depth, leading to  $(d+2) + n \times (d+1)!$  operations. The improvement is significant: the new complexity is the logarithm of the former one. This conclusion also holds with global edgewise subdivisions.

In the case of iterated generalized Delaunay barycentric or Delaunay edgewise subdivisions, we cannot use the same definition of rooted trees  $\mathcal{T}$ . Indeed, the complex  $\text{sub}^{i+1}(K)$  may not be a subdivision of  $\text{sub}^i(K)$ , hence some simplices of  $\text{sub}^{i+1}(K)$  may not be subsets of a simplex of  $\text{sub}^i(K)$ . However, we can adapt the construction as follows: for any maximal simplex  $\sigma \in \text{sub}^i(K)$ ,  $\mathcal{T}(\sigma)$  is defined as the set of simplices of  $\text{sub}^{i+1}(K)$  that intersect  $\sigma$ . The structure  $\mathcal{T}$  is now a directed graph, which can still be used recursively to compute the location map of the sphere. It is worth noting that our construction of  $\mathcal{T}$  is close to incremental constructions of Delaunay triangulations, such as the *Delaunay tree* or the *Delaunay hierarchy* [13, 24].

**4.3.3 Triangulation of the ball** Let us now describe explicitly the function `TriangulateBall` of Algorithm 4. Let  $f: K \rightarrow L$  be a simplicial map. As described in §4.1.3, the simplicial mapping cone  $\text{Cone}^s(f)$  can be obtained by gluing the simplicial cone  $\text{C}^s(K)$  to  $L$ . Moreover,  $\text{C}^s(K)$  is obtained from the product  $K \times I$  by coning  $K \times \{0\}$  to a new vertex  $x^*$ .

In our context,  $K$  is a triangulation of the sphere  $\mathbb{S}^d$ , hence  $\text{C}^s(K)$  is a triangulation of the ball  $\overline{\mathcal{B}}^{d+1}$ . Based on a geometric realization  $|K| \subset \mathbb{R}^{d+1}$  with  $|K^0| \subset \mathbb{S}^d$ , we can deduce a geometric realization for  $\text{C}^s(K)$  into  $\mathbb{R}^{d+1}$  as follows. Let  $\iota: K^0 \rightarrow \mathbb{S}^d$  be the embedding of the vertices of  $K$  into  $\mathbb{R}^{d+1}$ , and let us separate the vertices of  $\text{C}^s(K)$  into those of the outer layer  $K \times \{1\}$ , those of the inner layer  $K \times \{0\}$ , and the coning point  $x^*$ . Now,

- the vertices  $x$  of  $K \times \{1\}$  are mapped to  $\iota(x)$ ,

- the vertices  $x$  of  $K \times \{0\}$  are mapped to  $\frac{1}{2}t(x)$ ,
- $x^*$  is mapped to the origin  $0 \in \mathbb{R}^{d+1}$ .

The resulting geometric realization is represented in Figure 31. In order to define a homeomorphism  $\overline{\mathcal{B}}^{d+1} \rightarrow |C^s(K)|$ , we enlarge the outer simplices of  $C^s(K)$ , so as to make  $|C^s(K)|$  cover  $\overline{\mathcal{B}}^{d+1}$ .

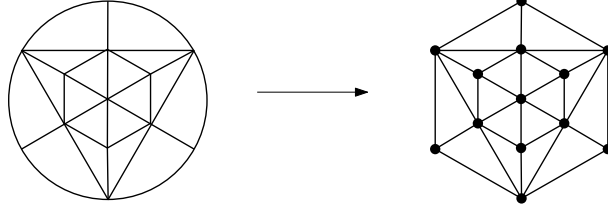


Figure 31: The homeomorphism  $\overline{\mathcal{B}}^2 \rightarrow |C^s(K)|$ .

*Remark 4.7.* In order to embed  $C^s(K)$  into  $\mathbb{R}^{d+1}$ , we arbitrarily placed the vertices of  $K \times \{0\}$  on the sphere of radius  $\frac{1}{2}$ . Of course, we can replace  $\frac{1}{2}$  by any real number in  $(0, 1)$ . This yields another homeomorphism  $\overline{\mathcal{B}}^d \rightarrow |C^s(K)|$ . In practice, we did not observe any significant improvement of the algorithm by changing this value.

**4.3.4 Fast location in the ball** In order to compute the location map  $\overline{\mathcal{B}}^{d+1} \rightarrow |C^s(K)|$ , we could test if every maximal simplex contains the point  $x$ . But this can be improved: as a preprocessing step, and for any maximal simplex  $\sigma$  of the sphere  $K$ , we record the maximal simplices of the ball that are in the ‘quadrant’ defined by  $\sigma$ , as in Figure 32. Now, in order to locate a point  $x \in \overline{\mathcal{B}}^{d+1}$ ,

- we compute the location map of the sphere for the normalized point  $\frac{x}{\|x\|}$ , and denote the output  $\sigma$
- for every simplex  $v$  in the quadrant of  $\sigma$ , we test whether it contains  $x$ ,
- we return the intersection of such simplices  $v$ .

If no simplex in the quadrant contains  $x$ , then  $x$  belongs to an outer simplex, hence we return the first simplex of the quadrant.

In practice, testing if  $x$  belongs to a simplex can be read in its barycentric coordinates, which amounts to performing a QR decomposition on a  $(d+1) \times (d+1)$  matrix. Compared to the naive implementation, subdividing in quadrants allows roughly to reduce the number of computations by a factor of  $d+2$ ,  $d+2$  being equal to the number of maximal simplices in a quadrant.

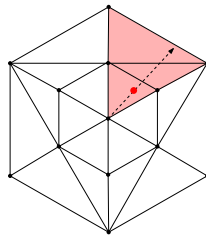


Figure 32: Localization of a point in  $C^s(K)$ . The corresponding quadrant is filled in red.

## 5 Applications

We now apply Algorithm 4 on three families of manifolds: the projective spaces in Subsection 5.1, the lens spaces in Subsection 5.2, and the Grassmannian in Subsection 5.3. We will not

verify the hypotheses of Theorem 4.5, hence we won't be able to conclude that the simplicial complexes have the correct homotopy type. We will only verify that they have the correct homology.

## 5.1 The projective spaces

For any  $n \geq 0$ , the projective space  $\mathbb{R}P^n$  can be defined as the quotient space of the  $n$ -sphere  $\mathbb{S}^n$  by the antipodal relation  $x \sim -x$ . This yields a degree two map  $\mathbb{S}^n \rightarrow \mathbb{R}P^n$ . It can be given the structure of a  $n$ -dimensional manifold. The integral homology groups of  $\mathbb{R}P^3$  are  $\mathbb{Z}$ ,  $\mathbb{Z}/2\mathbb{Z}$ , 0 and  $\mathbb{Z}$ .

**5.1.1 Cell structure for  $\mathbb{R}P^n$**  The projective space admits a cell structure with one cell for each dimension [45, Example 0.4]. Iteratively, one obtains  $\mathbb{R}P^{n+1}$  by attaching a  $(n+1)$ -cell to  $\mathbb{R}P^n$ , whose gluing map is the quotient map  $\mathbb{S}^n \rightarrow \mathbb{R}P^n$  previously defined.

**5.1.2 Result of our algorithm** We now apply Algorithm 4 to triangulate  $\mathbb{R}P^4$ , for the four subdivision methods: barycentric, edgewise, Delaunay barycentric and Delaunay edgewise. For the four of them, we also apply the simplification step of contractions (see Subsection 3.4), and for the Delaunay subdivisions, we apply the Delaunay simplifications (see §3.3.4). We indicate in the following table the number of vertices of the output of the algorithm. Moreover, we indicate in parenthesis the number of vertices before applying edge contractions.

	$\mathbb{R}P^1$	$\mathbb{R}P^2$	$\mathbb{R}P^3$	$\mathbb{R}P^4$
Barycentric	3 (4)	7 (32)	739 (7498)	×
Edgewise	3 (4)	7 (32)	46 (1328)	×
Delaunay barycentric	3 (4)	7 (10)	16 (56)	577 (1923)
Delaunay edgewise	3 (4)	6 (11)	15 (73)	708 (2664)

Table 4: Number of vertices of the output complexes of Algorithm 4 on  $\mathbb{R}P^4$ .

When subdividing the last cell with the barycentric or edgewise subdivision method, our personal computer ran out of memory. On the contrary, Delaunay subdivisions take up little space. This is because of the Delaunay simplification step, which reduces the number of vertices drastically. For instance, with Delaunay barycentric subdivisions, one finds a weak simplicial approximation for the last cell after subdividing  $\mathbb{S}^3$  up to 168'463 vertices. Then, this cell is simplified into a complex with only 1905 vertices. Similarly, with the Delaunay edgewise subdivisions, the Delaunay simplification allows to go from 96'737 to 2647 vertices.

At each step of the algorithm, a triangulation of the ball, `Balls[i]`, is built, whose boundary is `Spheres[i]`, as well as a simplicial map from the sphere to `Skeleton[i-1]`. We represent in the two following figures these balls, in the case of edgewise and Delaunay edgewise subdivisions, up to dimension 3. The colors on the boundary of the balls corresponds to the simplicial maps computed by the algorithm.



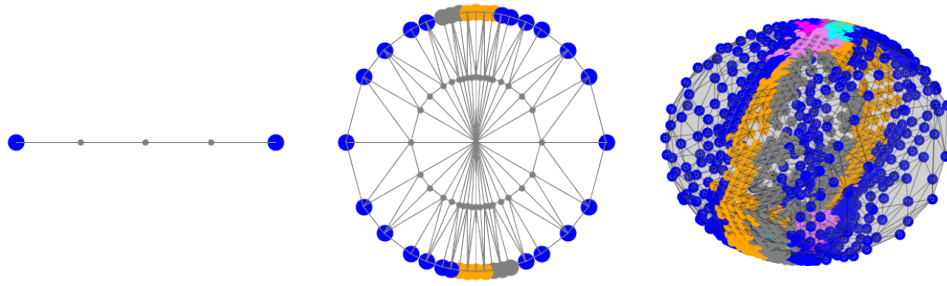


Figure 33: The Balls[i] in Algorithm 4, using edgewise subdivisions.

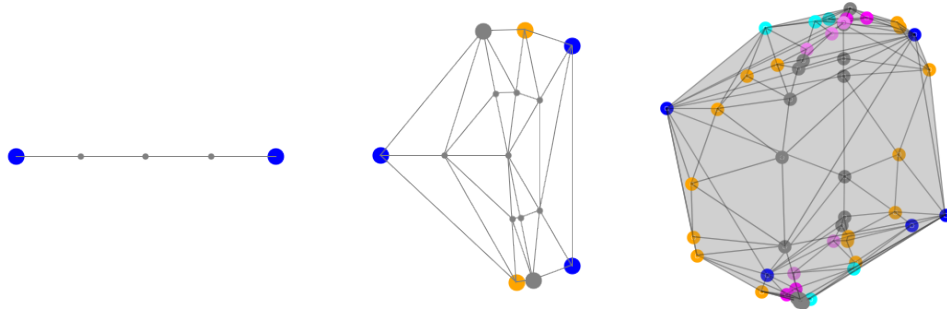


Figure 34: The Balls[i] in Algorithm 4, using Delaunay edgewise subdivisions and simplifications.

**5.1.3 Comparison with minimal triangulations of  $\mathbb{R}P^n$**  It is known that the minimal number of vertices of a triangulation of  $\mathbb{R}P^3$  is 11, and of  $\mathbb{R}P^4$  is 16. Surprisingly, Algorithm 4 may output way larger simplicial complexes. This is the case with barycentric subdivisions on  $\mathbb{R}P^3$ , whose output contains 739 vertices after edge contractions. As a high-level explanation of this phenomenon, we could say that the algorithm tends to produce ‘combinatorially complex’ simplicial approximations, this complexity being inherited to the following cells.

In order to illustrate this comment, let us use Algorithm 4 to glue the last cell of  $\mathbb{R}P^3$ , but now starting with the 7-vertices triangulation of  $\mathbb{R}P^2$  of Kühnel [49]. We obtain simplicial complexes with the following number of vertices: 28 (328 before contraction) for barycentric and 16 (160) for edgewise. These values are lower than the ones obtained in Table 4.

It seems reasonable to conclude that our algorithm does not produce small triangulations in general. In order to obtain triangulations with less vertices, one could use procedures of simplifications of simplicial complexes, such as bistellar moves, studied in the work of Lutz [51].

## 5.2 The 3-dimensional lens spaces

Let  $p$  and  $q$  be two relatively prime integers. The 3-dimensional lens space  $L(p, q)$  can be defined as a quotient of the 3-sphere as follows. Let  $\mathbb{S}^3 \subset \mathbb{C}^2$  be the unit sphere of  $\mathbb{C}^2$ . We consider the action of  $\mathbb{Z}/p\mathbb{Z}$  on  $\mathbb{S}^3$  generated by

$$(z_1, z_2) \mapsto (e^{2i\pi/p} z_1, e^{2i\pi q/p} z_2).$$

It is a free action, and the quotient space is called the lens space  $L(p, q)$ . It can be given the structure of a 3-dimensional smooth manifold.

The lens spaces are interesting objects in algebraic topology: they are not all homotopy equivalent, but the usual invariants do not allow to distinguish them. For instance, we know that  $L(p, q)$  and  $L(p, q')$  are homotopy equivalent if and only if  $qq'$  or  $-qq'$  is a quadratic residue

modulo  $p$ . However, they have the same fundamental group,  $\mathbb{Z}/p\mathbb{Z}$ , as well as the same integral homology groups, equal to  $\mathbb{Z}, \mathbb{Z}/p\mathbb{Z}, 0$  and  $\mathbb{Z}$ .

**5.2.1 Cell structure for  $L(p, q)$**  In order to give it a cell structure, consider the closed unit ball  $\overline{\mathcal{B}} \subset \mathbb{R}^3$ , and define the closed upper and lower hemispheres  $\partial\overline{\mathcal{B}}_+$  and  $\partial\overline{\mathcal{B}}_-$ . Let  $r : \partial\overline{\mathcal{B}}_+ \rightarrow \partial\overline{\mathcal{B}}_+$  be the direct rotation by  $2\pi\frac{q}{p}$  around the  $z$ -axis, and  $\rho : \partial\overline{\mathcal{B}}_+ \rightarrow \partial\overline{\mathcal{B}}_-$  the reflection along the  $(x, y)$ -plane. Then  $L(p, q)$  is homeomorphic to the quotient of  $\overline{\mathcal{B}}$  by the map  $\rho \circ r : \partial\overline{\mathcal{B}}_+ \rightarrow \partial\overline{\mathcal{B}}_-$ . This directly gives a cell structure for  $L(p, q)$ , with one cell per dimension: the first two cells form a circle, the 2-cell is a disk glued by a degree  $p$  map, and the 3-cell is glued by differentiating the two hemispheres, one is glued normally, the other one with a rotation  $2\pi\frac{q}{p}$ .

**5.2.2 Result of our algorithm** We apply Algorithm 4 on  $L(p, q)$  for various values of  $p$  and  $q$ , and for the Delaunay edgewise subdivision method only. We applied the edge contractions and Delaunay simplification steps. We indicate in the following table the number of vertices of the simplicial complexes output by the algorithm.

$q \backslash p$	2	3	4	5	6	7
1	13	19	24	41	48	77
2		16		35		80
3	18		36	30		65
4		21		43		80
5	13	18	28		56	71
6				38		79
7	12	19	27	52	75	

Table 5: Number of vertices of the output complexes of Algorithm 4 on  $L(p, q)$ .

**5.2.3 Lusternik-Schnirelmann (LS) category** We now propose to analyse the triangulations we obtained. In their study of critical points on manifolds, Lusternik and Schnirelmann introduced an invariant of topological spaces, now known as the LS category [50]. Given a topological space  $X$ , we say that an open set  $U \subset X$  is *categorical* if it can be contracted to a point in the ambient space  $X$ . Then  $\text{cat}(X)$  is defined as the minimal number of categorical open sets needed to cover  $X$ , minus one. For instance, the LS category of a contractible space is 0. As other examples, we have  $\text{cat}(\mathbb{S}^n) = 1$ ,  $\text{cat}((\mathbb{S}^1)^n) = n$ ,  $\text{cat}(\mathbb{R}P^n) = n$  [36] and  $\text{cat}(L(p, q)) = 3$  [48].

The Lusternik-Schnirelmann theorem states that, if  $X$  is a smooth manifold satisfying some hypotheses, then the number of critical points of any Morse function on  $X$  is lower bounded by  $\text{cat}(X)$  [22]. Besides, the LS category is linked to the notion of *topological complexity* of a topological space, which has seen applications in the problem of motion planning [32].

The definition of LS category has been adapted to simplicial complexes in several ways. In the sense of [34], a simplicial subcomplex  $L \subset K$  is *categorical* if there exists vertex  $v \in K$  such that the inclusion map  $L \rightarrow K$  and the constant map  $L \rightarrow \{v\} \subset K$  are in the same contiguity class. The minimal number of categorical subcomplexes needed to cover  $K$ , minus one, is defined as the *simplicial LS category*, and is denoted  $\text{scat}(K)$ . The original and the simplicial LS category are linked by the inequality  $\text{cat}(|K|) \leq \text{scat}(K)$ .

As another variation, the notion of *geometric category*, denoted  $\text{gcat}(X)$ , has been introduced in [1]. It has the same definition as the LS category, but an open set is said categorical if it is contractible. This condition being stronger, we have  $\text{cat}(X) \leq \text{gcat}(X)$ . It is worth noting that the geometric category is not a homotopy type invariant, and the previous inequality may be strict.

This notion is adapted to simplicial complexes as follows. We say that the *discrete geometric pre-category* of  $K$  is the minimal number of *collapsible* subcomplexes needed to cover  $K$ , minus one. The *discrete geometric category* is defined as the minimal discrete geometric pre-category over all subcomplexes  $L \subset K$  on which  $K$  collapses. It is denoted  $\text{dgc}at(K)$ . As before, we have  $\text{gcat}(|K|) \leq \text{dgc}at(K)$ . In [42] is proposed an algorithm to estimate the discrete geometric category of  $K$ . This algorithm is random, and outputs an upper bound on  $\text{dgc}at(K)$ . We implemented the algorithm and ran it a thousand times on each triangulations of the lens spaces we obtained in §5.2.2. The following table gathers the lowest values we obtained.

$q \backslash p$	2	3	4	5	6	7
1	3	5	8	8	13	17
2		5		11		18
3	3		9	10		16
4		4		12		18
5	3	5	8		14	17
6				11		19
7	3	5	8	11	15	

Table 6: Upper bound on the discrete geometric category of our triangulations of  $L(p, q)$  using the algorithm of [42].

Of course, these upper bounds are not lower than 3, the LS category of  $L(p, q)$ . However, one observes that they tend to increase with  $p$ . This may be caused by two reasons: either the discrete geometric category of these simplicial complexes are greater than 3, or the algorithm we used has not been able to find an optimal cover of the simplicial complexes. It would be interesting to design an algorithm to compute exactly the discrete geometric category of these spaces. However, as pointed out in [42], the problem of collapsibility of simplicial complexes is undecidable, hence one cannot expect to be able to compute this quantity in general.

### 5.3 The Grassmannian $\mathcal{G}(2, 4)$

The Grassmannians  $\mathcal{G}(d, n)$  form a family of smooth manifolds, indexed by two integers  $d$  and  $n$  such that  $0 \leq d \leq n$ . These parameters being fixed,  $\mathcal{G}(d, n)$  can be understood as the set of  $d$ -dimensional linear subspaces of  $\mathbb{R}^n$ . In particular,  $\mathcal{G}(1, n)$  corresponds to the projective space  $\mathbb{R}P^n$ . In general,  $\mathcal{G}(d, n)$  can be given a structure of a manifold of dimension  $d(n - d)$ . It can also be described as a submanifold of  $\mathcal{M}(\mathbb{R}^n)$ , the space of  $n \times n$  matrices. Namely, it the subset formed by the orthogonal projection matrices of rank  $d$ .

In this subsection, we are interested in  $\mathcal{G}(2, 4)$ , the Grassmannian of planes in  $\mathbb{R}^4$ . It is a manifold of dimension 4, whose integral homology groups are  $\mathbb{Z}$ , 0,  $\mathbb{Z}/2\mathbb{Z}$ ,  $\mathbb{Z}/2\mathbb{Z}$  and  $\mathbb{Z}$ .

**5.3.1 Cell structure for  $\mathcal{G}(2, 4)$**  The classical CW structure for  $\mathcal{G}(d, n)$  is based on Schubert cells [54]. We present here this construction, in the particular case of  $\mathcal{G}(2, 4)$ , but the general case is similar.

The first step consists in parametrizing the planes of  $\mathbb{R}^4$  via their Schubert symbol. To do so, let us endow  $\mathbb{R}^4$  with its canonical basis, and let  $\mathbb{R}^1, \mathbb{R}^2, \mathbb{R}^3$  and  $\mathbb{R}^4$  be the linear subspaces of  $\mathbb{R}^4$  respectively spanned by the first one, two, three and four coordinates. For any plane  $T \in \mathcal{G}(2, 4)$ , the integers

$$\dim(T \cap \mathbb{R}^1), \dim(T \cap \mathbb{R}^2), \dim(T \cap \mathbb{R}^3) \text{ and } \dim(T \cap \mathbb{R}^4)$$

form a non-decreasing sequence, whose steps are at most 1. Consequently, there exist a unique

pair of integers  $\sigma = (\sigma_1, \sigma_2)$  in  $\llbracket 1, 4 \rrbracket$  such that

$$\begin{cases} \dim(T \cap \mathbb{R}^{\sigma_1}) = 1, & \dim(T \cap \mathbb{R}^{\sigma_1-1}) = 0 \\ \dim(T \cap \mathbb{R}^{\sigma_2}) = 2, & \dim(T \cap \mathbb{R}^{\sigma_2-1}) = 1 \end{cases}$$

This pair is called the *Schubert symbol* of  $T$ . The admissible Schubert symbol for planes of  $\mathbb{R}^4$  are the followings:  $(1, 2)$ ,  $(1, 3)$ ,  $(2, 3)$ ,  $(1, 4)$ ,  $(2, 4)$  and  $(3, 4)$ . By denoting  $e_\sigma$  the set of planes that admits  $\sigma$  as a Schubert symbol, we obtain a partition of  $\mathcal{G}(2, 4)$ :

$$\mathcal{G}(2, 4) = e_{1,2} \sqcup e_{1,3} \sqcup e_{1,4} \sqcup e_{2,3} \sqcup e_{2,4} \sqcup e_{3,4}.$$

Next, one shows that each set  $e_\sigma$  is homeomorphic to an open ball. In order to describe this homeomorphism, let us consider, for any integer  $k \in \llbracket 1, 4 \rrbracket$ , the subset  $H^k$  of  $\mathbb{R}^4$  consisting of vectors whose  $k^{\text{th}}$  coordinate is positive, and whose last  $4 - k$  coordinates are zero. Also, let  $s_{\sigma_1}$  be the vector of  $\mathbb{R}^4$  whose coordinates are all zero, except the  $\sigma_1^{\text{th}}$  one which is 1. Now, any plane of  $e_\sigma$  admits a unique orthonormal basis  $(v_1, v_2)$  such that  $v_1 \in H^{\sigma_1}$  and  $v_2 \in H^{\sigma_2}$ , called its *reduced echelon form*. We have an homeomorphism  $e_\sigma \rightarrow \mathcal{B}^{\sigma_1-1} \times \mathcal{B}^{\sigma_2-2}$  given by the composition

$$(v_1, v_2) \mapsto (v_1, R(v_1, v_2)) \mapsto (v'_1, R(v_1, v_2)')$$

where we define

$$R(v_1, v_2) = v_2 - \frac{(s + v_1) \cdot v_2}{1 + s_{\sigma_1} \cdot v_1} (s + v_1) + 2(v_1 \cdot v_2),$$

and where  $v'_1$  is the vector consisting of the first  $\sigma_1 - 1$  coordinates of  $v_1$ , and  $R(v_1, v_2)'$  is the vector consisting of the first  $\sigma_2 - 1$  coordinates of  $R(v_1, v_2)$ , with the  $\sigma_1^{\text{th}}$  one removed. The inverse homeomorphism  $\mathcal{B}^{\sigma_1-1} \times \mathcal{B}^{\sigma_2-2} \rightarrow e_\sigma$  is given by the composition

$$(x, y) \mapsto (x', y') \mapsto (x', R^{-1}(x', y')),$$

where  $x'$  is the vector obtained by adding a last coordinate  $\sqrt{1 - \|x\|^2}$  to  $x$ , and  $y'$  is the vector obtained by adding a last coordinate  $\sqrt{1 - \|y\|^2}$  to  $y$ , and a coordinate 0 at the  $\sigma_1^{\text{th}}$  place. Note that this homeomorphism extends to a continuous map  $\mathcal{B}^{\sigma_1-1} \times \mathcal{B}^{\sigma_2-2} \rightarrow \overline{e_\sigma}$ , where  $\overline{e_\sigma}$  denote the closure of  $e_\sigma$  in  $\mathcal{G}(2, 4)$ . In practice, we can use the following simplified expressions:

$$\begin{aligned} R(v_1, v_2) &= v_2 - \frac{v_2^i}{1 + v_1^i} (s_{\sigma_1} + v_1) \quad \text{when } v_1 \cdot v_2 = 0, \\ R^{-1}(v_1, v_2) &= v_2 - \frac{v_1 \cdot v_2}{1 + v_1^i} (s_{\sigma_1} + v_1) \quad \text{when } s_{\sigma_1} \cdot v_2 = 0, \end{aligned}$$

where  $v_1^i$  and  $v_2^i$  denote the  $i^{\text{th}}$  coordinates of  $v_1$  and  $v_2$ .

**5.3.2 Result of our algorithm** We apply Algorithm 4 on  $\mathcal{G}(2, 4)$ , for the Delaunay edgewise subdivision only, and performing the edge contractions and Delaunay simplification steps. The following table gathers the number of vertices of the complexes at each step, and we indicate in parenthesis the number before edge contractions.

Schubert symbol $\sigma$	(1, 2)	(1, 3)	(2, 3)	(1, 4)	(2, 4)	(3, 4)
Number of vertices	1	3 (4)	6 (10)	10 (13)	22 (93)	825 (3450)

Table 7: Number of vertices of the complexes output by Algorithm 4 on  $\mathcal{G}(2, 4)$ .

We verified that the last complex has the homology of  $\mathcal{G}(2, 4)$ , but we did not verified that it has the same homotopy type.

**5.3.3 Persistent Stiefel-Whitney classes** We now propose an application of the triangulation of  $\mathcal{G}(2,4)$  we obtained: the practical estimation of Stiefel-Whitney classes. These classes, and more generally characteristic classes, are a powerful tool from algebraic topology, defined for any topological space  $X$  endowed with a vector bundle  $\xi$  [54]. The  $i^{\text{th}}$  Stiefel-Whitney class, denoted  $w_i(\xi)$ , is an element of the cohomology group  $H^i(X)$  over  $\mathbb{Z}/2\mathbb{Z}$ . It contains information about the vector bundle. For instance,  $w_1(\xi)$  is zero if and only if  $\xi$  is orientable. In particular, if  $X$  is a compact manifold and  $\xi$  its tangent bundle, then the manifold  $X$  is orientable if and only if  $w_1(\xi) = 0$ .

A few recent works aimed towards the estimation of these classes from datasets. For instance, in [61] are developed several notions of vector bundle adapted to finite simplicial complexes, as well as algorithms to compute the first two Stiefel-Whitney classes. In [66], we proposed a definition of *persistent Stiefel-Whitney classes*, inspired by the theory Persistent Homology. Given a point cloud  $X \subset \mathbb{R}^n$ , a  $d$ -dimensional vector bundle on it, and an integer  $i$ , we also designed an algorithm to compute its  $i^{\text{th}}$  persistent Stiefel-Whitney class. However, this algorithm relies on a triangulation of the Grassmannian  $\mathcal{G}(d,n)$ . At the time we wrote the article, only triangulations of  $\mathcal{G}(1,n)$  were available. Using the triangulation of  $\mathcal{G}(2,4)$  we obtained in this section, we can compute the persistent Stiefel-Whitney classes of bundles of dimension 2.

As a concrete example of application, consider the two sets

$$\left\{ \begin{pmatrix} \cos(\theta) \\ \sin(\theta) \\ t \\ 0 \end{pmatrix} \mid \begin{matrix} \theta \in [0, 2\pi) \\ t \in [-1, 1] \end{matrix} \right\} \quad \text{and} \quad \left\{ \begin{pmatrix} \cos(\theta) \\ \sin(\theta) \\ t \cos(\theta/2) \\ t \sin(\theta/2) \end{pmatrix} \mid \begin{matrix} \theta \in [0, 2\pi) \\ t \in [-1, 1] \end{matrix} \right\}.$$

The first one is homeomorphic to the cylinder  $\mathbb{S}^1 \times [0, 1]$ , and the second one to the Möbius strip. These spaces are not homeomorphic, although their homology groups agree. We generate samples of these sets, denoted  $X$  and  $Y$ , consisting respectively of 1392 and 1370 points.

In Topological Data Analysis, one studies a point cloud dataset by computing its persistence barcodes [17, 19]. We represent on Figure 35 the  $H_1$ -persistence barcodes of the Rips filtration of  $X$  and  $Y$  over  $\mathbb{Z}/2\mathbb{Z}$ . Both on them consists of one salient bar, representing a persistent class in  $H_1$ . As we see, the persistence barcodes do not allow to differentiate between  $X$  and  $Y$ , just as the homology groups do not allow to differentiate between the cylinder and the Möbius strip.

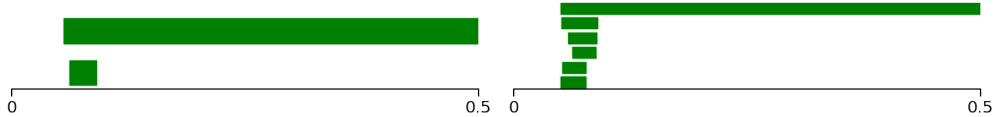


Figure 35:  $H_1$ -persistence barcodes of the Rips filtration of  $X$  and  $Y$  over  $\mathbb{Z}/2\mathbb{Z}$ .

We will now compute the characteristic classes. First,  $X$  and  $Y$  have to be endowed with a vector bundle. To do so, we estimate their tangent bundles, using local Principal Component Analysis, as described in [65]. We then compute their first persistent Stiefel-Whitney classes, following [66]. The information given by such a class is summarized in the *lifebar*, that we represent on Figure 36. One reads that the persistent Stiefel-Whitney class of  $X$  is trivial up to  $t = 0.1$ , while the one of  $Y$  is non-trivial from  $t \approx 0.05$ . This indicates that the  $X$  has been sampled from an orientable space, and  $Y$  from a non-orientable one. In conclusion, we have been able to estimate that these point clouds come from non-homeomorphic spaces.



Figure 36: Lifebars of the first persistent Stiefel-Whitney classes of the estimated tangent bundles of  $X$  and  $Y$ .

## 6 Conclusion

In this paper, we presented and analysed Algorithm 4, an implementation of simplicial approximation to CW complexes. We applied it to  $\mathbb{R}P^4$ , the lens spaces and the Grassmannian  $\mathcal{G}(2, 4)$ . The correctness of the algorithm, stated in Theorem 4.5, depends on some additional verifications, that we did not implement.

The algorithm is not deterministic: various random choices are made, when selecting a weak simplicial approximation, when contracting edges, and when applying Delaunay simplifications. It would be interesting to investigate how to make optimal choices, in the sense that the algorithm would yield complexes with fewer vertices.

In order to perform simplicial approximation, we implemented the edgewise and barycentric subdivisions, and adapted these methods to Delaunay complexes. When dealing with Delaunay complexes, however, we can think of more specific subdivision processes. For instance, we could add the points that corresponds to the center of the Delaunay spheres of the complex.

A last remark concerning the limitations of our algorithm. In our examples, we considered manifold of dimension at most 4. Applying the algorithm on higher dimensional manifolds may lead to memory limitation problems. As an example, in order to triangulate manifolds of dimension 5, one has to glue 5-dimensional cells, whose boundaries are 4-spheres. Applying only 5 global barycentric subdivisions to the 4-sphere  $\partial\Delta^{4+1}$  yields a simplicial complex with  $(4+2)(4+1)!^5$  maximal simplices, that is, approximately 140 Gigabytes of memory, more than a common personal computer. We plan to investigate such memory limitations in a further work.

## A Notations

Throughout the paper, we adopt the following notations:

- $\mathbb{Z}$  is the set of integers and  $\mathbb{Z}/n\mathbb{Z}$  the cyclic group of order  $n$ . If  $i$  and  $j$  are integers such that  $i \leq j$ , then  $[i, j]$  denotes the set of integers between  $i$  and  $j$  included.
- $\mathbb{R}^n$  is the Euclidean space of dimension  $n$ ,  $\mathbb{S}^d$  the unit sphere of  $\mathbb{R}^{d+1}$ ,  $\mathcal{B}^{d+1}$  and  $\overline{\mathcal{B}}^{d+1}$  the open and closed unit balls of  $\mathbb{R}^{d+1}$ . Moreover,  $\|\cdot\|$  denotes the Euclidean norm on  $\mathbb{R}^n$  and  $d_{\mathbb{S}^d}(\cdot, \cdot)$  the geodesic distance on  $\mathbb{S}^d$ .
- If  $X$  is a topological space,  $H_i(X)$  (resp.  $H^i(X)$ ) denotes its  $i^{\text{th}}$  singular homology (resp. cohomology) group over a specified ring. If  $f: X \rightarrow Y$  is a continuous map,  $f_*: H_i(X) \rightarrow H_i(Y)$  (resp.  $f^*: H^i(X) \leftarrow H^i(Y)$ ) is the map induced in homology (resp. cohomology). Also,  $\pi_d(X)$  denotes the  $d^{\text{th}}$  homotopy group of  $X$ , and  $[X, Y]$  the set of homotopy classes of maps  $X \rightarrow Y$ .
- Moreover, if  $\mathcal{U}$  is an open cover of  $X$ ,  $\Lambda_{\mathcal{U}}$  denotes its local Lebesgue number (see §3.4.3).
- If  $K$  is an abstract simplicial complex,  $K^i$  denotes its  $i$ -skeleton. For every vertex  $v \in K^0$ ,  $\text{St}(v)$  and  $\overline{\text{St}}(v)$  denote its open and closed star. For any simplex  $\sigma \in K$ ,  $\text{Lk}(\sigma)$  denotes its link, and  $\overline{\sigma}$  the subcomplex of  $K$  consisting of  $\sigma$  and all its subsets. The simplicial homology and cohomology groups of  $K$  are denoted  $H_i(K)$  and  $H^i(K)$ .
- Moreover, the first barycentric or edgewise subdivision of  $K$  are denoted  $\text{sub}(K)$ , and iterated subdivisions  $\text{sub}^i(K)$  (see Subsection 2.3). If  $L \subset K$  is a simplicial subcomplex,  $\text{sub}(K; L)$  is the generalized subdivision of  $K$  holding  $L$  fixed (see §3.3.1).
- If  $K, L$  are two *ordered* simplicial complexes,  $K \times L$  denotes their product (see §4.1.1).
- If  $X \subset \mathbb{S}^d$  is a finite subset,  $\text{Del}(X)$  is its Delaunay complex (see §3.2.3). Its iterated barycentric or edgewise Delaunay subdivisions are denoted  $\text{sub}^i(\text{Del}(X))$  (see

§3.2.4). Its generalized subdivision holding a subcomplex  $L \subset \text{Del}(X)$  fixed is denoted  $\text{sub}(\text{Del}(X); K)$  (see §3.3.3).

- If  $K$  is a geometric simplicial complex, its geometric realization is denoted  $|K|$ , and the geometric realization of any subset  $L \subset K$  is  $|L|$ . Its location map is denoted  $\mathcal{L}_K: |K| \rightarrow K$ . If  $h: X \rightarrow |K|$  is a continuous map, its location map is denoted  $\mathcal{L}_h: X \rightarrow K$  (see §2.2.1).
- Moreover,  $\delta(K)$  denotes the length of the largest edge of  $K$ . If  $|K^0| \subset \mathbb{S}^d$ , then  $\delta_{\mathbb{S}^d}(K)$  denotes the largest length with respect to the geodesic distance.
- If  $X$  is a topological space,  $C(X)$  is its cone. If  $f$  is a continuous map,  $\text{Cyl}(f)$  and  $\text{Cone}(f)$  are its mapping cylinder and mapping cone (see §2.1.2).
- If  $K$  is a simplicial complex,  $C^s(K)$  is its simplicial cone. If  $f$  is a simplicial map,  $\text{Cyl}^s(f)$  and  $\text{Cone}^s(f)$  are its simplicial mapping cylinder and simplicial mapping cone (see Subsection 4.1).
- $\mathbb{R}P^n$  is the projective space of dimension  $n$ ,  $L(p, q)$  the 3-dimensional lens space with parameters  $p$  and  $q$ , and  $\mathcal{G}(2, \mathbb{R}^4)$  is the Grassmannian of 2-planes in  $\mathbb{R}^4$ .
- $\ell$  is the map introduced in Lemma 3.3.

## B Supplementary results

In this appendix, we expose our choices for the generalized edgewise subdivision, introduced in §3.3.1. We then prove Lemma B.1, used in the proof of Lemma 4.2, and Lemma B.2, used in Subsection 5.3.

**Generalized edgewise subdivisions** In order to define generalized *edgewise* subdivisions, as discussed in §3.3.1, we have to solve the following problem: given a simplex  $\sigma$  and  $\mathcal{E} \subset \sigma^1$  a subset of edges, give a triangulation  $K(\sigma)$  of  $\sigma$  such that the vertices of  $K$  are the vertices of  $\sigma$  plus the midpoints of edges in  $\mathcal{E}$ . Moreover, we impose the following hereditary condition: if  $v$  is a face of  $\sigma$ , then  $K(v)$  is a simplicial sub-complex of  $K(\sigma)$ . We will expose our choices for simplices only up to dimension 3, although we think that this method can be extended to arbitrary dimension.

If  $\sigma$  has dimension  $d$ , then its set of edges has cardinal  $d + 1$ , and there are  $2^{d+1}$  choices for  $\mathcal{E}$ . Hence we have to distinguish 8 cases in dimension 2, and 16 cases in dimension 3. However, not all of these cases will happen in practice. Indeed, as described in §3.3.2, the edges in  $\mathcal{E}$  come from particular construction: they are the edges that intersect a subset of vertices  $V$  of  $\sigma$ . Hence we only have to describe the subdivided complex  $K(\sigma)$  for a choice of vertices  $V \subset \sigma^0$ . Our choices are gathered in the following Tables 8 and 9, respectively for  $\sigma$  of dimension 2 and of dimension 3. If  $[a, b]$  is an edge of  $K$ , we denote by  $\widehat{ab}$  its midpoint.

Vertices $V$	Edges $\mathcal{E}$	Simplices $K(\sigma)$
$\emptyset$	$\emptyset$	$[0, 1, 2]$
0	$[0, 1], [0, 2]$	$[0, \widehat{01}, \widehat{02}], [\widehat{01}, 1, 2], [\widehat{01}, \widehat{02}, 2]$
1	$[0, 1], [1, 2]$	$[\widehat{01}, 1, \widehat{12}], [\widehat{01}, \widehat{12}, 2], [0, \widehat{01}, 2]$
2	$[0, 2], [1, 2]$	$[\widehat{02}, 1, \widehat{12}], [0, \widehat{02}, 1], [\widehat{02}, \widehat{12}, 2]$
$\left. \begin{array}{l} 0, 1 \\ 0, 2 \\ 1, 2 \end{array} \right\}$ $0, 1, 2$	$[0, 1], [0, 2], [1, 2]$	$[\widehat{01}, 1, \widehat{12}], [0, \widehat{01}, \widehat{02}], [\widehat{02}, \widehat{12}, 2], [\widehat{01}, \widehat{02}, \widehat{12}]$

Table 8: Our choices for the generalized edgewise subdivisions of the triangle  $\Delta^2$ .

Vertices $V$	Edges $\mathcal{E}$	Simplices $K(\sigma)$
$\emptyset$	$\emptyset$	$[0, 1, 2, 3]$
0	$[0, 1], [0, 2], [0, 3]$	$[\widehat{01}, \widehat{02}, \widehat{03}, 3], [0, \widehat{01}, \widehat{02}, \widehat{03}], [\widehat{01}, 1, 2, 3], [\widehat{01}, \widehat{02}, 2, 3]$
1	$[0, 1], [1, 2], [1, 3]$	$[0, \widehat{01}, 2, 3], [\widehat{01}, \widehat{12}, \widehat{13}, 3], [\widehat{01}, 1, \widehat{12}, \widehat{13}], [\widehat{01}, \widehat{12}, 2, 3]$
2	$[0, 2], [1, 2], [2, 3]$	$[0, \widehat{02}, 1, 3], [\widehat{02}, 1, \widehat{12}, 3], [\widehat{02}, \widehat{12}, \widehat{23}, 3], [\widehat{02}, \widehat{12}, 2, \widehat{23}]$
3	$[0, 3], [1, 3], [2, 3]$	$[\widehat{03}, \widehat{13}, \widehat{23}, 3], [\widehat{03}, 1, \widehat{13}, 2], [\widehat{03}, \widehat{13}, 2, \widehat{23}], [0, \widehat{03}, 1, 2]$
0, 1	$[0, 1], [0, 2], [0, 3], [1, 2], [1, 3]$	$[\widehat{01}, \widehat{03}, \widehat{12}, \widehat{13}], [\widehat{02}, \widehat{03}, \widehat{12}, 3], [0, \widehat{01}, \widehat{02}, \widehat{03}], [\widehat{01}, \widehat{02}, \widehat{03}, \widehat{12}], [\widehat{03}, \widehat{12}, \widehat{13}, 3], [\widehat{02}, \widehat{12}, 2, 3], [\widehat{01}, 1, \widehat{12}, \widehat{13}]$
0, 2	$[0, 1], [0, 2], [0, 3], [1, 2], [2, 3]$	$[\widehat{01}, \widehat{03}, \widehat{12}, 3], [\widehat{03}, \widehat{12}, \widehat{23}, 3], [0, \widehat{01}, \widehat{02}, \widehat{03}], [\widehat{01}, \widehat{02}, \widehat{03}, \widehat{12}], [\widehat{02}, \widehat{03}, \widehat{12}, \widehat{23}], [\widehat{01}, 1, \widehat{12}, 3], [\widehat{02}, \widehat{12}, 2, \widehat{23}]$
0, 3	$[0, 1], [0, 2], [0, 3], [1, 3], [2, 3]$	$[0, \widehat{01}, \widehat{02}, \widehat{03}], [\widehat{01}, \widehat{02}, \widehat{03}, \widehat{23}], [\widehat{03}, \widehat{13}, \widehat{23}, 3], [\widehat{01}, 1, \widehat{13}, 2], [\widehat{01}, \widehat{03}, \widehat{13}, \widehat{23}], [\widehat{01}, \widehat{13}, 2, \widehat{23}], [\widehat{01}, \widehat{02}, 2, \widehat{23}]$
1, 2	$[0, 1], [0, 2], [1, 2], [1, 3], [2, 3]$	$[\widehat{01}, \widehat{12}, \widehat{13}, \widehat{23}], [\widehat{01}, \widehat{02}, \widehat{23}, 3], [\widehat{01}, \widehat{13}, \widehat{23}, 3], [0, \widehat{01}, \widehat{02}, 3], [\widehat{01}, \widehat{02}, \widehat{12}, \widehat{23}], [\widehat{01}, 1, \widehat{12}, \widehat{13}], [\widehat{02}, \widehat{12}, 2, \widehat{23}]$
1, 3	$[0, 1], [0, 3], [1, 2], [1, 3], [2, 3]$	$[\widehat{03}, \widehat{13}, \widehat{23}, 3], [\widehat{01}, \widehat{03}, \widehat{12}, \widehat{13}], [\widehat{03}, \widehat{12}, 2, \widehat{23}], [0, \widehat{01}, \widehat{03}, 2], [\widehat{01}, \widehat{03}, \widehat{12}, 2], [\widehat{01}, 1, \widehat{12}, \widehat{13}], [\widehat{03}, \widehat{12}, \widehat{13}, \widehat{23}]$
2, 3	$[0, 2], [0, 3], [1, 2], [1, 3], [2, 3]$	$[\widehat{03}, \widehat{13}, \widehat{23}, 3], [0, \widehat{02}, \widehat{03}, 1], [\widehat{02}, \widehat{03}, \widehat{12}, \widehat{23}], [\widehat{03}, 1, \widehat{12}, \widehat{13}], [\widehat{03}, \widehat{12}, \widehat{13}, \widehat{23}], [\widehat{02}, \widehat{03}, 1, \widehat{12}], [\widehat{02}, \widehat{12}, 2, \widehat{23}]$
0, 1, 2	$\left. \begin{array}{l} [0, 1], [0, 2], [0, 3], [1, 2], [1, 3], [2, 3] \end{array} \right\}$	$[\widehat{03}, \widehat{13}, \widehat{23}, 3], [\widehat{01}, \widehat{03}, \widehat{12}, \widehat{13}], [0, \widehat{01}, \widehat{02}, \widehat{03}], [\widehat{01}, \widehat{02}, \widehat{03}, \widehat{12}], [\widehat{02}, \widehat{03}, \widehat{12}, \widehat{23}], [\widehat{01}, 1, \widehat{12}, \widehat{13}], [\widehat{03}, \widehat{12}, \widehat{13}, \widehat{23}], [\widehat{02}, \widehat{12}, 2, \widehat{23}]$
0, 1, 3		
0, 2, 3		
1, 2, 3		
0, 1, 2, 3		

Table 9: Our choices for the generalized edgewise subdivisions of the tetrahedron  $\Delta^3$ .



In the following figure, we represent the subdivided complexes  $K(\sigma)$  for some subsets  $V \subset \sigma^0$ , represented in red.

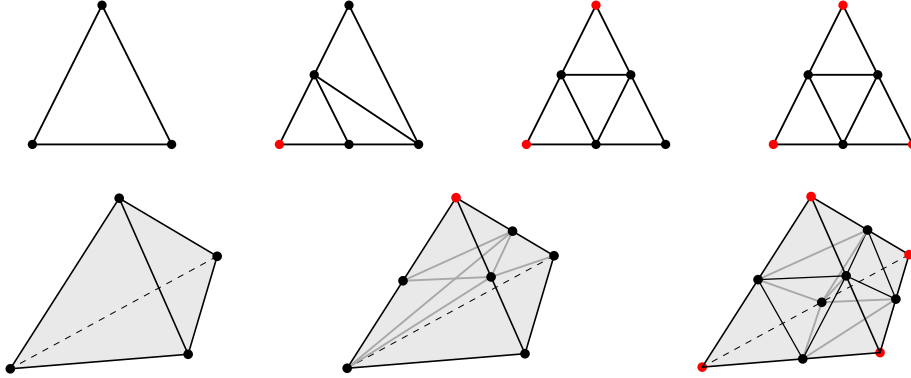


Figure 37: Examples of generalized edgewise subdivisions in dimension 2 and 3.

**Technical lemmas** The following result has been used in §4.1.3.

**Lemma B.1.** *Let  $X$  be a CW complex,  $A' \subset A \subset X$  subcomplexes, and  $r: A \rightarrow A'$  a retraction that comes from a deformation retraction. Let  $X/r$  be the quotient space obtained by identifying each  $x \in A$  to  $r(x)$ . Then the quotient map  $q: X \rightarrow X/r$  is a homotopy equivalence.*

*Proof.* The proof is almost identical to [45, Proposition 0.17]. Let  $f: A \times [0, 1] \rightarrow A$  be a homotopy between the identity map on  $A$  and the retraction  $r$ . Since  $(X, A)$  is a CW pair, it has the extension property [45, Proposition 0.16], hence we can extend the homotopy to  $f: X \times [0, 1] \rightarrow X$ . By definition of a deformation retraction,  $f$  satisfies  $f(a, t) = a$  for all  $a \in A'$ , and so does  $q \circ f_t$ . Consequently, the maps  $q \circ f_t$  descends to the quotients. We denote them  $\bar{f}_t$ . Besides, the map  $f_1$  hence satisfies  $f_1(a) = r(a)$  for all  $a \in A$ . Hence it induces a map  $g: X/r \rightarrow X$ . We obtain the two following commutative diagrams:

$$\begin{array}{ccc} X & \xrightarrow{f_t} & X \\ \downarrow q & & \downarrow q \\ X/r & \xrightarrow{\bar{f}_t} & X/r \end{array} \qquad \begin{array}{ccc} X & \xrightarrow{f_1} & X \\ \downarrow q & \nearrow g & \downarrow q \\ X/r & \xrightarrow{\bar{f}_1} & X/r \end{array}$$

We now see that  $(q, g)$  forms a homotopy equivalence between  $X$  and  $X/r$ , since  $g \circ q$  is homotopic to the identity  $X \rightarrow X$  via  $f_t$ , and  $q \circ g$  is homotopic to the identity  $X/r \rightarrow X/r$  via  $\bar{f}_t$ .  $\square$

This last lemma is used in Subsection 5.3.

**Lemma B.2.** *Let  $\bar{\mathcal{B}}^n$  denote the closed unit ball of  $\mathbb{R}^n$ . For any  $n, m \geq 0$ , we have a homeomorphism  $\bar{\mathcal{B}}^{n+m} \rightarrow \bar{\mathcal{B}}^n \times \bar{\mathcal{B}}^m$  given by*

$$(x_1, \dots, x_n, y_1, \dots, y_m) \mapsto \frac{\|(x, y)\|}{\max(\|x\|, \|y\|)}(x, y)$$

and whose inverse is

$$(x_1, \dots, x_n, y_1, \dots, y_m) \mapsto \frac{\max(\|x\|, \|y\|)}{\|(x, y)\|}(x, y).$$

**Acknowledgements** I wish to thank Marc Glisse, Kristóf Huszár and Mathijs Wintraecken for interesting discussions and references.

## References

- [1] Aaronson, S., Scoville, N.A.: Lusternik–Schnirelmann category for simplicial complexes. *Illinois Journal of Mathematics* **57**(3), 743–753 (2013)
- [2] Adiprasito, K., Avvakumov, S., Karasev, R.: A subexponential size triangulation of  $RP^n$ . *Combinatorica* pp. 1–8 (2021)
- [3] Akbulut, S., McCarthy, J.D.: Casson’s invariant for oriented homology 3-spheres, volume 36 of. *Mathematical Notes* pp. 217–231 (1990)
- [4] Amenta, N., Choi, S., Dey, T.K., Leekha, N.: A simple algorithm for homeomorphic surface reconstruction. In: *Proceedings of the sixteenth annual symposium on Computational geometry*, pp. 213–222 (2000)
- [5] Attali, D., Lieutier, A., Salinas, D.: Efficient data structure for representing and simplifying simplicial complexes in high dimensions. *International Journal of Computational Geometry & Applications* **22**(04), 279–303 (2012). URL <https://hal.archives-ouvertes.fr/hal-00579902/document>
- [6] Barber, C.B., Dobkin, D.P., Huhdanpaa, H.: The quickhull algorithm for convex hulls. *ACM Transactions on Mathematical Software (TOMS)* **22**(4), 469–483 (1996)
- [7] Bauer, U.: Ripser: efficient computation of Vietoris–Rips persistence barcodes. *Journal of Applied and Computational Topology* pp. 1–33 (2021)
- [8] Bell, M., Hall, T., Schleimer, S.: Twister (computer software). [https://bitbucket.org/Mark\\_Bell/twister/](https://bitbucket.org/Mark_Bell/twister/) (2008–2014). Version 2.4.1
- [9] Biss, D.K.: The homotopy type of the matroid Grassmannian. *Annals of mathematics* pp. 929–952 (2003)
- [10] Biss, D.K.: Erratum to “the homotopy type of the matroid grassmannian”. *Annals of mathematics* **170**(1), 493–493 (2009)
- [11] Boissonnat, J.D., Chazal, F., Yvinec, M.: In: *Geometric and topological inference*, vol. 57. Cambridge University Press (2018)
- [12] Boissonnat, J.D., Ghosh, A.: Manifold reconstruction using tangential Delaunay complexes. *Discrete & Computational Geometry* **51**(1), 221–267 (2014)
- [13] Boissonnat, J.D., Teillaud, M.: On the randomized construction of the Delaunay tree. *Theoretical Computer Science* **112**(2), 339–354 (1993)
- [14] Bosma, W., Cannon, J., Playoust, C.: The Magma algebra system. I. The user language. *J. Symbolic Comput.* **24**(3–4), 235–265 (1997). DOI 10.1006/jSCO.1996.0125. URL <http://dx.doi.org/10.1006/jSCO.1996.0125>. Computational algebra and number theory (London, 1993)
- [15] Brown, K.Q.: Geometric transforms for fast geometric algorithms. Tech. rep., Carnegie-Mellon Univ Pittsburgh PA Dept Of Computer Science (1979)
- [16] Burton, B.A., Budney, R., Pettersson, W., et al.: Regina: Software for low-dimensional topology. <http://regina-normal.github.io/> (1999–2021)
- [17] Carlsson, G.: Topology and data. *Bulletin of the American Mathematical Society* **46**(2), 255–308 (2009)
- [18] Caroli, M., de Castro, P.M., Lorient, S., Rouiller, O., Teillaud, M., Wormser, C.: Robust and efficient Delaunay triangulations of points on or close to a sphere. In: *International Symposium on Experimental Algorithms*, pp. 462–473. Springer (2010)

- [19] Chazal, F., Michel, B.: An introduction to Topological Data Analysis: fundamental and practical aspects for data scientists. *Frontiers in Artificial Intelligence* **4** (2021)
- [20] Cheeger, J.: A combinatorial formula for Stiefel-Whitney classes. In: *Proceedings of Georgia topology conference*, pp. 470–471 (1969)
- [21] Cohen, M.M.: Simplicial structures and transverse cellularity. *Annals of Mathematics* pp. 218–245 (1967)
- [22] Cornea, O., Lupton, G., Oprea, J., Tanré, D., et al.: Lusternik-Schnirelmann category. 103. *American Mathematical Soc.* (2003)
- [23] Culler, M., Dunfield, N.M., Goerner, M., Weeks, J.R.: SnapPy, a computer program for studying the geometry and topology of 3-manifolds. Available at <http://snappy.computop.org> (02/12/2021)
- [24] Devillers, O.: The Delaunay hierarchy. *International Journal of Foundations of Computer Science* **13**(02), 163–180 (2002)
- [25] Dey, T.K., Edelsbrunner, H., Guha, S., Nekhayev, D.V.: Topology preserving edge contraction. In: *Publ. Inst. Math.(Beograd)*. Citeseer (1998)
- [26] Dey, T.K., Hirani, A.N., Krishnamoorthy, B., Smith, G.: Edge contractions and simplicial homology. *arXiv preprint arXiv:1304.0664* (2013). URL <https://arxiv.org/pdf/1304.0664.pdf>
- [27] Edelsbrunner, H., Grayson, D.R.: Edgewise subdivision of a simplex. *Discrete & Computational Geometry* **24**(4), 707–719 (2000)
- [28] Edelsbrunner, H., Letscher, D., Zomorodian, A.: Topological persistence and simplification. In: *Proceedings 41st annual symposium on foundations of computer science*, pp. 454–463. *IEEE* (2000)
- [29] Edelsbrunner, H., Shah, N.R.: Triangulating topological spaces. In: *Proceedings of the tenth annual symposium on Computational geometry*, pp. 285–292 (1994)
- [30] Effenberger, F., Spreer, J.: simpcomp - a GAP toolkit for simplicial complexes, Version 2.1.14 (2022)
- [31] Eilenberg, S., Steenrod, N.: *Foundations of algebraic topology*. Princeton University Press (2015)
- [32] Farber, M.: Topological complexity of motion planning. *Discrete and Computational Geometry* **29**(2), 211–221 (2003)
- [33] Feder, T., Hell, P.: List homomorphisms to reflexive graphs. *Journal of Combinatorial Theory, Series B* **72**(2), 236–250 (1998)
- [34] Fernández-Ternero, D., Macías-Virgós, E., Vilches, J.A.: Lusternik–Schnirelmann category of simplicial complexes and finite spaces. *Topology and its Applications* **194**, 37–50 (2015)
- [35] Filakovský, M., Franek, P., Wagner, U., Zhechev, S.: Computing simplicial representatives of homotopy group elements. *Journal of applied and computational topology* **2**(3), 177–231 (2018)
- [36] Fişekci, S., Vandembroucq, L.: On the LS-category and topological complexity of projective product spaces. *Journal of Homotopy and Related Structures* **16**(4), 769–780 (2021)
- [37] Franek, P., Ratschan, S.: Effective topological degree computation based on interval arithmetic. *Mathematics of Computation* **84**(293), 1265–1290 (2015)

- [38] Gaifullin, A.A.: Configuration spaces, bistellar moves, and combinatorial formulae for the first pontryagin class. *Proceedings of the Steklov Institute of Mathematics* **268**(1), 70–86 (2010)
- [39] Goldstein, R.Z., Turner, E.C.: A formula for Stiefel-Whitney homology classes. *Proceedings of the American Mathematical Society* **58**(1), 339–342 (1976)
- [40] Gorodkov, D.: A 15-vertex triangulation of the quaternionic projective plane. *Discrete & Computational Geometry* **62**(2), 348–373 (2019)
- [41] Govc, D., Marzantowicz, W., Pavešić, P., et al.: How many simplices are needed to triangulate a Grassmannian? *Topological Methods in Nonlinear Analysis* (2020)
- [42] Green, B., Scoville, N.A., Tsuruga, M.: Estimating the discrete Lusternik-Schnirelmann category. *Topological Methods in Nonlinear Analysis* **45**(1), 103–116 (2015)
- [43] Group, T.G.: Gap – groups, algorithms, and programming, version 4.11.1. <https://www.gap-system.org> (2021)
- [44] Harker, S., Mischaikow, K., Mrozek, M., Nanda, V., Wagner, H., Juda, M., Dlotko, P.: The efficiency of a homology algorithm based on discrete morse theory and coreductions. *Image-A: Applicable Mathematics in Image Engineering*, 1 (1), 41-48 (2010)
- [45] Hatcher, A.: *Algebraic topology*. Cambridge University Press (2002)
- [46] Knudson, K.P.: Approximate triangulations of Grassmann manifolds. *Algorithms* **13**(7), 172 (2020)
- [47] Kozlov, D.: *Combinatorial algebraic topology*. Springer Science & Business Media (2008)
- [48] Krasnosel’skii, M.: On special coverings of a finite-dimensional sphere. In: *Dokl. Akad. Nauk SSSR (NS)*, vol. 103, pp. 961–964 (1955)
- [49] von Kühnel, W.: Minimal triangulations of Kummer varieties. In: *Abhandlungen aus dem Mathematischen Seminar der Universität Hamburg*, vol. 57, pp. 7–20. Springer (1987)
- [50] Lusternik, L., Schnirelmann, L., Kravtchenko, J.: Méthodes topologiques dans les problèmes variationnels. première partie: Espaces à un nombre fini de dimensions. *Revue de Métaphysique et de Morale* **42**(1) (1935)
- [51] Lutz, F.H.: *Triangulated manifolds with few vertices and vertex-transitive group actions* (1999)
- [52] Manolescu, C.: Lectures on the triangulation conjecture. arXiv preprint arXiv:1607.08163 (2016)
- [53] Maria, C., Boissonnat, J.D., Glisse, M., Yvinec, M.: The gudhi library: Simplicial complexes and persistent homology. In: *International congress on mathematical software*, pp. 167–174. Springer (2014)
- [54] Milnor, J., Stasheff, J.D.: *Characteristic classes*.(am-76). Princeton university press (2016)
- [55] Mischaikow, K., Gameiro, M.: CHomP - Computation Homology Project software. <http://chomp.rutgers.edu/>. Accessed: 2021-12-12
- [56] Munkres, J.R.: *Elements of algebraic topology*. CRC Press (2018)
- [57] Niyogi, P., Smale, S., Weinberger, S.: Finding the homology of submanifolds with high confidence from random samples. *Discrete & Computational Geometry* **39**(1-3), 419–441 (2008)

- [58] Oudot, S.Y.: Persistence theory: from quiver representations to data analysis. American Mathematical Soc. (2017)
- [59] Real, P.: An algorithm computing homotopy groups. *Mathematics and Computers in Simulation* **42**(4-6), 461–465 (1996)
- [60] Renka, R.J.: Algorithm 772: Stripack: Delaunay triangulation and Voronoi diagram on the surface of a sphere. *ACM Transactions on Mathematical Software (TOMS)* **23**(3), 416–434 (1997)
- [61] Scoccola, L., Perea, J.A.: Approximate and discrete euclidean vector bundles. *arXiv preprint arXiv:2104.07563* (2021)
- [62] Sergeraert, F.: Triangulations of complex projective spaces. In: *Contribuciones científicas en honor de Mirian Andrés Gómez*, pp. 507–519. Universidad de La Rioja (2010)
- [63] Sugihara, K.: Laguerre Voronoi diagram on the sphere. *Journal for Geometry and Graphics* **6**(1), 69–81 (2002)
- [64] Tierny, J., Favelier, G., Levine, J.A., Gueunet, C., Michaux, M.: The topology toolkit. *IEEE transactions on visualization and computer graphics* **24**(1), 832–842 (2017)
- [65] Tinarrage, R.: Recovering the homology of immersed manifolds (2019)
- [66] Tinarrage, R.: Computing persistent Stiefel–Whitney classes of line bundles. *Journal of Applied and Computational Topology* pp. 1–61 (2021)
- [67] Whitehead, J.H.: Combinatorial homotopy. I. *Bulletin of the American Mathematical Society* **55**(3. P1), 213–245 (1949)
- [68] Whitehead, J.H.C.: Simplicial spaces, nuclei and m-groups. *Proceedings of the London mathematical society* **2**(1), 243–327 (1939)
- [69] Zeeman, E.C.: Relative simplicial approximation. In: *Mathematical Proceedings of the Cambridge Philosophical Society*, vol. 60, pp. 39–43. Cambridge University Press (1964)
- [70] Zomorodian, A., Carlsson, G.: Computing persistent homology. *Discrete & Computational Geometry* **33**(2), 249–274 (2005)